FORT NELSON TEST SITE – SITE CHARACTERIZATION REPORT

Plains CO_2 Reduction (PCOR) Partnership Phase III
Task 4 – Deliverable D65
Task 4 – Milestone M29

Prepared for:

Andrea M. Dunn

National Energy Technology Laboratory
U.S. Department of Energy
626 Cochrans Mill Road
PO Box 10940
Pittsburgh, PA 15236-0940

DOE Cooperative Agreement No. DE-FC26-05NT42592

Prepared by:

James A. Sorensen
Charles D. Gorecki
Edward N. Steadman

Energy & Environmental Research Center
University of North Dakota
15 North 23rd Street, Stop 9018
Grand Forks, ND 58202-9018

January 2012
Revised February 2014
Approved

2014-EERC-03-02

EERC DISCLAIMER

LEGAL NOTICE This research report was prepared by the Energy & Environmental Research Center (EERC), an agency of the University of North Dakota, as an account of work sponsored by the U.S. Department of Energy (DOE). Because of the research nature of the work performed, neither the EERC nor any of its employees makes any warranty, express or implied, or assumes any legal liability or responsibility for the accuracy, completeness, or usefulness of any information, apparatus, product, or process disclosed or represents that its use would not infringe privately owned rights. Reference herein to any specific commercial product, process, or service by trade name, trademark, manufacturer, or otherwise does not necessarily constitute or imply its endorsement or recommendation by the EERC.

ACKNOWLEDGMENT

This material is based upon work supported by the U.S. Department of Energy National Energy Technology Laboratory under Award No. DE-FC26-05NT42592.

DOE DISCLAIMER

This report was prepared as an account of work sponsored by an agency of the United States Government. Neither the United States Government, nor any agency thereof, nor any of their employees, makes any warranty, express or implied, or assumes any legal liability or responsibility for the accuracy, completeness, or usefulness of any information, apparatus, product, or process disclosed, or represents that its use would not infringe privately owned rights. Reference herein to any specific commercial product, process, or service by trade name, trademark, manufacturer, or otherwise does not necessarily constitute or imply its endorsement, recommendation, or favoring by the United States Government or any agency thereof. The views and opinions of authors expressed herein do not necessarily state or reflect those of the United States Government or any agency thereof.

NDIC DISCLAIMER

This report was prepared by the EERC pursuant to an agreement partially funded by the Industrial Commission of North Dakota, and neither the EERC nor any of its subcontractors nor the North Dakota Industrial Commission nor any person acting on behalf of either:

(A) Makes any warranty or representation, express or implied, with respect to the accuracy, completeness, or usefulness of the information contained in this report or that the use of any information, apparatus, method, or process disclosed in this report may not infringe privately owned rights; or

(B) Assumes any liabilities with respect to the use of, or for damages resulting from the use of, any information, apparatus, method, or process disclosed in this report.

TABLE OF CONTENTS

Continued…

TABLE OF CONTENTS (continued)

LIST OF FIGURES

LIST OF TABLES

FORT NELSON TEST SITE – SITE CHARACTERIZATION REPORT

EXECUTIVE SUMMARY

The Plains CO_2 Reduction (PCOR) Partnership, led by the Energy & Environmental Research Center (EERC), is working with Spectra Energy Transmission (SET) to determine the feasibility of large-scale injection of carbon dioxide (CO_2) into a deep brine-saturated carbonate formation near Fort Nelson, British Columbia, Canada, for the purpose of CO_2 storage. Site characterization must be conducted prior to large-scale injection of CO_2 at the Fort Nelson test site. Effective characterization supports modeling; risk assessment; and monitoring, verification, and accounting (MVA) programs that will constantly evolve to suit the project's needs. Site characterization activities have been conducted to address three critical issues affecting the viability of the Fort Nelson test site: 1) the capacity of the target formation, 2) injectivity, and 3) containment – the potential for leakage of the injected CO_2 into overlying formations and/or the near-surface environment.

Geochemical, mineralogical/petrophysical, geomechanical, and hydrogeological data have been collected for the purpose of supporting modeling, risk assessment, and MVA activities. The geology, stratigraphy, and lithology have been evaluated, delineated, and described for the entire sedimentary succession from the base of the Devonian age Presqu'ile reef complex to the top of the Fort Simpson shale (cap rock) in the Fort Nelson project area. The structural elements of the reef complex have been investigated to identify any existing faults and/or fractures that would allow migration of any reservoir and/or injected fluids out of the storage reservoir. On this basis, a geologic model has been built, with particular attention given to the Devonian injection interval and overlying and underlying sealing formations.

Key findings of the characterization activities to date include:

- The Slave Point, Sulphur Point, and Keg River Formations appear to have adequate storage- and injectivity-related properties to serve as primary sinks.
- The Fort Simpson and Muskwa Formations appear to have the tightness, competency, thickness, and lateral continuity necessary to be the primary seals.
- Evidence suggests the Slave Point, Sulphur Point, and Keg River Formations are in hydraulic communication (laterally and vertically) with each other.
- Surface, shallow subsurface, and deep subsurface characterization data are limited because of the remote nature of the Fort Nelson area and because of the lack of producer wells in the area being considered for CO_2 storage.

- The storage capacity of the Presqu'ile reef complex in the Fort Nelson area has been estimated to range from 100 to over 240 million tonnes of CO_2.

- It is anticipated that future characterization activities will include drilling and testing of a new exploratory well, collecting new seismic survey data, detailed technical analyses, and conducting laboratory-based geochemical and geomechanical investigations.

It is important to note that this report presents the site characterization information, analyses, and interpretation as of 2010. Further site investigations and analyses have been ongoing since 2010, and some of the interpretations and conclusions presented in this report may be subject to change as warranted because of results generated after 2010.

FORT NELSON TEST SITE – SITE CHARACTERIZATION REPORT

INTRODUCTION

Spectra Energy Transmission's (SET) Fort Nelson gas-processing plant is located in northeastern British Columbia, Canada, and is the largest sour gas-processing plant in North America. Spectra Energy's Fort Nelson gas-processing plant (FNGP) is located on the southern edge of the Horn River shale basin which is expected to undergo significant development of unconventional gas reserves which will be processed at the FNGP. In the near future, the FNGP is anticipated to be running at its full 1.0 Bcf/d raw gas-processing capacity, emitting approximately 3 million tonnes of CO_2 a year.

With the combination of the projected emissions for the FNGP and the growing tendency toward greenhouse gas regulations by both local and federal governments, SET is proactively exploring the addition of carbon capture and storage (CCS) technology to its FNGP. The goal of CCS at the Fort Nelson plant would be to capture the formation CO_2 that is separated by gas processing at the FNGP and store it in a deep saline formation. The application of CCS technology at the FNGP is anticipated to inject and permanently store approximately 2.2 million tonnes of formation CO_2 a year, thereby reducing the FNGP overall CO_2 emissions from 3 Mt/year to approximately 0.8 Mt/year. The injected stream is expected to consist of 95% CO_2, 4% H_2S, and 1% residual methane.

To support efforts to determine the feasibility of the proposed Fort Nelson CCS project, an initial baseline site characterization undertaking has been performed. This effort was required in order to understand the geology and near-surface conditions of the area. Characterization of the Fort Nelson area is crucial in understanding the reservoir; the containment; developing geologic models; performing predictive simulations; conducting risk management activities; and developing cost-effective monitoring, verification, and accounting (MVA) strategies with the overall goal of safely and cost-efficiently storing sour CO_2.

PROJECT BACKGROUND/GOALS

The governments of Canada and British Columbia are pursuing ways to encourage industry to reduce atmospheric CO_2 emissions. CO_2 storage in geologic media has been identified as an important means for reducing anthropogenic greenhouse gas emissions into the atmosphere (Bradshaw et al., 2006). Several means for geologic storage of CO_2 are available, such as depleted oil and gas reservoirs, deep brine-saturated formations (often referred to in literature as "saline formations" or "saline aquifers"), and CO_2 enhanced oil recovery (EOR) operations. Regional characterization activities conducted by the Plains CO_2 Reduction (PCOR)

Partnership (Peck and others, 2007) and other published literature (Bachu et al., 2003) indicate that brine-saturated formations represent the largest-volume opportunities for long-term storage of CO_2 in North America. In an effort to significantly reduce CO_2 emissions from their natural gas-processing operations in northeastern British Columbia (Figure 1), SET is taking steps to initiate the first CCS project in British Columbia to inject up to 2.2 million tonnes/year of CO_2 into a saline reservoir.

The PCOR Partnership, covering nine U.S. states and four Canadian provinces, is one of seven Regional Carbon Sequestration Partnerships established by the U.S. Department of Energy in 2003. The primary objective of the PCOR Partnership is to assess the technical and economic feasibility of capturing and storing CO_2 emissions from stationary sources in the central interior of North America. The partnership comprises more than 100 private and public sector groups from the nine states and four provinces, among them SET; Natural Resources Canada (NRCan); and the British Columbia Ministry of Energy, Mines, and Petroleum Resources (BCMEMPR). The 10-year Phase III program being conducted by the PCOR Partnership aims to demonstrate the efficacy of large-scale CO_2 storage in two locations, including the Fort Nelson CCS project being planned by SET.

Figure 1. SET's natural gas-processing plant Fort Nelson, British Columbia, Canada.

The brine-saturated carbonate formations that are being considered in the Fort Nelson area as targets for large-scale injection are similar in many respects to deep carbonate rocks that are not only found in sedimentary basins of the PCOR Partnership region (Figure 2) but also around the world. It is, therefore, anticipated that the results generated at the Fort Nelson site will provide insight and knowledge that can be directly and readily applied throughout the world.

Developing cost-effective approaches to predict and determine the fate of the injected CO_2 is an important aspect of the emerging CCS technology. Site characterization activities are critical to developing accurate models and simulation, risk management, and MVA plans designed to minimize leakage. Laboratory and modeling analysis programs can generate results

Figure 2. Location of the Fort Nelson demonstration site and sedimentary basins within the PCOR Partnership region.

that can be used in conjunction with site characterization to establish baseline conditions at the site. The baseline conditions subsequently provide a point of comparison to predict and document the effects of the large-scale sour CO_2 injection on the geochemical/geomechanical integrity of both the target injection formation and its overlying seal. The results of laboratory-based geotechnical evaluations coupled with robust modeling based on those results can guide the development of injection schemes that maximize the efficiency of injection and MVA plans that can detect if leakage has occurred or not.

BACKGROUND/GOALS OF SITE CHARACTERIZATION

The integrated philosophy of the PCOR Partnership is to combine site characterization, modeling and simulation, risk assessment, and MVA strategies into an iterative process to produce superior quality results (Figure 3). Elements of any of these activities are crucial for understanding or developing the other activities. As new knowledge is gained for site characterization, for example, it reduces a given amount of uncertainty in geological assumptions. This reduced uncertainty can then propagate through modeling and simulation, risk assessment, and MVA efforts.

Site characterization activities have been conducted to address three critical issues affecting the viability of the Fort Nelson test site: 1) the capacity of the target formation, 2) injectivity, 3) containment and the potential for leakage of the injected CO_2 into overlying formations and/or the near-surface environment. This process began with a literature review of all known geologic information for the region of interest in order to gain a broad-based understanding of the geologic systems that may serve as sinks or seals. Robust sets of relevant data that may assist in describing the current subsurface geologic conditions, in particular, those that relate to storage reservoir injectivity, capacity, and integrity, were acquired. Those data were analyzed and interpreted to identify potential injection horizons and well locations for more detailed study. Once potential sinks and seals were identified, the data were then used as the basis for static and dynamic modeling activities to provide stakeholders and decision makers with insight regarding the viability of the area of interest with respect to CO_2 storage. Risk assessment activities have been conducted and used to identify which aspects of the program require additional characterization. Potential MVA technologies have been identified which will ultimately serve as the primary means by which the storage operation can be managed from a risk perspective. Over the course of the project, the cycle will repeat as the results of the first iteration of site characterization are used to guide the acquisition of additional data through more focused characterization activities. The initial site characterization cycle for the Fort Nelson project (the results of which are presented in this report) relied on information from readily available literature or publicly accessible databases, proprietary technical reports commissioned by SET, and a variety of data generated by the drilling of an exploratory well and acquisition of seismic surveys.

However, subsequent iterations will generally require the acquisition of more robust, site-specific data, such as that associated with seismic surveys or additional exploratory well-drilling activities and detailed analyses and interpretation.

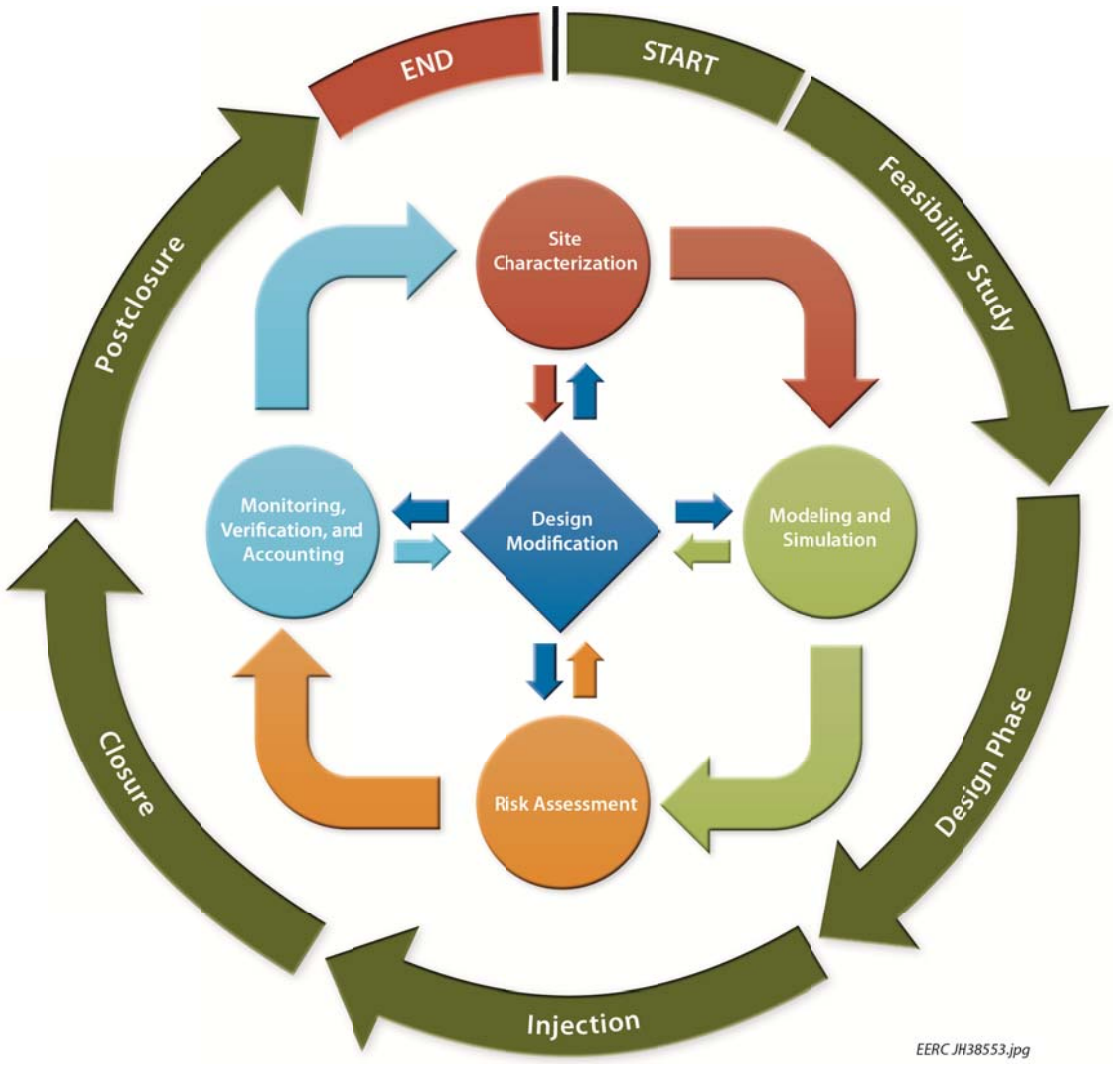

Figure 3. Graphic expression of the relationship between site characterization and other elements of the Fort Nelson CCS project. Each of these elements feeds into another, iteratively improving results and the efficiency of evaluation.

ELEMENTS OF THE FORT NELSON CCS SITE

The key elements of any CCS site being considered for long-term, permanent storage of CO_2 that must be characterized include the surface and shallow subsurface environments, deep injection target formations (sinks) and their associated sealing formations (seals), other formations that may be of interest to project stakeholders, and structural features that may control or affect the movement and ultimate fate of the injected CO_2. These key elements as they apply to the Fort Nelson CCS site are described below.

Surface and Shallow Subsurface

The potential leakage of sour CO_2 could have adverse impacts on the flora and fauna occupying the surface and near-surface environment of the Fort Nelson CCS site area. Establishing baseline conditions for the surface and near-surface environment is essential to effectively monitor for impacts potentially caused by leakage. For the purpose of this report, the surface environment is defined as including the soil, water, and air at the ground surface. The shallow subsurface environment is considered to encompass the unsaturated (vadose) soil zone and shallow groundwater resources. In the Fort Nelson area, shallow groundwater resources are considered to extend to a depth of approximately 150 to 200 meters.

The surface of the Fort Nelson CCS project area is a largely uninhabited boreal forest/ muskeg landscape, a vast majority of which is not easily accessible. Because of the lack of surface development and accessibility, very little quantitative data exist on the nature of soils and shallow groundwater in the area. Efforts to characterize the near-surface and shallow subsurface environment of the Fort Nelson area have largely been based on information provided in readily available technical literature, data obtained from the few shallow groundwater wells that do exist, and aerial images of surface features. More extensive baseline testing of the surface and shallow subsurface would likely be prudent prior to project implementation.

Deep Storage Reservoir and Containment System

Exploration activities for mineral and energy resources over the last 50 years have yielded a significant amount of information about the geology of northeastern British Columbia and northwestern Alberta. Data sets associated with the exploration activities include wireline well logs, core and fluid analyses, seismic surveys, production, water disposal operations, and the results of reservoir-testing activities. These data sets provide quantitative information on key formation parameters such as depth, thickness, lithology, porosity, permeability, and structure. Examination and evaluation of these historical data sets indicate that that the Devonian-age reef system that underlies much of the Fort Nelson area can provide a storage reservoir–containment system that is world-class in terms of injectivity, storage capacity, and containment.

The sedimentary succession in the Fort Nelson area consists, in ascending order from the Precambrian crystalline basement to the surface, of Middle and Upper Devonian carbonates and shales, Mississippian carbonates, and Lower Cretaceous shales overlain by Quaternary glacial drift unconsolidated sediments. Figure 4 shows a stratigraphic column that presents the relative position of the key rock formations of interest that make up the sink–seal system for the Fort Nelson area.

With respect to potential reservoir, the carbonate platforms and reefs of the Middle Devonian formations that make up the Presqu'ile reef structure in the northern Alberta Basin are known to contain large quantities of sour natural gas (10% CO_2 and 1.5% H_2S naturally) underlain by a very large hydrodynamic regional saltwater aquifer which suggests that the formations have adequate porosity, permeability, and trapping mechanisms to support the long-term storage of large volumes of CO_2 (Sorensen and others, 2005; Stewart and Bachu, 2000). In the Fort Nelson area, it is anticipated that brine-saturated reservoirs within the underlying Middle

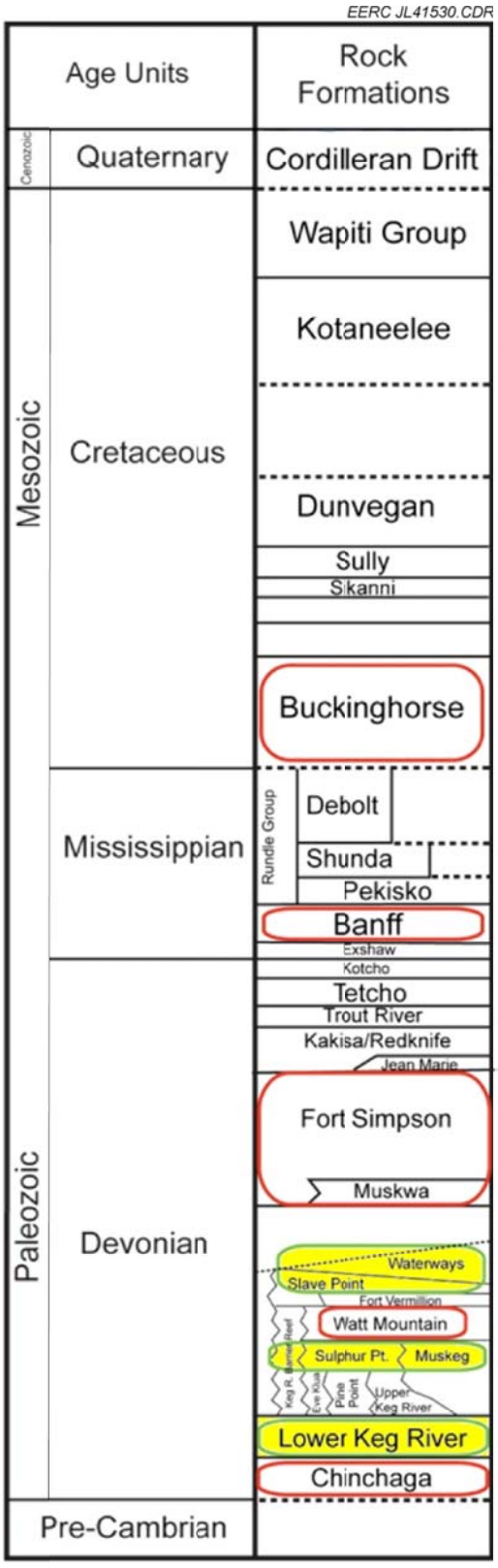

Figure 4. Stratigraphic column at the Fort Nelson CCS project site. Seal formations are circled in red; potential sink formations are highlighted yellow.

Devonian Sulphur Point Formation and/or Keg River Formation will be the primary target injection zones for the Fort Nelson CCS project. It is anticipated that the overlying Slave Point Formation will also be part of the storage unit because it is hydrodynamically connected to the Sulphur Point and Upper Keg River Formations. However, because of the presence of natural gas reserves in the Slave Point, it will likely not be a target formation for CO_2 injection.

With respect to primary containment, the Devonian reef complex in the Fort Nelson area is overlain by thick, laterally extensive shales of the Devonian Muskwa and Fort Simpson Formations. Shales and low-meability carbonate rocks within the Mississippian Banff and the Cretaceous Buckinghorse Formations, which are above the Fort Simpson Formation, also serve as additional laterally extensive barriers to the upward migration of CO_2 and are considered to provide additional overlying containment for the Fort Nelson CCS project.

The key formations that have been characterized as part of the Fort Nelson CCS project are described in greater detail below. These descriptions are based on published literature and the examination of data from well logging and core analysis activities, both historical and those conducted over the course of this project.

Storage

The Sulphur Point and Keg River Formations have been identified as being the most likely target injection formations for the Fort Nelson CCS project. The Sulphur Point Formation and the Keg River Formation are both part of the sequence of rocks that make up the Presqu'ile reef complex, a Middle Devonian age barrier reef that occurs across tens of thousands of square kilometers in the northern Alberta Basin. The rocks of the Presqu'ile reef complex comprise a succession of shallow-water carbonates. In the Fort Nelson area, the target for CCS is the reef front consisting of Slave Point, Sulphur Point, and Keg River Formations. These formations are dominated by clean carbonate rocks (limestones and dolomites) with prominent reef and/or bank structures that have porosity and permeability characteristics adequate for large-scale CO_2 injection. While looking for gas reserves, only a few wells have been drilled into the Sulphur Point and Keg River Formations and only into the top of the Slave Point in the vicinity of the FNGP because of the lack of natural gas resources in those formations in the Fort Nelson area. Therefore, data on the porosity and permeability below the top of the Slave Point rock formations in the area are sparse. Although rock property data for the area are limited, the data that do exist suggest that porosity and permeability are likely adequate to support large-scale injection of CO_2. Existing data indicate that the Sulphur Point Formation has an average thickness of about 40 meters in the Fort Nelson area, with average porosity ranging from 3% to 11% and permeability estimates as high as 1000 mD. The Upper and Lower Keg River Formation in the area has an average combined thickness of about 150 meters, with an average porosity range of 6% to 11% and permeability averaging tens to hundreds of mDs.

Containment

Shales of the Muskwa and Fort Simpson Formations directly overlie the Mid-Devonian carbonate reef and the potential CO_2 storage reservoirs of the Slave Point, Sulphur Point, and Keg River Formations. The Muskwa and Fort Simpson shales exhibit considerable thickness and

have a vast extent, making them the primary containment formations with respect to vertical migration of injected CO_2. Together, the Fort Simpson and Muskwa Formations represent a formidable cap rock of approximately 560 meters in total thickness.

Other Formations in the System

Although the sink and seal formations provide the most critical elements of an effective CCS operation (i.e., storage capacity and containment), it is important to note that there may be other rock formations in the project area that may play important roles in a successful CCS project. There are several published interpretations of the stratigraphy of the Fort Nelson area, with anywhere from 20 to 25 distinctly identifiable rock units being present in the area's stratigraphic column. Of the rock units that will not serve as either primary sinks or seals, four have nonetheless been identified as being of importance to the Fort Nelson CCS project: the Devonian age Slave Point, Watt Mountain, and Otter Park Formations, which are part of the Presqu'ile reef complex, and the Mississippian age Debolt Formation, which is the first locally porous and permeable zone above the primary seals.

The Slave Point Formation is a complex carbonate platform that is approximately 60 meters thick. It represents the top of the Devonian carbonate reef complex. Although it is known to have zones of reasonably high porosity and permeability, it is not considered to be a candidate injection target formation for CO_2 storage because two commercially operated gas reservoirs are in relatively close proximity to the sites being considered for the Fort Nelson CCS project. It is imperative that CO_2 injection and storage operations do not interfere with those commercial gas production operations, either through contamination of the gas pools with sour CO_2 or pressure interference that CO_2 injection may have with gas production and/or produced water disposal operations. In fact, one of the primary goals of the dynamic reservoir modeling for the project is to predict the effects that large-scale injection may have on those gas fields, particularly with respect to the timing and magnitude of those effects under different injection scheme scenarios. With this in mind, it is critical to obtain characterization data for Slave Point that are of similar nature and detail as those obtained for the Fort Nelson sinks and seals.

The Devonian age Watt Mountain Formation is a primarily silty mudstone unit with low permeability that discontinuously overlies the Sulphur Point Formation and underlies the Slave Point. However, because it is relatively thin (approximately 5 meters thick or less in some parts of the Fort Nelson area), it is discontinuous and lacks consistent porosity and permeability. It is considered to be a local, low-permeability barrier within the reef retarding upward movement of injected CO_2 in the Sulphur Point. However, it may serve as a baffle to upward migration of CO_2, thereby affecting the movement and three-dimensional geometry of the plume before it gets to the base of the primary seal formation.

Directly underlying the Muskwa Formation is the Devonian age Otter Park Formation, in the off reef, seaward side, a tight, often calcareous shale with occasional zones of dolomite that serve as unconnected streaks of porosity (Belyea and Norris, 1962). It generally sits on top of the Keg River Formation off the reef front, where it typically ranges in thickness from 100 to 200 meters. Chronostratigraphically, the Otter Park is roughly equivalent to the Slave Point Formation. As such, the Otter Park is usually not present where the Slave Point occurs but does

sometimes thinly drape over it. The primary role of the Otter Park Formation will be to serve as an important lateral seal for CO_2 storage in the Fort Nelson area.

The Mississippian age Debolt Formation is approximately 240 meters thick and consists mainly of brown, cherty, massive bioclastic limestone, with some dolomite and shale (Macauley, 1958). The Debolt Formation is of interest to the Fort Nelson CCS project for two reasons. Firstly, it is the first largely porous and permeable formation that occurs above the Fort Simpson shales of the primary seal, and as such, it will likely be monitored for the first signs of CO_2 leakage outside the primary seal–sink system

Structural Elements

Understanding the structural elements of an area is crucial to predicting the movement and ultimate containment of the plume and the nature of pressure propagation through the sink–seal system. Structural elements of the Fort Nelson CCS project study area include the three-dimensional geometry of the reef complex, faults, fractures, and hydrothermal sag features. The strike, dip, and surface relief of formations and the strike and dip of faults and fractures are particularly crucial to accurately predict the movement of buoyant fluids such as CO_2. These elements can be identified and incorporated into a static geologic model using data from well logs, seismic surveys, and the analysis of core and cuttings.

The reef structure will influence the distribution of porosity and permeability throughout the various formations that make up the reef. The distribution of those properties can, in turn, influence the movement of fluids through those formations. Because CO_2 is buoyant, the structure of the reef complex will also affect the movement and geometry of the CO_2 plume. The presence of faults in the system can have a significant impact on the movement of CO_2 and the propagation of pressure, with closed faults serving as barriers and open faults providing fast-flow vertical pathways. Fractures generally increase the overall permeability of a rock system, although they do so in a complex manner that can be difficult to incorporate into a model. Zones of high fracturing can be associated with reef structures, faults, and hydrothermal sag features. Hydrothermal sag features are known to occur in Devonian carbonate rocks in the Fort Nelson area. These features are typically chimney-shaped zones within the Devonian carbonates through which hydrothermal fluids migrated long after deposition of the formations. As with faults, some hydrothermal sag features may be closed, thereby serving as barriers to lateral and vertical migration. However, open hydrothermal sag features can affect the CO_2 movement and pressure propagation by serving as fast-flow vertical conduits. All of these structural elements must be considered when characterization data are gathered and geologic modeling exercises are conducted.

Hydrogeological Regime

The direction and rate of fluid flow in three dimensions within a rock formation or between a group of formations are collectively referred to as the hydrogeological regime of that geologic system. For a CCS project, a thorough and accurate understanding of the hydrogeological regime of the sink–seal system is essential for predicting both the movement and fate of the injected CO_2 and the dissipation of pressure within the reservoir. Hydrogeological data, including formation

pressure and reservoir fluid chemistry data, can be used to determine the existence and nature of hydraulic connectivity between different rock units.

The hydrogeological regime in the Fort Nelson area is influenced by a variety of factors. At the regional scale, in situ formation water flow within the Devonian system is generally eastward, flowing away from the Rocky Mountains. However, at the local scale, flow within the Devonian system in the Fort Nelson area is complicated by the effects of reef structure and architecture, the distribution of porosity and permeability, and the impact of localized pressure drawdown as a result of major gas production from portions of the reef. With respect to flow rates, the available head data suggest very slow natural in situ brine flow in the Fort Nelson area (Burnie, 2010).

FORT NELSON CHARACTERIZATION EFFORTS AND RESULTS TO DATE

The following subsections present and discuss the key results of characterization activities that have been conducted by SET and the PCOR Partnership as of May 2011. Because the Fort Nelson CCS project is in the feasibility stage of development, it is important to bear in mind that these results should not be considered comprehensive or final in nature. Rather, the findings presented here are intended to provide a general understanding of the nature of the Fort Nelson CCS project technical team's knowledge of the key elements of the area being considered to host the Fort Nelson CCS project.

Surface and Shallow Subsurface Characterization Results

Initial efforts by the PCOR Partnership and SET to characterize the Fort Nelson test site surface area have included a thorough literature review and examination of regional and local surface maps and aerial photos. While future surface characterization activities may include the collection and analysis of topsoil, soil gas, surface water, and near-surface air samples, no historical data on these properties have been identified, likely because of the remote and undeveloped nature of the area.

The Fort Nelson CCS project is located within the northwestern portion of the Alberta Basin approximately 10 miles (16 km) southwest of the town of Fort Nelson, British Columbia, Canada, near Alaskan Highway Mile 300. Figure 5 is a map depicting the location of the Fort Nelson CCS project study area. The Fort Nelson project surface area is largely dominated by rural boreal forest which is a complex mosaic of fens, bogs, swamps and pools, and scrubby forest (Royal British Columbia Museum, 2011) and is scarcely populated. The topography is generally flat, with slow flowing rivers (i.e., the Muskwa, Prophet, and Sikanni Chief Rivers), lakes (most notably, Clarke, Milo, and Klowee Lakes), and creeks being the only distinctive features. Regionally, the soil type is a poorly drained silty clay.

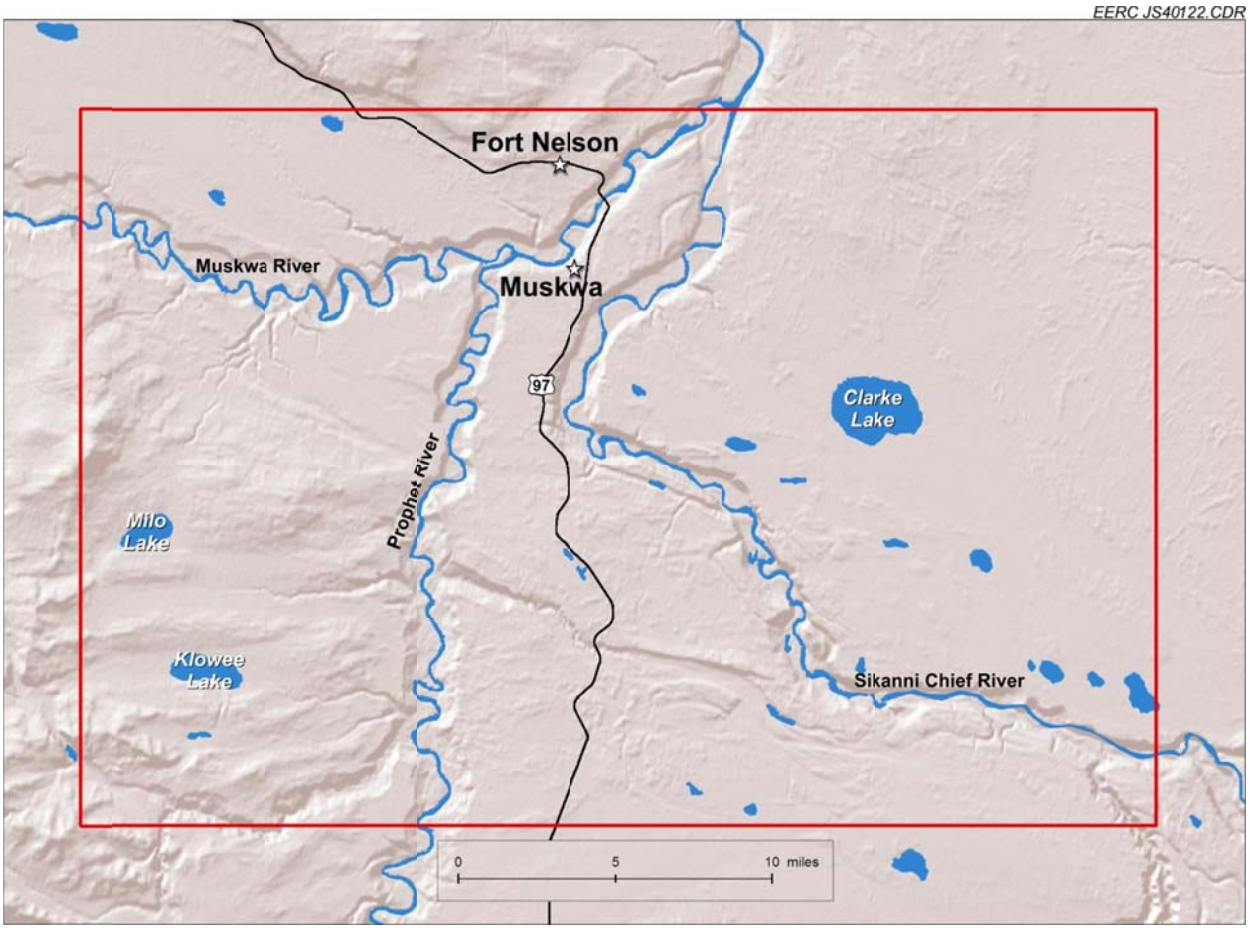

Figure 5. Representing surface features (lakes, rivers, roads) of the Fort Nelson study area.

The land in the Fort Nelson project area is Provincial Crown land, owned by the province of British Columbia, Canada, and within the traditional territory of the Fort Nelson and Prophet River First Nations. Because of the remote nature of the Fort Nelson project area and lack of permanent roads, surface land use activities are limited to natural gas exploration and production as well as forestry, trapping, hunting, and fishing. The climate regime of the area is considered to be a muskeg or a taiga "subarctic" plain having an average mean summer temperature of 12°C (54°F), an average mean winter temperature of −15°C (5°F), and a mean annual precipitation range of 400 to 500 mm (16–20 in.).

Shallow subsurface characterization has focused primarily on the drilling and subsequent sampling of shallow groundwater wells in the vicinity of SET's deep exploratory well. Roy Northern Environmental Ltd. (Roy Northern) was contracted by Canadian Petroleum Engineering Inc. (CPE) to conduct water sampling from four groundwater wells drilled near the SET CCS Services Inc. Milo c-61-E/94-J-10 location (Figure 6). The four wells were initially sampled on May 19, 2009, and again in January 2010. Results were compiled into a report dated August 4, 2009. All of the wells were used to supply water for drilling operations as well as to supply water for the campsite.

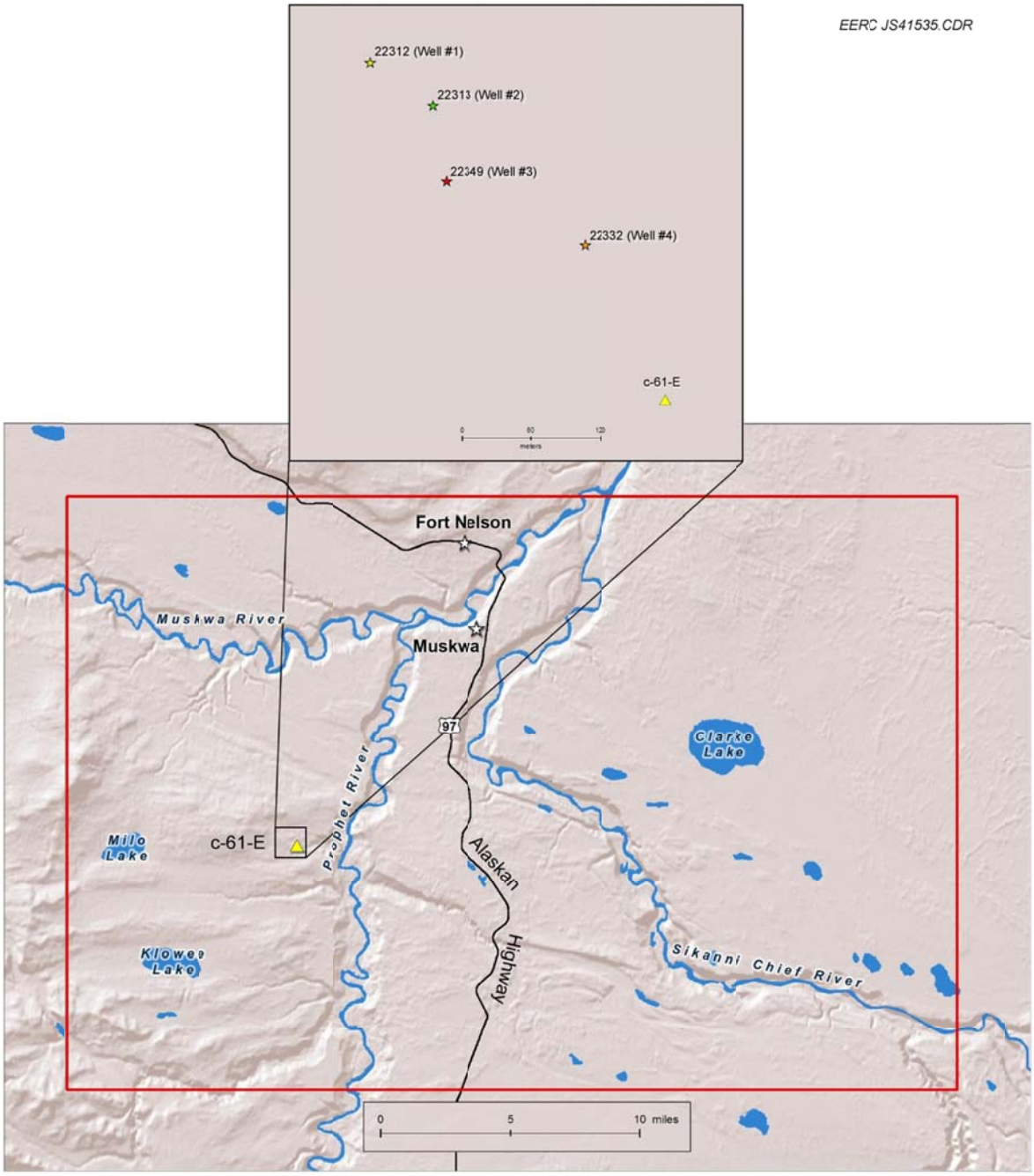

Figure 6. Location of Groundwater Wells 1–4 used in the baseline data collection relative to the planned Injection Well c-61-E.

The primary purpose of the groundwater-monitoring wells is to provide baseline data regarding the quality of shallow groundwater resources. These baseline data can then be used as points of comparison to later postinjection sampling events to determine what effects, if any, the storage of sour CO_2 may have on the shallow groundwater. The results from the samples collected in both May 2009 and January 2010 were used to determine baseline parameters for

water quality in the area; additional future sampling may be beneficial for observation of seasonal variance, if such variance exists. A continuing water-monitoring program for the duration of the active injection operations and for a postinjection period yet to be determined will need to be implemented once the injection well is in use. However, it is important to note that naturally driven, long-term changes in surface conditions may affect shallow groundwater parameters. Such phenomena may need to be factored into deviations from baseline data, should deviations occur once injection is taking place.

Shallow groundwater sampling was conducted in accordance with procedures described in the "British Columbia Field Sampling Manual for Continuous Monitoring and the Collection of Air, Air-Emission, Water, Wastewater, Soil, Sediment, and Biological Samples," 2003 Edition (Permitee). Below is a description of measurements and methods.

Based on the results from the four groundwater-monitoring wells, shallow groundwater near c-61-E appears to have little variation in quality. Field measurements were collected using a multiparameter instrument and flow-through cell at the time of sampling and included the following:

- Temperature
  - Range of 2.6° to 3.9°C with a mean of 3.4°C

- pH
  - Range of 6.8 to 7.5 with a mean of 7.2

- Electric conductivity (EC)
  - Range of 909 to 1181 μS/cm with a mean of 1089 μS/cm

- Dissolved oxygen (DO)
  - Range of 3.9% to 18.9% with a mean of 12

- Total dissolved solids (TDS)
  - Range of 1003 to 1396 mg/L with a mean of 1205 mg/L

- Salinity
  - Range of 0.86 to1.09 ppt with a mean of 0.94 ppt

Field titration kits were utilized to estimate:

- Total alkalinity
  - Range of 750 to 1035 mg/L with a mean of 901 mg/L

- Free CO_2
  - Range of 37 to 87 mg/L with a mean of 57 mg/L

- Chloride concentrations
  - Range of <10 to 125 mg/L

Storage and Containment System Results

As of January 2012, SET and the EERC had completed numerous analytical activities, modeling exercises, and investigations to characterize the potential sinks, their associated primary seals, and other formations relevant to the project. These characterization activities included purchase and interpretation of available historical 2-D and 3-D seismic surveys, drilling and testing a deep test hole in 2009, and drilling and testing a sidetrack of the 2009 vertical hole in 2010. Laboratory-based analytical activities using cuttings and core samples were conducted and continue to be ongoing. Figure 7 illustrates the location of the investigative work undertaken, including Spectra's interpretation of the Slave Point reef edge, and outlines of recognized natural gas pools.

On April 4, 2009, Spectra initiated drilling of the first Fort Nelson CCS project test well at location c-61-E /94-J-10 referred to as "c-61-E." The c-61-E well was drilled down through the carbonate barrier reef complex, penetrating the Chinchaga Formation and reaching a total depth of 2561 meters. In December 2009, the c-61-E well was reentered and a second borehole (designated d-61-E and referred to as the "sidetrack" wellbore) drilled at an angle of approximately 30 degrees away from the previously existing vertical borehole. The sidetrack wellbore extended from approximately 8 meters below the casing shoe in the Muskwa and ended at a depth of 2282 meters in the Upper Keg River Formation. Specific characterization activities in the Fort Nelson exploratory well included the running of well logs, the collection of core, and

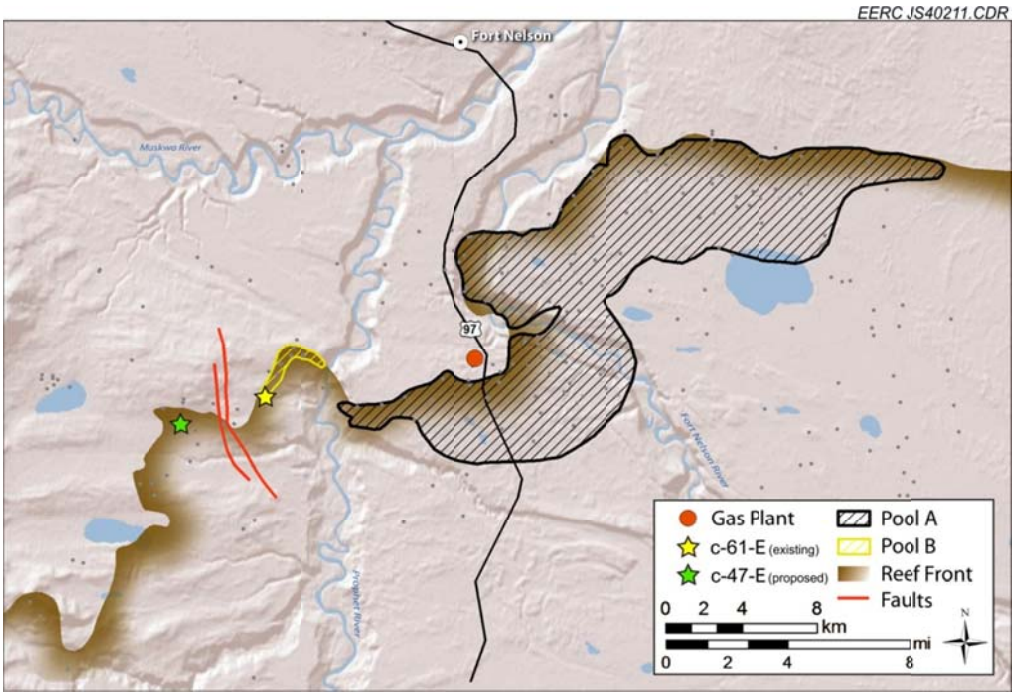

Figure 7. Location of Fort Nelson CCS project area of review.

injection-related tests. The primary goal of these drilling and testing programs was to determine the storage capacity, injectivity, and containment characteristics of the seals; sinks; and other relevant deep formations in the Fort Nelson CCS project area.

A standard suite of well logs, including gamma ray, neutron porosity, lithodensity, and spontaneous potential/induction logs, were run through most of the Devonian portion of the wellbore. Sonic and formation microimaging (FMI) logs were also run in the Presqu'ile reef portion of the well. Generally speaking, the results of the wireline logging showed that the stratigraphy, depths, and properties of the formations and zones of interest were consistent with past characterization efforts and within the range of what is typically expected from those formations. Figure 8 shows gamma and lithology logging results in the portion of the well that includes the Fort Nelson sink and seal system.

Primary Containment Results

The Fort Simpson Formation is considered to be the primary seal with respect to vertical leakage for the Fort Nelson CCS project. The Muskwa Formation, which immediately underlies the Fort Simpson, is also a tight formation that will serve as a barrier to upward migration of CO_2. Together, the Fort Simpson and Muskwa Formations represent a thick, competent, geographically widespread cap rock of approximately 560 meters total thickness in the Fort Nelson area. It is to be noted that the Muskwa/Fort Simpson shales have contained the Slave Point gas and brine for millions of years, providing further evidence of their competence as a cap rock for CCS. To evaluate the characteristics of the primary sealing formations, SET ran a suite of well logs and cored part of the Fort Simpson and Muskwa shales. Core and cutting samples were used to conduct a suite of analytical studies to evaluate the mineralogical, geochemical, and geomechanical properties of the seals.

A petrographic assessment was performed on samples from three intervals of Fort Simpson and Muskwa Formations corresponding to depths of approximately 2030, 2042, and 2045 m (Figure 8). The assessment evaluated geochemical stability, mineralogy, and rock properties pertinent to CO_2 containment. A variety of analyses were conducted in order to collect properties, provide supporting data, correlate findings, and provide illustrations and explanations of results. Specifically, testing included the following:

- X-ray diffraction (XRD) for bulk mineralogy
- X-ray fluorescence (XRF) for trace element analysis
- Petrographic analysis via thin section for mineralogy and rock fabric descriptions
- Quantitative evaluation of minerals by scanning electron microscopy (QEMSEM) for mineralogical mapping
- SEM with energy-dispersive spectrometry (EDS) for mineralogical identification and rock fabric descriptions

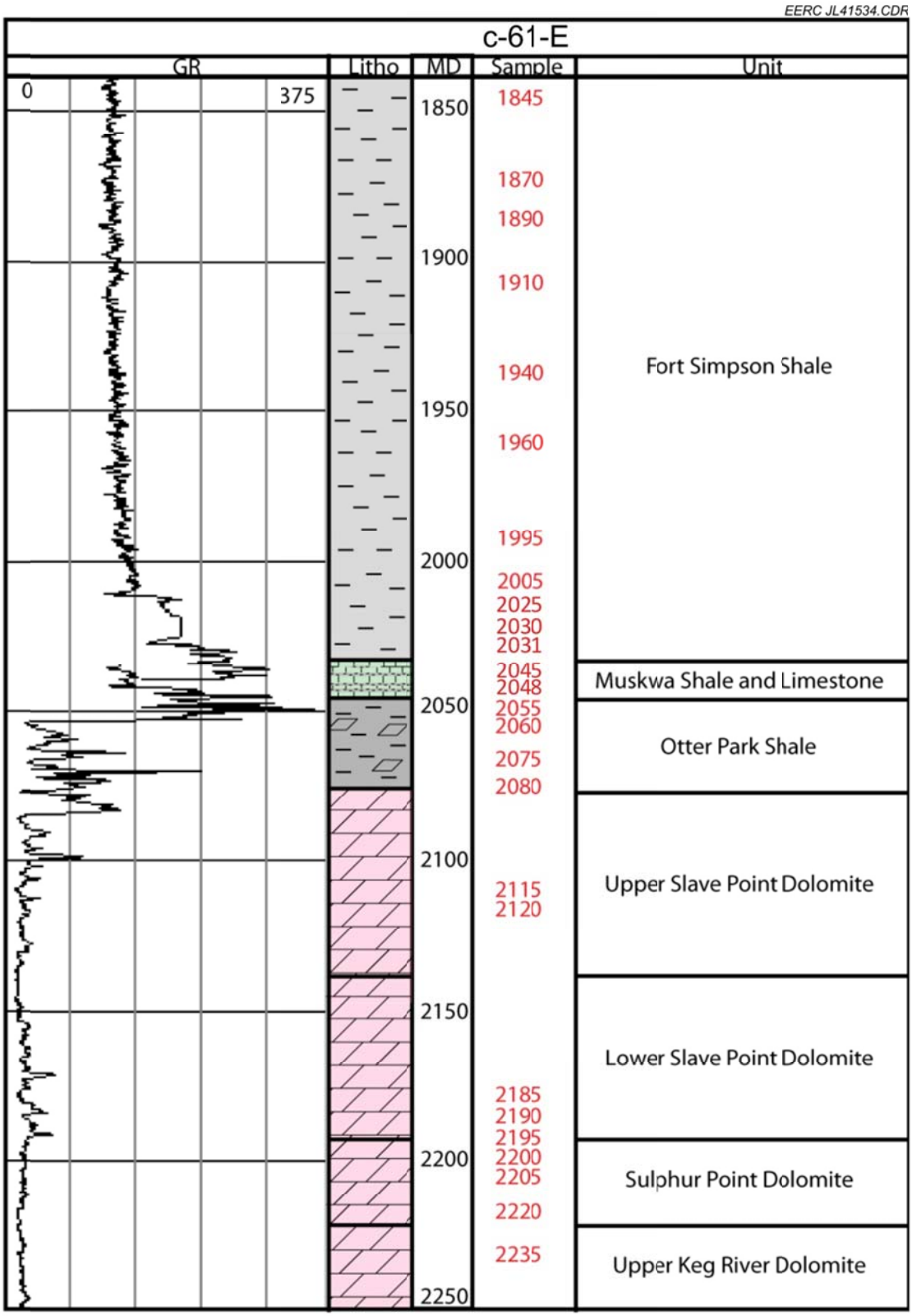

Figure 8. Gamma and lithology logs from Well c-61-E, with marked sample locations from the Fort Simpson, Muskwa, Otter Park, Slave Point, Sulphur Point, and Keg River Formations.

- CHN/S measurements for elemental composition information
- Surface area to determine reactive surface
- Skeletal density to support mineralogy and examination of total vs. effective porosity
- Degree of cementation
- Inductively coupled plasma–mass spectroscopy to examine trace element abundance

All three specimens represent various tight cap rock characteristics ideal for the Fort Nelson CCS site, such as having tight partially mineralized collection of stable minerals with low porosity, low permeability, and small pore throat diameter. The first two intervals were very similar, containing high percentages of clay, with variable pyrite, silt, and fine-grained carbonate, while the third interval contained a much higher degree of sparry carbonate growth. No microstructure was visible in any of the sections. Test results confirm the Fort Simpson and Muskwa Formations will provide a significant barrier to sour CO_2 vertical flow. The complete Fort Nelson Cap Rock Petrographic Analysis – July 2011 can be found in Appendix A.

Weatherford Laboratories (Canada) Ltd. conducted a cap rock study using cap rock material from Well c-61-E. The objective of this study was to evaluate the competency of the cap rock for this reservoir, pore-size distribution, and capillary pressure characteristics using the mercury injection method. Mechanical property testing to evaluate the integrity of the cap rock was performed, as well as analyses of routine petrophysical parameters taken from full-diameter core samples. The complete Weatherford Laboratories report is found in Appendix B; the highlights of the study are presented below.

The structural integrity and leak resistance of the Fort Nelson cap rocks were investigated by measuring the capillary pressures along with rock mechanical testing. Each of the cap rocks was found to be completely impermeable to sour CO_2 at injection pressures of more than 10,000 kPa and exhibited effective permeabilities to sour CO_2-saturated brine of 4.6 nD (Fort Simpson) and 0.9 nD (Muskwa) at injection pressures of 5500 kPa (798 psi). Both of these values are many orders of magnitude less than the commonly accepted maximum permeability to fluid value of 0.001 mD. While these lab results are encouraging, it should be noted that the Muskwa is part of the Horn River shale gas "reservoir," and these traditional lab techniques should be treated with caution. Different lab techniques and analyses are required in evaluating unconventional shale gas.

Mercury injection capillary pressure (MICP) testing was completed on Fort Simpson (2031 meters) and Muskwa Formations (2048 meters). Mercury injection (intrusion) provides for the rapid quantification of a sample's interconnected pore system and the size distribution of pore apertures (capillaries) that strongly influence saturations and fluid flow (permeability). Both Fort Simpson and Muskwa Formations are characterized as having a pore throat type of 100% micropores (pore diameter of less than 1 μm). The MICP testing also yielded a threshold intrusion pressure of 24,790 kPa (3595 psia) for each of the formations, which further supports the conclusion that these formations are competent seals for a large-scale CO_2 storage operation.

To date, only the Muskwa Formation (2045 meters) has been evaluated for mechanical properties. Specifically, triaxial compressive strength and dynamic elastic parameters were determined using two representative plugs 0.14 meters apart. The average compressive strength of the Muskwa shales was 202,750 kPa (29400 psi), which is ten times higher than the expected Fort Nelson CCS project operating pressures.

The results of the Fort Nelson Cap Rock Petrographic Analysis – July 2011 along with Weatherford's Energy Reservoir Engineering study begin to provide confidence that Fort Nelson cap rocks will serve as a competent vertical seal for the injection of sour CO_2. However further testing and characterization the Muskwa and Fort Simpson Formations must be done at a larger scale to determine the presence and condition of fractures and faults that may exist in those formations in the Fort Nelson area.

Potential Storage Reservoir Results

Together, the Sulphur Point and Upper Keg River Formations appear to have sufficient porosity, permeability, and lateral continuity to serve as zones for large-scale injection of CO_2 in the Fort Nelson area. These reservoirs together with the Slave Point are the principal storage reservoirs in the project area. Using the c-61-E well, SET ran a suite of well logs and also attempted to collect core from the Slave Point, Sulphur Point, and Keg River Formations to evaluate the characteristics of the potential reservoir storage formations. The core recovery was incomplete for the Slave Point, Sulphur Point, and Upper Keg River Formations because of the presence of vugs and fractures. Available core and cuttings samples were used to conduct a suite of analytical studies to evaluate the mineralogical, geochemical, and permeability properties of the potential reservoirs. Specific laboratory analyses included XRD, XRF, QEMSEM, and SEM–EDS for mineralogical and geochemical evaluations. Laboratory-based permeability testing could only be conducted on rock samples representing the Slave Point because not enough core was recovered from the Sulphur Point or Keg River Formations. Field-based drillstem tests (DSTs) were also conducted on several porous sections within the Slave Point, Sulphur Point, and Keg River zones of Well c-61-E to evaluate injectivity.

The following summarizes the characteristics of the Presqu'ile reef carbonate section and the related potential sinks that were found to occur at the c-61-E well location:

- The c-61-E well encountered a 346-meter-thick reef complex comprising:
  - 103 meters of Slave Point – primarily dolomite which has a porous and permeable section into which the well began to lose drilling fluid, which is indicative of high permeability.
  - 5-meter-thick Watt Mountain – tight silty dolomitic mudstone, which will serve as a baffle, but not necessarily a seal, for upward migration of CO_2.
  - 42 meters of Sulphur Point – fractured vuggy dolomite, into which the well lost drilling fluids, indicating significant permeability. Because of large vugs, core was unobtainable.
  - 129 meters of Upper Keg River – dolomite reef with some porosity.

The c-61-E test well penetrates three potential reservoirs upon which SET conducted DSTs. These in situ tests provide valuable data that can be used to estimate the permeability and injectivity of a reservoir. DSTs were conducted on the Slave Point, Sulphur Point, and Keg River intervals of the exploratory well. The key results of the DSTs are summarized below:

- Slave Point Formation:
  - A net effective pay thickness of 28.5 meters.
  - The radius of investigation was approximately 145 meters.
  - Permeability to water of 48 mD.
  - Results implied a reservoir of moderate permeability.

- Sulphur Point Formation:
  - A net effective pay thickness of 22.1 meters (8.1% porosity).
  - Permeability to water of 572 to 797 mD.
  - Radius of investigation was approximately 66 meters.
  - Results implied a reservoir with excellent permeability.

- Keg River Formation:
  - A net effective pay thickness of 12.3 meters (6% porosity).
  - Permeability to water of 24 to 42 mD.
  - Radius of investigation was approximately 186 meters.
  - Results implied a reservoir of moderate permeability.

The results of the exploratory drilling program, in situ testing, well log analyses, water injection test and subsequent analyses of core and cuttings from Slave Point, Sulphur Point, and Upper Keg River Formations provide substantial evidence that those formations have sufficient porosity/thickness (storage capacity) and permeability (injectivity) to serve as sinks for the Fort Nelson CCS project.

Current Understanding of Structural Elements

The current understanding of the structural elements of the Fort Nelson CCS project area is based on the synthesis and evaluation of historical 2-D and 3-D seismic survey data, well log data from a total of 96 wells (29 of which penetrate the Sulphur Point Formation), test well information, all DST information available within the project study area, cross sections, and review of facies determinations from core, cuttings, and well logs. The parts of the study area for which 2-D and 3-D seismic data were available are shown in Figure 9, while Figure 10 is a map showing the locations of the 96 wells for which well log data were available. Based on this information and utilizing a barrier reef depositional environment as the overall framework for the system, structure maps were developed for the top of each formation in the reef from the top of the Fort Simpson shale to the Chinchaga. Other structural features that have been identified include the presence of hydrothermal sags and a fault/graben system that cuts in a north-south trending direction across the reef front approximately 1 km west of c-61-E. Figure 11 presents a structure map for the top of the Sulphur Point Formation in the vicinity of c-61-E in which hydrothermal sags and the fault/graben system can be clearly identified.

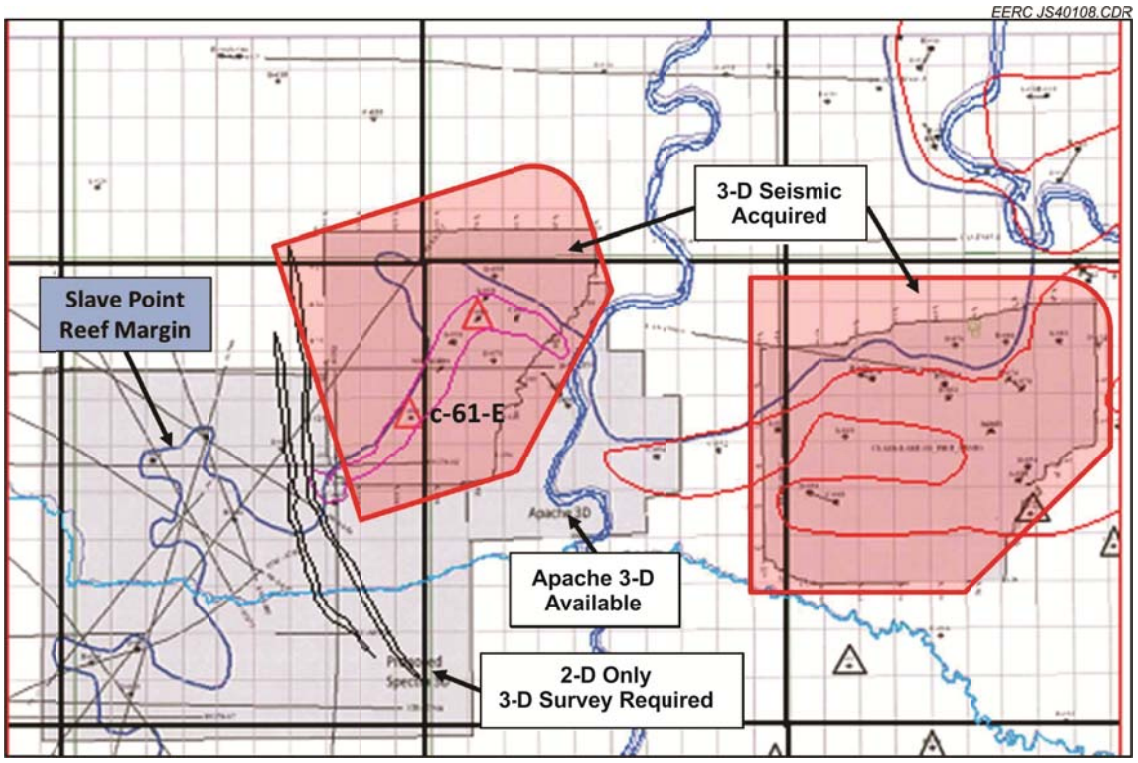

Figure 9. Acquired and available seismic survey locations within the Fort Nelson study area.

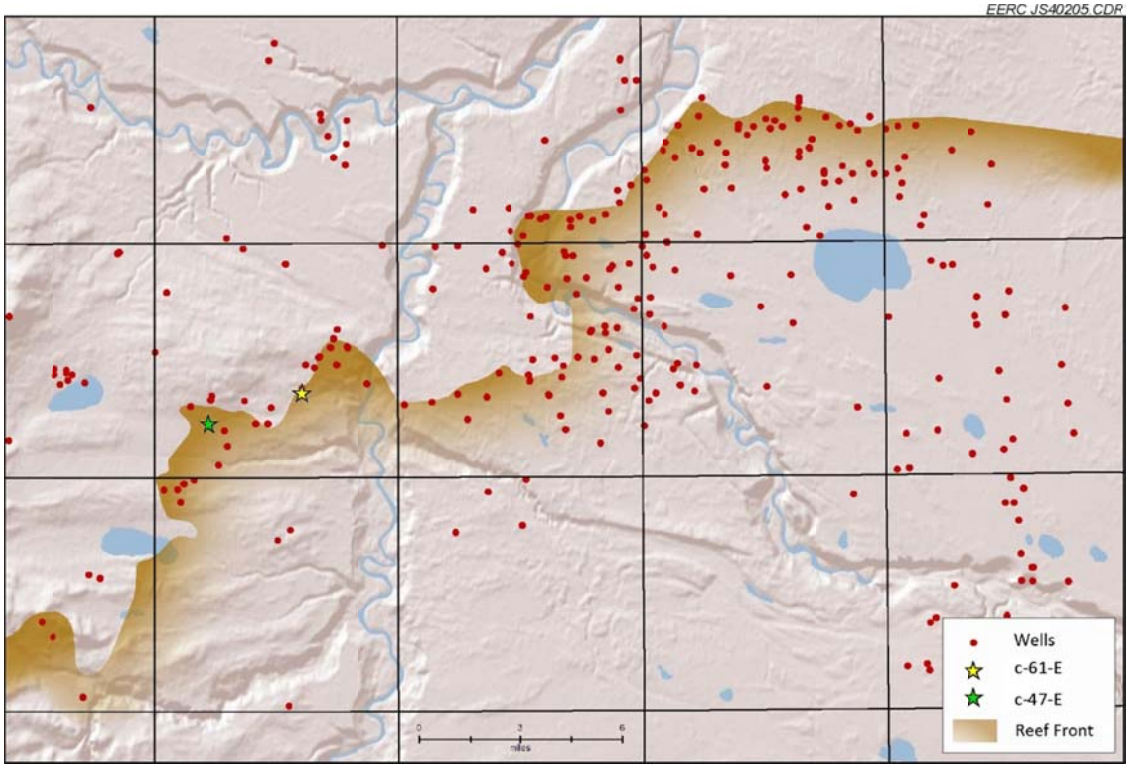

Figure 10. Location of Fort Nelson CCS project area surrounding wells.

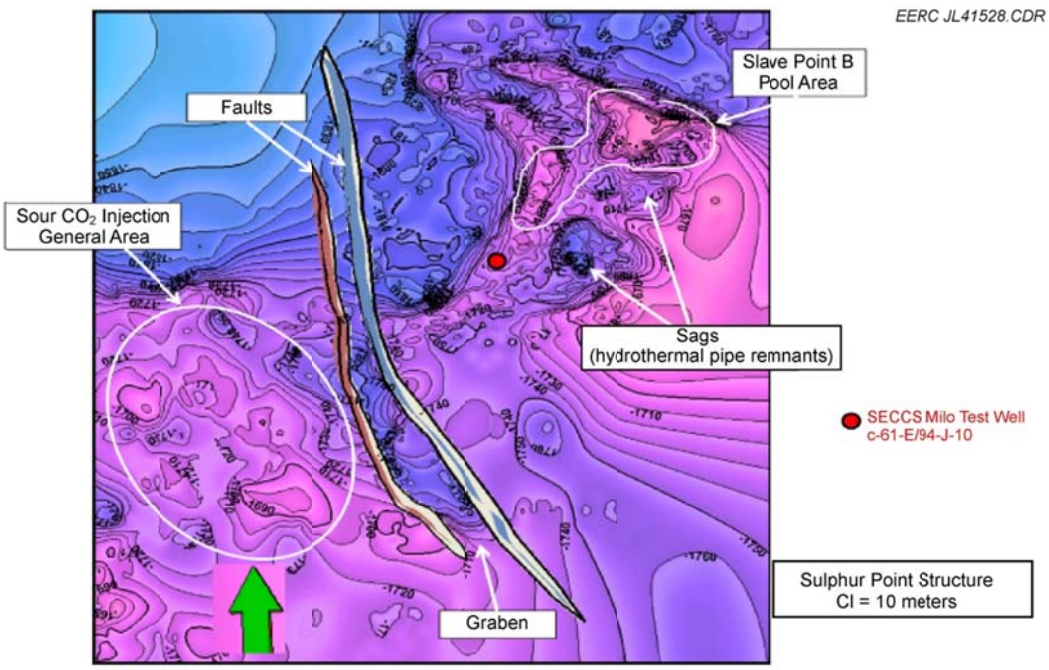

Figure 11. A structure map of the top of the Sulphur Point Formation in the vicinity of the c-61-E well.

The structural interpretations for the reef were integrated along with porosity and permeability distribution interpretations to create static geologic models for the Fort Nelson CCS project area. Figure 12 shows a cross-sectional example from west to east taken from the base-case version of the static model. This cross section illustrates the structural complexity that exists within the Presqu'ile reef complex in the Fort Nelson area. Within the cross section, the fault/ graben system and at least two sag features can be clearly identified. It is worth noting that Figures 11 and 12 are example images that only provide insight to very specific parts of the reef complex. The properties of the rock units and structural elements within the static models are populated in three dimensions, and any given vertical cross section will reveal different aspects of the stratigraphy and structural features. It is also important to bear in mind that the precise locations of features and distribution of rock properties are largely based on the interpretations of a team of geologists, geophysicists, and reservoir engineers, and such interpretations inherently include a degree of uncertainty. Relative to a commercially operated oil or gas field, the amount of seismic and well-based data available for the Fort Nelson CCS project area is sparse, and the level of uncertainty associated is related to the lack of data at this stage of the investigations. The acquisition of additional data is necessary to reduce the uncertainty associated with the current knowledge of the Presqu'ile reef in the Fort Nelson area.

Current Understanding of Hydrogeological Regime and Reservoir Communication

In 2008, SET commissioned a thorough study of the hydrogeological regime in the Fort Nelson area (Burnie, 2010). The results of that study provide valuable insight into the nature of fluid flow into and within the Presqu'ile reef complex. The key findings of that study relative to

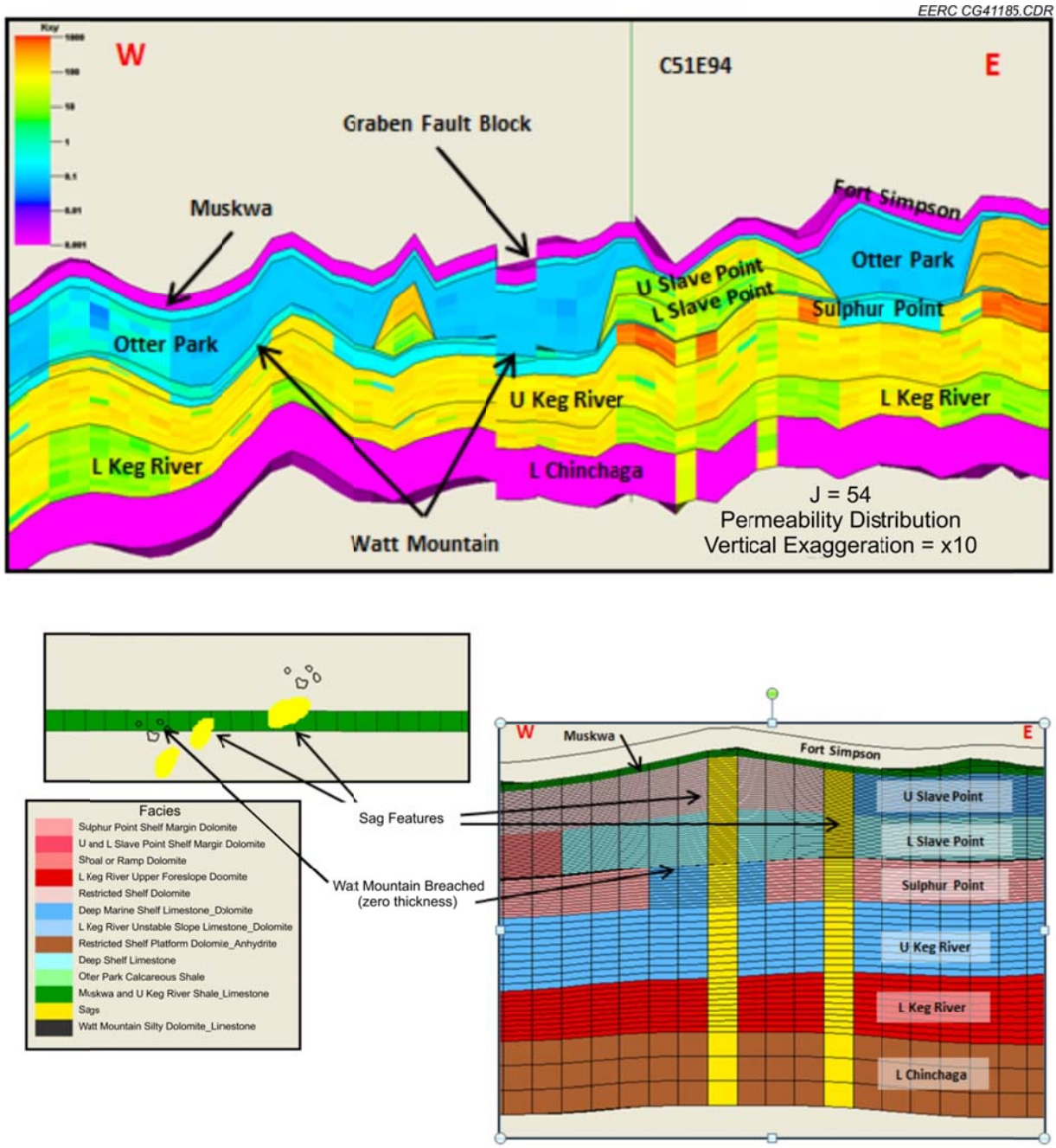

Figure 12. Fort Nelson CCS project area static model cross section.

the Fort Nelson CCS project are discussed below in the context of characterizing the nature and extent of hydraulic and pressure communication between the various rock units of the sink–seal system.

In the Fort Nelson CCS project, the current design calls for injection and storage of sour CO_2 into either the Sulphur Point or Keg River Formations. The high permeability and great

extent of these formations will accommodate the injected sour CO_2, specifically facilitating pressure dissipation and the movement of the in situ brine away from the point of injection. The other factor that controls the movement of injected sour CO_2 is bed dip and the related factor, buoyancy. By injecting lower in the reef, in the Sulphur Point or Keg River Formations, the sour CO_2 will tend to migrate vertically and structurally updip, as permitted by permeability and fractures. The following discussion looks at evidence for vertical and lateral communication within the reef for three important reasons:

- Likely the Slave Point and Sulphur Point are connected within the area (partially separated by the discontinuous Watt Mountain), as a result the injected sour CO_2 will, at some point, migrate upward into the Slave Point where the Watt Mountain is thin and/or fractured. The overlying seals (Muskwa/Fort Simpson shales) will, for the most part, contain the buoyant movement of the injected fluid and force it to migrate updip to structural highs where it could be trapped.

  Likely all of the reservoirs in the reef complex are connected, and consequently, an extensive brine-saturated hydrogeological system exists in the deep subsurface, which will facilitate pressure dissipation for the large volume of injected sour CO_2. Understanding the nature of pressure dissipation would be beneficial to the Fort Nelson CCS project from both an operational and regulatory perspective.

- As there is remaining Slave Point gas production along the reef complex, principally the Clarke Lake Slave Point A gas pool, it will be important not to contaminate the pools with injected sour CO_2 or adversely impact offsetting operations with a pressure increase from the Fort Nelson CCS project. Therefore, it is important to establish the extent of any connectivity along the reef to the gas pools which are currently under production. Contamination of the current production or altering the current pressure profile in the producing areas is a risk that can be managed by careful selection of injection sites and appropriate monitoring to allow for mitigation techniques.

Flow Within the Presqu'ile Reef and Communication Between Formations

As part of the Fort Nelson characterization activities, a head map was constructed for the Presqu'ile reef hydrogeological system in order to interpret the brine flow pattern. The head values were calculated according to Hubbert (1940) and include only head values from hydrogeological tests or wells with short gas columns and from data that are distant in time/ location from major production at the Clarke Lake Slave Point A and Clarke Lake Slave Point B pool and that are outside the pressure transient from the production area. Figure 13 shows the resulting head map for the Fort Nelson project area prior to any major gas production. The contouring was done independently from knowledge of the bank edge, and as a result, the close grouping of contours at the northern edge of Figure 13 only partially follows the bank edge. The widely spaced contours on the western edge of the head map reflect flow from the recharge area in the mountains to the west.

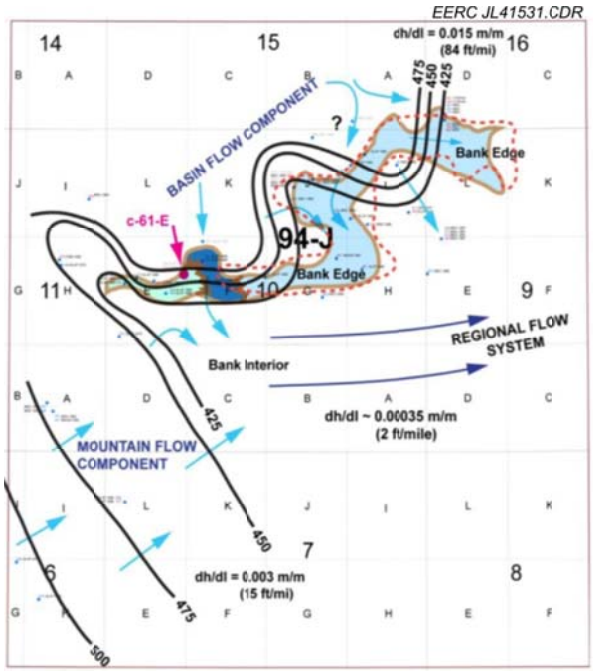

Figure 13. Local Fort Nelson CCS project area head map (modified from Burnie, 2010).

Flow in the system, indicated by the blue arrows in Figure 13, is perpendicular to the contour lines and from higher head values to lower head values. The direction of flow is southward from the Keg River platform underlying the shale basin toward the Middle Devonian carbonate bank and from the southwest to the northeast along the bank interior. There is little data control in the bank interior, but the few head determinations suggest a very slow natural in situ brine flow (on the order of a few centimeters per year) in the Fort Nelson CCS area. The head gradient varies from average to the southwest (15 ft/mile) to moderate (84 ft/mile) along the higher permeable bank edge. This natural brine flow will have some influence on the injected sour CO_2 in the postinjection phase along with other factors such as buoyancy and the various trapping mechanisms.

In addition to understanding the natural brine flow in the Middle Devonian reef, there is another strong influence on flow within the reefal system, and that is the pressure drawdown in the local Fort Nelson CCS project area because of gas production. Just to the east of the proposed CO_2 injection area is the major Clarke Lake Slave Point A gas pool which has been in production since 1961 and has produced just over 1.69 Tcf (47,741,279 m^3) of raw sour gas and just under 226 million barrels (35,930,557 m^3) of formation water. The operator injects the produced formation water back into the Slave Point and Sulphur Point Formations underlying this gas cap.

Current understanding of the impacts of historic gas production on the pressure profile of the Presqu'ile reef complex in the Fort Nelson area is illustrated in Figures 14 and 15. Figure 14 shows initial pressure distribution in the reef before gas production and produced water disposal injection operations, while Figure 15 shows two interpretations (one based on actual

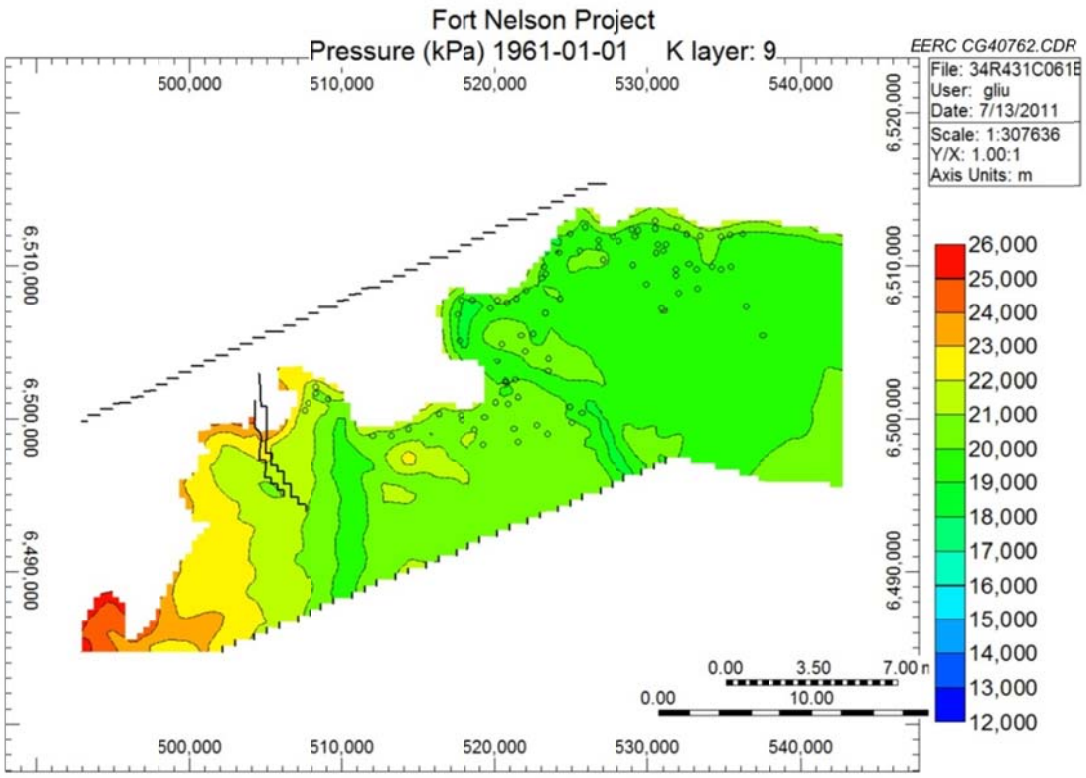

Figure 14. Pressure profile. Initial pressure before production and injection operations.

measurements and the other on simulations) of current pressure distribution within the reef. Comparison of these pressure profiles indicates that gas field production operations have resulted in a significant overall lowering of the pressure regime in the reef complex, which in turn further complicates the direction and magnitude of fluid flow in the Devonian system. There are two points to note here:

- The produced saline water is disposed of with no measurable pressure buildup on the injection well, indicating that the pressure in the underlying hydrogeological system is the regional pressures, which are all less than hydrostatic and define a regionally underpressured hydrogeological system. Also considering the large volumes of water that have been disposed of without significant pressure increases shows it to be a large, well-connected underlying aquifer in the reef.

- The removal of gas from the Slave Point A and B pools creates a cone of depression or a low-pressure area about the pools, particularly for the A pool, which widens and deepens with time. This low-pressure area will deflect the regional flow toward the producing pools.

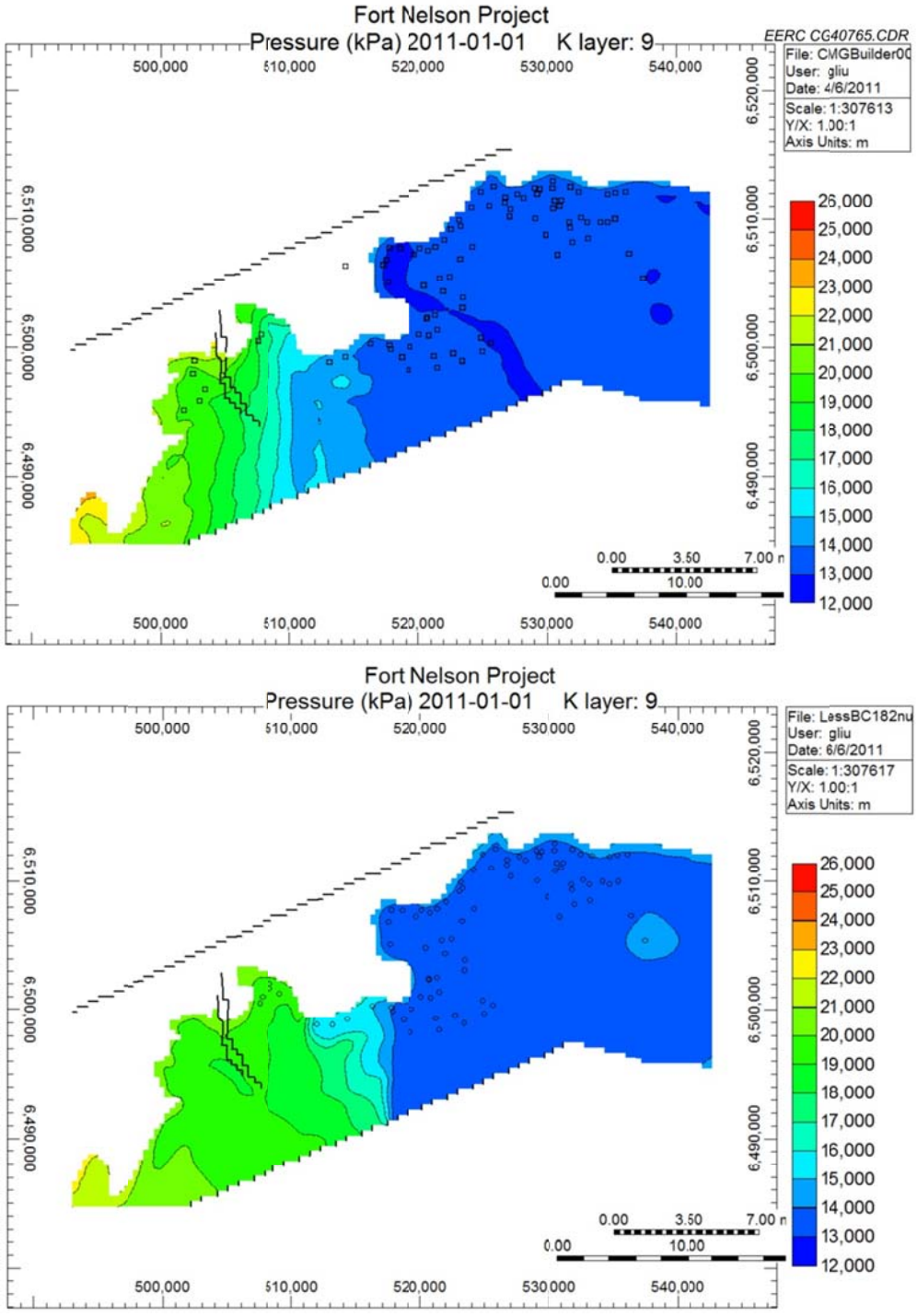

Figure 15. Pressure profile comparisons between measured distributions (top, after production but before injection operations) and simulation results (bottom, after history matching before injection operations).

Figure 16 (from Burnie, 2010) presents a pressure versus elevation plot for the wells along the reef edge. The graph shows the initial pressure in the preproduction to early production phases of the Clarke Lake Slave Point A pool and then how the pressure has dropped over time. On the graph, the 2009 and 2010 pressures from the Spectra Test Well c-61-E and Sidetrack d-61-E have been plotted. These pressures are affected by drawdown from producing Slave Point pools some 15+ kilometers away. The plot of the pressures from the Spectra test wells also shows the impact of Slave Point gas production on the Sulphur Point and Keg River deeper hydrogeological systems, which indicates communication between all three hydrogeological systems over a large area.

There is only minor production from the Clarke Lake Slave Point B pool, which also has a small water disposal scheme in place; therefore, the main impact to flow in the Middle Devonian hydrogeological system in the Fort Nelson project area is production from the Clarke Lake Slave Point A pool. During injection at the Fort Nelson project site, the influence of the expanding cone of pressure drawdown, from the Clarke Lake Slave Point A pool, will tend to direct any sour CO_2 plume toward this gas pool. Consequently, it is vital to understand the brine flow pattern, taking into consideration the drawdown effects from Clarke Lake along with the key reservoir properties that impact plume migration (i.e., permeability, permeability trends, fractures, structure, and the buoyant properties of sour CO_2). These factors impact the choice of the early injection sites for the Fort Nelson CCS project that may have to be placed an appropriate distance from the currently producing pools with closer sites drilled only when these producing Slave Point gas pools become uneconomical.

Vertical and Lateral Communication Indications (c-61-E and d-61-E pressure data)

As part of conducting DSTs in the c-61-E well and injection testing at the Sidetrack d-61-E wellbore, pressure, temperature, and fluid data were obtained. Figure 17 presents a pressure vs. depth graph with the pressure data points identified by formation and by year (i.e., c-61-E is 2009, and d-61-E is 2010). Review of the information on the pressure depth graph indicates the following:

- The Slave Point and Sulphur Point pressure data show that they are on the same pressure gradient, suggesting vertical communication.

- The 2009 Keg River pressure point is very close to the 2009 Slave Point/Sulphur Point water line, so it may be in the same system/aquifer. The Keg River is likely connected to the Sulphur Point based on knowledge of the geology in that area, and the slight difference in pressure can be accounted for being within the margin of error of the pressure gauges or by slight differences in the flow paths and, hence, the potential/pressure field. Based on this knowledge, it is possible that the Sulphur Point and Keg River may be parts of one extensive dynamic brine-saturated hydrogeological system.

- Pressure values from the 2010 data are slightly less than the 2009 pressures in both the Slave Point and Sulphur Point Formations by about 72 kPa. This pressure difference is significant, and it likely shows that the pressure decline because of production from the Clarke Lake Slave Point A pool has reached at least as far as the c-61-E location.

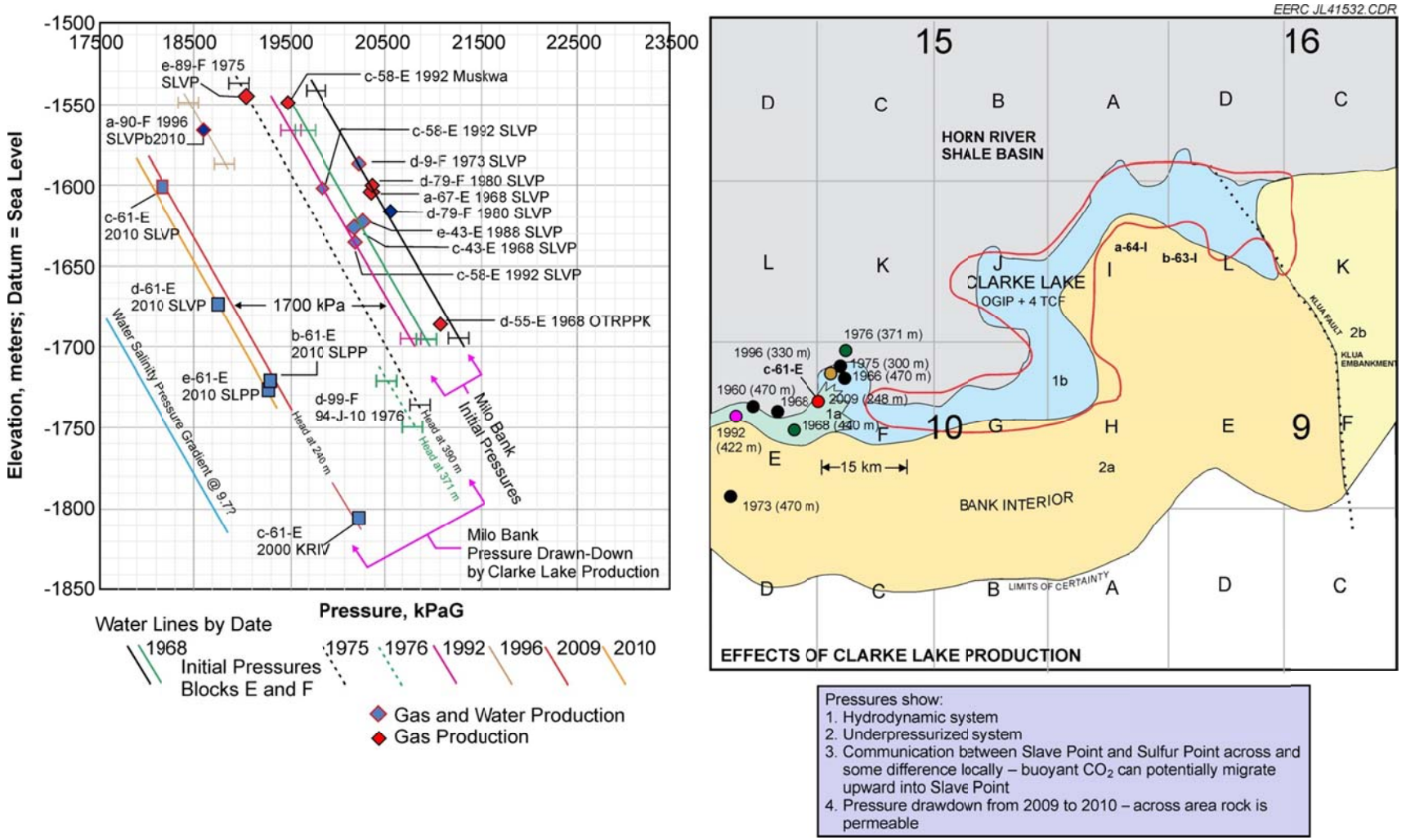

Figure 16. Fort Nelson Project brine reservoir communication (modified from Burnie, 2010).

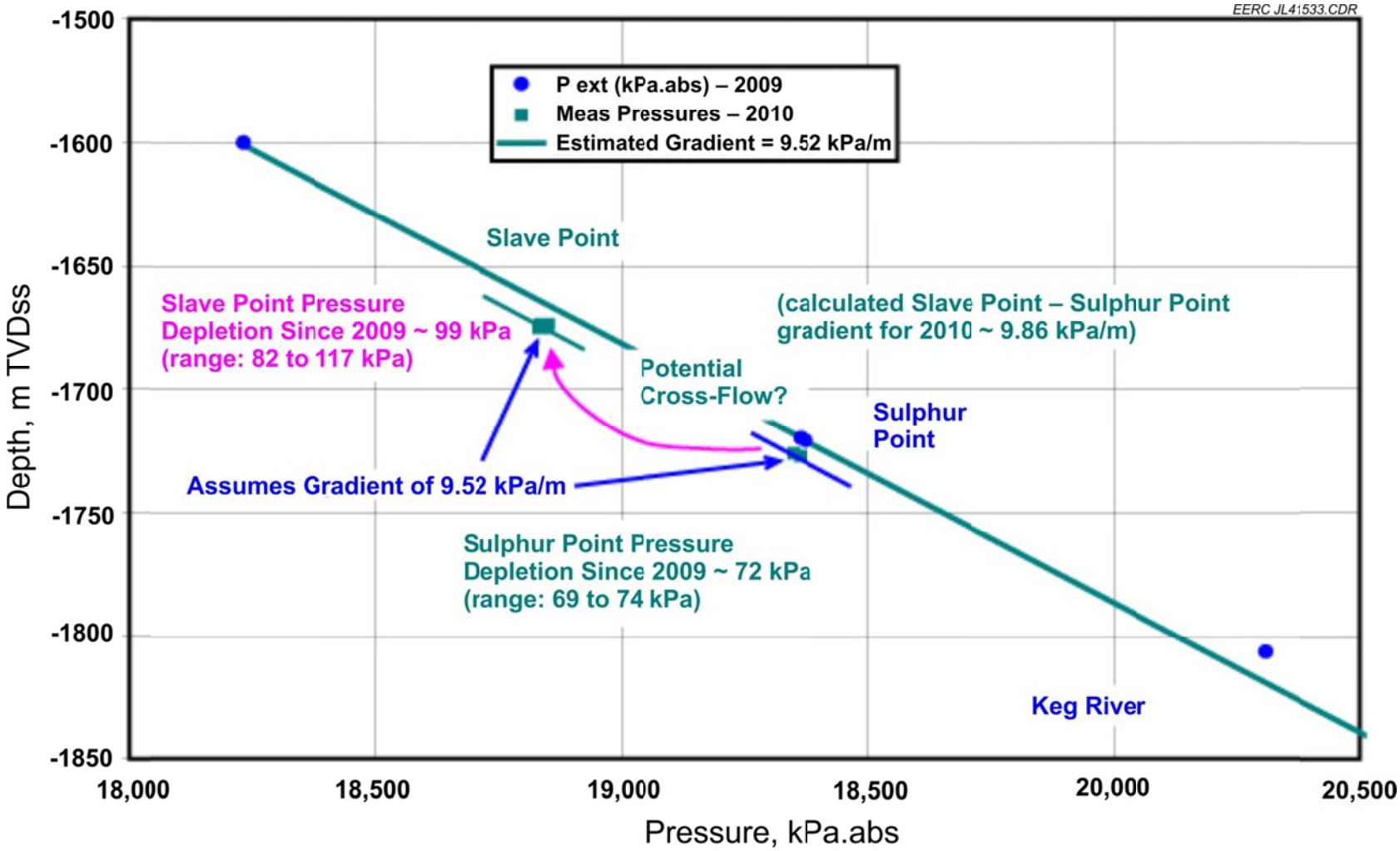

Figure 17. Pressure/depth plot (c-61-E well and sidetrack well); modified from Burnie (2010).

- Clarke Lake Slave Point A pool production effects have reached at least as far as the c-61-E location. This means that there is connectivity in the Slave Point and Sulphur Point reservoirs from the c-61-E location across the Fort Nelson project area to this producing pool. In addition, it shows there is communication between Slave Point and Sulphur Point Aquifers because the production at the Clarke Lake A Pool is from the upper Slave Point. For pressure to be drawn down in the Sulphur Point as well, it means that the two formations are in communication in this area. At this time, reservoir information in the lower Slave Point to Keg River is sparse, and on the western part of the Fort Nelson CCS study area, there is a lack of Sulphur Point and Keg River reservoir information as most wells were drilled only into the top part of the upper Slave Point.

- Review of the pressure data along with temperature data and spontaneous potential well log information suggests brine flow took place from Sulphur Point to Slave Point. The brine flow, however, is not large. It is believed that in the general vicinity of the c-61-E wellbore, the Slave Point and Sulphur Point, although connected regionally, are separated locally by a tight Watt Mountain Formation (i.e., petrophysical analyses on c-61-E sidetrack shows it is 4.8 m thick and has no effective net pay). This is understandable as the carbonate reef sequence is very heterogeneous in nature, so permeability connections will vary locally, but overall communication via various tortuous routes will occur. In the seismic interpretation and analyses to date, there are local features, such as sags and associated seismic character changes, that suggest a very thin or absent Watt Mountain in some areas of the Fort Nelson project area where seismic information exists. It is postulated that hydrothermal pipes or sags, seen as circular features on the seismic, penetrate through the Watt Mountain and other local aquitard layers. Also, the thin to absent Watt Mountain locations and small fractures may be potential avenues of vertical communication between the Slave Point and Sulphur Point reservoirs.

In summary, the evidence suggests that there is communication (laterally and vertically) across the Fort Nelson project study area in the Slave Point, Sulphur Point, and Keg River Formations. Locally, there may be separation depending on the areal extent and thickness of the Watt Mountain aquitard and the amount of fracturing and the degree of dolomitization of the interval between the Slave Point and Sulphur Point reservoirs. The reefal sequence between the Sulphur Point and Keg River has low permeability based on log porosities and limited core. However, intense dolomitization and fracturing are suspected to be common and have been identified in the c-61-E logs, making it likely that communication occurs between these two reservoirs. This is supported by the pressure data from well tests.

STORAGE CAPACITY

Having a thorough understanding of the storage capacity of a given sink is necessary to determine the long-term viability of a CCS project. Simply stated, a target injection zone may have adequate injectivity to support high rates of CO_2 injection, but if there are physical constraints that limit the sustainability of those injection rates, then that zone will have limited

storage capacity. Subsurface characterization data provide the basis for estimating storage capacity. Using much of the data described above, storage capacity estimates for the Slave Point, Sulphur Point, and Keg River Formations in the Fort Nelson CCS project study area were developed in late 2010. These estimates were based on the available geologic characterization data and modeling conducted prior to December 31, 2010. A description of the approach used to develop these storage capacity estimates and the results are presented as follows.

Void Replacement

A simple mass balance (i.e., void replacement) was performed by calculating the volume of fluids entering and leaving the Presqu'ile reef in the modeled area (2000 km^2), which includes the Clark Lake Slave Point A and B gas pools. Based on the volume of gas and water removed from the system, it was estimated that there is a CO_2 storage volume equivalent to approximately 137 million tonnes. This estimate was determined by adding up the total volume of gas and water produced from the Clark Lake Slave Point A and B gas pools and subtracting the volume of water injected back into the Presqu'ile reef in the modeled area. These volumes were converted to reservoir conditions using estimated formation volume factors for both the water and gas. The reservoir volume that was removed (i.e., the reservoir volume made available for CO_2 storage) from the Presqu'ile reef in the modeled area was then multiplied by the expected reservoir density of the injected sour CO_2 under the assumed reservoir conditions to yield 137 million tonnes of potential CO_2 storage (Table 1). Therefore, injecting 100 million tonnes of sour CO_2 into these formations over a 50-year period should not raise the regional formation pressure to the initial pressure, even if the system were closed (which it is not).

Pore Volume Estimates

In addition to the void replacement calculations, it is estimated that the pore space in the Slave Point, Sulphur Point, and Keg River Formations combined exceeds 29 billion m^3. This pore volume was determined by estimating the pore volume in the formations from the reservoir model, without consideration of the produced fluids; i.e., pore space is the product of the area, thickness, and porosity of the formation. Since it is known that the pore space is full of formation fluids, only a portion of this "pressure space" is available for CO_2 storage. From the literature (IEA Greenhouse Gas Programme, 2009; U.S. Department of Energy, 2010), it is reasonable

Table 1. Simple Mass Balance (i.e., void replacement) CO_2 Storage Capacity Estimate

	Standard Conditions, m^3	Reservoir Conditions,* m^3	CO_2 Mass,** tonnes
Gas Produced	50,344,931,159	326,000,000	135,000,000
Water			
Produced	39,456,222		
Injected	34,183,587		
Net Water Produced	5,272,635	5,000,000	2,000,000
Total Voidage Created by Production Operations		331,000,000	137,000,000

* Conversion to reservoir volumes was done using a formation volume factor of $B_g = 0.00648$ for natural gas and $B_w = 1.04$ for formation water.

** A CO_2 reservoir density of 415 kg/m^3 (average CO_2 density in the reservoir) was used to calculate the CO_2 storage mass.

to estimate that 1% to 4% of the total pore space is available for an entire formation and an even higher percentage is available for a specific area within a formation. For the Fort Nelson site, a very conservative estimate of available pore space (1%–2%) was assumed in the assessment of the formation. On this basis, if the reservoir was not already depleted and injections were into a virgin reservoir, then 100 million tonnes of sour CO_2 would utilize less than 1% of the available pore volume in the study area. On the same basis, 2% of the pore volumes in the three permeable and porous formations in the study area are sufficient to store more than 240 million tonnes of sour CO_2 (Table 2).

Modeled Storage Capacity

Storage capacity was also evaluated and estimated using numerical simulation techniques. The results of the numerical modeling are presented and discussed in detail in Lin and others (2011), but key findings with respect to storage capacity are summarized as follows:

- In addition to voidage replacement and pore volume simulations of storage capacity, numerical simulations were also performed.

- After the model was history-matched, a three-well injection pattern simulation was run injecting ~2 million tonnes CO_2 a year for 50 years. Results show that 100 million tonnes was stored, only increasing reservoir pressure/injection pressure about 2000 kPa above initial pressures.

- Results were in good agreement with voidage replacement and pore volume estimation methodologies, further supporting the conclusion that the Presqu'ile reef in the Fort Nelson area is an excellent CO_2 storage site based on capacity.

SUMMARY OF KEY FINDINGS FROM SITE CHARACTERIZATION

The key findings from the characterization activities conducted as of May 2011 include the following:

- Sampling and analysis events in May 2009 and January 2010 provide baseline data for shallow groundwater quality in the area of Well c-61-E. Based on the results from those activities, shallow groundwater near c-61-E appears to have little variation in quality.

Table 2. Effective Storage Volume of the 2000-km^2 Study Area at the Fort Nelson CCS Site

Formations	Pore Volume, m^3	Storage Mass* (E = 1.00%), tonnes	Storage Mass* (E = 2.00%), tonnes
Slave Point	4,340,000,000	18,000,000	36,000,000
Sulphur Point	2,920,000,000	12,100,000	24,200,000
Keg River	22,200,000,000	92,100,000	184,200,000
Sum	29,460,000,000	122,200,000	244,400,000

* A CO_2 density of 415 kg/m^3 was used to calculate the storage mass (average CO_2 density in the reservoir).

- There are anywhere from 20 to 25 distinctly identifiable rock units present in the stratigraphic column of the Fort Nelson CCS project area. Multiple units above the Devonian age Presqu'ile reef complex have the potential to serve as either sinks or seals for CO_2 storage to impede upward of migration.

- The Slave Point, Sulphur Point, and Keg River Formations have been identified as being the most likely primary sinks for the Fort Nelson CCS project.

- The shales of the Fort Simpson and Muskwa Formations have been identified as being the primary seals for CO_2 storage.

- The Devonian age Watt Mountain Formation, which is an internal reef aquitard but whose occurrence is discontinuous in the Fort Nelson area, may locally serve as a baffle to upward migration of CO_2 from the underlying Sulphur Point Formation.

- The Debolt Formation has been identified as a formation of interest to the Fort Nelson CCS project because it is the first locally porous and permeable formation that occurs above the Fort Simpson shales of the primary seal. It will, therefore, likely be monitored for the first signs of CO_2 leakage outside the primary seal–sink system.

- The results of a variety of laboratory testing on samples of the Fort Simpson and Muskwa shales from c-61-E provide encouraging evidence that these formations will serve as competent vertical containment for the storage of sour CO_2.

- The results of the in situ testing of the exploratory c-61-E and subsequent d-61-E wells and subsequent analyses of pressure transients, from Slave Point, Sulphur Point, and Upper Keg River Formations indicate that those formations have sufficient injectivity to serve as storage reservoirs for the Fort Nelson CCS project.

- Seismic survey data and well log data from 96 wells indicate that structural complexity exists within the Presqu'ile reef complex in the Fort Nelson area. Structural elements that have been identified include a fault/graben system west of c-61-E and multiple hydrothermal sag features. These structural elements can exert considerable influence on the mobility and fate of injected CO_2 and the dissipation of pressure from the reservoir.

- Hydrogeological evidence suggests that there is communication (laterally and vertically) across the Fort Nelson project study area in the Slave Point, Sulphur Point, and Keg River Formations.

- Compared to an oil or gas field, the amount of subsurface characterization data available for the Fort Nelson CCS project area is sparse. The acquisition of additional data is necessary to increase the confidence level in this reservoir for large scale CCS.

- Estimates of the sour CO_2 storage capacity of the Presqu'ile reef complex in the Fort Nelson CCS project area range from 100 million to over 240 million tonnes. These

results are supported by numerical predictive simulations based on a history-matched model indicating that 100 million tons can be injected in 50 years using three wells without increasing reservoir pressure above the maximum limit.

THE RELATIONSHIP BETWEEN SITE CHARACTERIZATION, MODELING, RISK ASSESSMENT, AND MVA AT FORT NELSON

The characterization data presented and discussed above provide the technical framework required to conduct the modeling, risk assessment, and MVA programs that are necessary for an effective and safe commercial CCS project. The collection and evaluation of characterization data and its integration with modeling, risk assessment, and MVA activities has occurred on an iterative basis since the earliest stages of the Fort Nelson CCS project. As of August 2011, the characterization data have been used as the basis for three rounds of modeling (presented in Liu and others, 2011), two rounds of risk assessment, the development of an MVA plan for the surface and shallow subsurface environment, and the initiation of the development of an MVA plan for the deep subsurface.

Planning for the next iteration of characterization activities is currently under way. The focal points for those activities will largely be determined by the nature of the risks that have been identified in the most recent risk assessment, which, in turn, will dictate the types of data that are necessary to address those risks. For example, risks related to the public perception of potential impact to shallow groundwater will lead to efforts to gather more baseline data on shallow groundwater quality from both existing and new shallow wells. Those baseline data in turn will be used to identify groundwater geochemistry parameters that will be best suited to providing an indication that leakage has occurred, thereby providing a basis for an important element of the surface and shallow subsurface environment MVA plan.

THE PATH FORWARD FOR FORT NELSON SITE CHARACTERIZATION

In keeping with the integrated, iterative approach to characterization, modeling, risk assessment, and MVA, the recommended path forward for characterization is based primarily on the findings of the most recent round of risk assessment activities combined with the expertise of the SET and EERC technical teams. While the results are encouraging that this is a good CCS site, more in-depth investigative work and further detailed technical analyses are warranted. Specifically, it is clear that drilling a new exploratory well and collecting additional data followed with detailed analyses will best support the next round of modeling, risk assessment, and MVA planning. It is anticipated that additional characterization activities will include a variety of laboratory and field-based investigations and detailed reservoir analyses. The results of all of that work will be reconciled and used to constrain input parameters for conceptual and predictive numerical modeling. The integration of the different components (laboratory tests, field observations, analyses, and numerical models) will provide a better understanding of the injection target reservoir and sealing units and will help in making safe and cost-effective site-specific operating decisions. The increased understanding of the target reservoir and sealing units

will also help constrain the likelihood of failure modes, thereby informing the project risk assessment and MVA plans.

REFERENCES

Bachu, S., and Adams, J.J., 2003, Sequestration of CO_2 in geological media in response to climate change—capacity of deep saline aquifers to sequester CO_2 in solution: Energy Conversion and Management, v. 44, p. 3151–3175.

Belyea, H., and Norris, A.W. 1962, Middle Devonian and older Paleozoic Formations of Southern District of Mackenzie and adjacent area: Geological Survey of Canada Paper 62-15, p. 76–79.

Bradshaw, J., Bachu, S., Bonijoly, D., Burruss, R., Holloway, S., Christensen, N.P., and Mathiassen, O.M., 2006, Storage capacity estimation—issues and development of standards: 8th International Conference on Greenhouse Gas Control Technologies, Trondheim, Norway, June 19–22, 2006.

Burnie, S., 2010, Hydrogeology of the Mid-Devonian carbonate back complex, Milo-Clarke area northeastern British Columbia. Unpublished report prepared for Spectra Energy, 54 p.

Hubbert, M.K., 1940, Theory of ground-water motion: The Journal of Geology, v. 48, no. 8, pt. 1, p. 785–94.

IEA Greenhouse Gas Programme, 2009, Development of storage coefficients for carbon dioxide storage in deep saline formations: Technical Study Report No. 2009/13, November.

Liu, G., Gorecki, C.D., Bailey, T.P., Saini, D., Braunberger, J.R., Sorensen, J.A., and Steadman, E.N., 2011, Fort Nelson Test Site—simulation report: Plains CO_2 Reduction (PCOR) Partnership Phase III Task 9 – Deliverable D67, 212 p.

Macauley, G., 1958, Late Paleozoic of Peace River area, Alberta, *in* Goodman, A.J., ed., Jurassic and Carboniferous of western Canada: American Association of Petroleum Geologists Allen Memorial, p. 289–308.

Peck, W.D., Botnen, B.W., Botnen, L.S., Daly, D.J., Harju, J.A., Jensen, M.D., O'Leary, E.M., Smith, S.A., Sorensen, J.A., Steadman, E.N., Wolfe, S.L., Damiani, D.R., Litynski, J.T., and Fischer, D.W., 2007, PCOR Partnership Atlas (2d ed.): Grand Forks, North Dakota, Energy & Environmental Research Center, 54 p.

Royal British Columbia Museum, 2011, Muskeg—what is it?: www.livinglandscapes.bc.ca/prnr/photo_journey/muskeg.htm (accessed September 2011).

Sorensen, J.A., Jensen, M.D., Smith, S.A., Fischer, D.W., Steadman, E.N., and Harju, J.A., 2005, Geologic sequestration potential of the PCOR Partnership region: Plains CO_2 Reduction

(PCOR) Partnership topical report, www.netl.doe.gov/technologies/carbon_seq/partnerships/phase1/pdfs/MDJ-Geologic%20Sequestration%20Potential.pdf (accessed October 15, 2007).

Stewart, S., and Bachu, S., 2000, Suitability of the western Canada sedimentary basin for carbon dioxide sequestration in geological media: Presented at the 2000 Canadian Society of Exploration Geophysicists Conference, August 6–11, 2000.

U.S. Department of Energy, 2010, Atlas, 3rd ed. www.netl.doe.gov/technologies/carbon_seq/refshelf/atlasIII/2010atlasIII.pdf (accessed May 2011).

APPENDIX A

FORT NELSON CAP ROCK PETROGRAPHIC ANALYSIS – JULY 2011

FORT NELSON CAP ROCK PETROGRAPHIC ANALYSIS – JULY 2011

Prepared for:

Dr. Ernie Perkins
Alberta Innovates Technology Futures

Prepared by:

Jordan M. Bremer
Corey D. Lindeman
Jonathan L. LaBonte
Benjamin W. Huffman
Alexander Azenkeng
Blaise A.F. Mibeck
Steven A. Smith
James A. Sorensen
Charles D. Gorecki
Edward N. Steadman
John A. Harju

Energy & Environmental Research Center
University of North Dakota
15 North 23rd Street, Stop 9018
Grand Forks, ND, 58202-9018

August 2011

DOE DISCLAIMER

This report was prepared as an account of work sponsored by an agency of the United States Government. Neither the United States Government, nor any agency thereof, nor any of their employees, makes any warranty, express or implied, or assumes any legal liability or responsibility for the accuracy, completeness, or usefulness of any information, apparatus, product, or process disclosed, or represents that its use would not infringe privately owned rights. Reference herein to any specific commercial product, process, or service by trade name, trademark, manufacturer, or otherwise does not necessarily constitute or imply its endorsement, recommendation, or favoring by the United States Government or any agency thereof. The views and opinions of authors expressed herein do not necessarily state or reflect those of the United States Government or any agency thereof.

NDIC DISCLAIMER

This report was prepared by the Energy & Environmental Research Center (EERC) pursuant to an agreement partially funded by the Industrial Commission of North Dakota, and neither the EERC nor any of its subcontractors nor the North Dakota Industrial Commission nor any person acting on behalf of either:

(A) Makes any warranty or representation, express or implied, with respect to the accuracy, completeness, or usefulness of the information contained in this report or that the use of any information, apparatus, method, or process disclosed in this report may not infringe privately owned rights; or

(B) Assumes any liabilities with respect to the use of, or for damages resulting from the use of, any information, apparatus, method, or process disclosed in this report.

Reference herein to any specific commercial product, process, or service by trade name, trademark, manufacturer, or otherwise does not necessarily constitute or imply its endorsement, recommendation, or favoring by the North Dakota Industrial Commission. The views and opinions of authors expressed herein do not necessarily state or reflect those of the North Dakota Industrial Commission

EERC DISCLAIMER

LEGAL NOTICE This research report was prepared by the Energy & Environmental Research Center (EERC), an agency of the University of North Dakota, as an account of work sponsored by the U.S. Department of Energy. Because of the research nature of the work performed, neither the EERC nor any of its employees makes any warranty, express or implied, or assumes any legal liability or responsibility for the accuracy, completeness, or usefulness of any information, apparatus, product, or process disclosed or represents that its use would not infringe privately owned rights. Reference herein to any specific commercial product, process, or service by trade name, trademark, manufacturer, or otherwise does not necessarily constitute or imply its endorsement or recommendation by the EERC.

TABLE OF CONTENTS

LIST OF FIGURES

Continued . . .

LIST OF FIGURES (continued)

LIST OF TABLES

EXECUTIVE SUMMARY

Petrographic assessment was performed on primary cap rock samples from the Fort Nelson area provided by Dr. Ernie Perkins of Alberta Innovates Technology Futures. The cap rock samples represent three intervals from Well C-61-E/94-J-10, corresponding to depths of 2030.4, 2042.11, and 2045.75 meters. The samples are dark gray to black pyritic, dolomitic shales that increase in hardness and degree of cementation with depth.

It is expected that the rock sequence in the area represents a brief regression from the productive carbonate reef-building time, leading to fluid enrichment and dolomitization. This was followed by a large-scale transgression that blankets the rocks under the thick Fort Simpson Shale. The rocks collected for analysis represent shale samples from above the reef complex that have received differential cementation because of hypersaline water (Meijer Drees, 2008).

A broad geochemical understanding of these samples is required to predict the cap rock integrity and reservoir security of large-scale acid gas injection. To collect geochemical and pertinent rock properties for the cap rock samples, the Energy & Environmental Research Center (EERC) submitted samples collaboratively between its Applied Geology, Analytical Research, and Natural Materials Research Laboratories, each with their own focus and expertise. In all, the following tests and measurements were performed:

- X-ray diffraction (XRD) for bulk mineralogy
- X-ray fluorescence (XRF) for trace element analysis
- Petrographic analysis via thin section for mineralogy and rock fabric descriptions
- QEMSEM (quantitative elemental mapping using scanning electron microscopy) for mineralogical mapping
- SEM with energy-dispersive spectroscopy for mineralogical identification and rock fabric descriptions
- Total carbon, hydrogen, and sulfur measurements for elemental composition information
- Surface area to determine reactive surface

- Skeletal density to support mineralogy and examination of total vs. effective porosity and degree of cementation

- Inductively coupled plasma–mass spectrometry (ICP–MS) to examine trace element abundance

Results from the various tests are shown to correlate well with one another, forming defensible conclusions regarding bulk and trace mineralogy and measured rock properties through several different methods and observations as follows:

- The cap rock intervals tested were found to be composed of a tight, dense collection of typically stable minerals.

- Bulk sample mineralogy, collected by XRD, QEMSEM, and thin-section analysis, is presented in Tables ES-1–ES-3. Mineralogy is supported by SEM images, XRF, and skeletal density measurements.

- Common trace elements and their relative percentages were collected by XRF and ICP–MS. These data are partially supported by SEM and CHN/S. Results for five trace metals from XRF (plus additional metals from Sample T-3) and the top 10 most abundant trace elements detected in ICP–MS for each sample are presented in Tables ES-4–ES-6.

- Rock property measurements and specifically measured elements including total porosity, effective porosity, skeletal density, total sulfur, total carbon, total hydrogen, and surface area are presented in Table ES-7.

While the testing and analysis were performed for the purpose of geochemical characterization, results may also be of additional use in petrophysical modeling, monitoring, verification, and accounting practices and other scientific and engineering aspects of the project.

Table ES-1. Mineralogy Report Summary for Sample TH-1, 2030.4 meters

	Common Mineral Phases							
Method	Illite	Kaolinite	Quartz	Carbonate	Pyrite	Feldspars	Apatite	Unit
XRD	47.0	ND[1]	41.6	1.8	7.0	0.8	ND	wt%
QEMSEM	74.9	6.65	6.21	1.38	8.14	0.53	0.08	% area
Thin Section	75		ND	15	10	ND	ND	% area

[1] Not detected.

Table ES-2. Mineralogy Report Summary for Sample T-1, 2042.11 meters

	Common Mineral Phases							
Method	Illite	Kaolinite	Quartz	Carbonate	Pyrite	Feldspars	Apatite	Unit
XRD	46.2	ND	40.9	2.7	6.5	2.5	ND	wt%
QEMSEM	75.83	6.37	6.59	2.50	3.71	0.99	0.05	% area
Thin Section	75		Trace	15	10	ND	ND	% area

Table ES-3. Mineralogy Report Summary for Sample T-3, 2045.75 meters

	Common Mineral Phases							
Method	Illite	Kaolinite	Quartz	Carbonate	Pyrite	Feldspars	Apatite	Unit
XRD	21.6	ND	31.0	41.1	3.5	0.6	ND	wt%
QEMSEM	16.11	3.96	12.91	46.65	4.04	3.90	0.08	% area
Thin Section	15		5	65	5	ND	ND	% area

Table ES-4. Trace Element Report Summary for Sample TH-1, 2030.4 meters

Method	Trace Elements										Unit
	K	Ti	Ba	Sr	Mn						
XRF	3.744	0.396	0.134	0.017	0.007						wt%
	Ti	Mn	Cr	V	Ni	Th	Ce	Cu	Gd	Y	
ICP–MS	1886	657	52.7	47.6	39.1	24.4	23.4	22.8	22.3	17.2	µg/g

Table ES-5. Trace Element Report Summary for Sample T-1, 2042.11 meters

Method	Trace Elements										Unit
	K	Mn	Ti	Ba	Sr						
XRF	3.943	1.780	0.640	0.140	0.008						wt%
	Ti	V	Ni	Cr	Mn	Zn	Ce	Cu	Th	La	
ICP–MS	3661	197.6	117.9	92.6	85.9	70.7	57.9	57.8	39.7	30.7	µg/g

Table ES-6. Trace Element Report Summary for Sample T-3, 2045.75 meters

Method	Trace Elements										Unit
	K	Cr	Ti	Mn	Ba	Y	Sr	V	Ni	Cu	
XRF	2.142	0.658	0.261	0.083	0.080	0.051	0.020	0.012	0.007	0.004	wt%
	Ti	Zn	V	Mn	Ni	Cr	Cu	Ce	Th	Pb	
ICP–MS	3473	266.7	202.0	167.0	101.8	92.1	76.8	46.9	42.0	31.1	µg/g

Table ES-7. Rock Property Report for Fort Nelson Cap Rock Samples

Sample	Skeletal Density, g/cm^3	Total Sulfur, wt%	Total Carbon, wt%	Total Hydrogen, wt%	Surface Area, m^2/g
TH-1	2.73	3.14	1.67	0.27	14.66
T-1	2.82	3.60	27.6	0.28	20.16
T-3	2.82	2.07	8.28	0.07	14.82

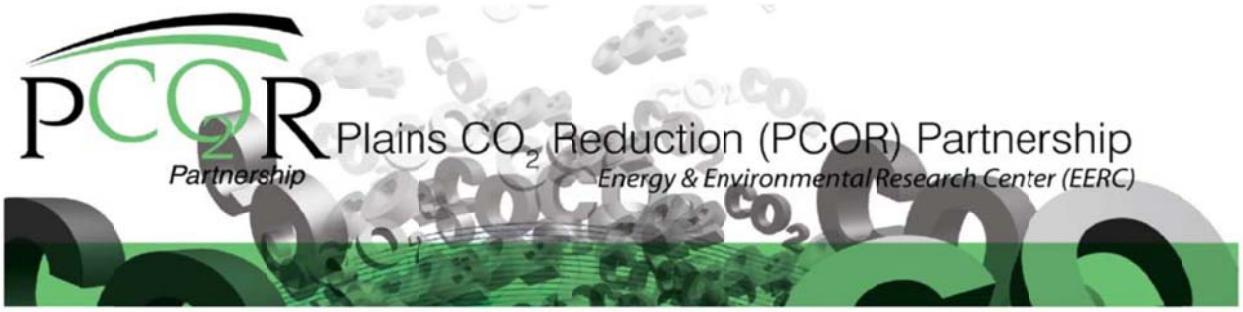

INTRODUCTION

The Energy & Environmental Research Center (EERC), through the Plains CO_2 Reduction (PCOR) Partnership, is working with Spectra Energy Transmission (SET) to investigate the feasibility of a carbon capture and storage (CCS) project to mitigate carbon dioxide (CO_2) emissions produced by SET's Fort Nelson Gas Plant (FNGP). The gas stream produced by the FNGP will include up to 5% sulfur dioxide (SO_2) and a small amount of methane (CH_4) and, as such, is referred to as a "sour" CO_2 stream. The sour CO_2 gas stream will be injected into a deep saline carbonate formation.

Over the past 50 years, exploration activities for mineral and energy resources in the area have yielded a significant amount of information about the geology of northeastern British Columbia and northwestern Alberta. The sedimentary succession in the Fort Nelson area consists, in ascending order from the Precambrian crystalline basement to the surface, of Middle and Upper Devonian carbonates, evaporates, and shales; Mississippian carbonates; and Lower Cretaceous shales overlain by Quaternary glacial drift and unconsolidated sediments (Figures 1–3).

With respect to formations that will prevent upward migration of the injected sour CO_2, shales of the overlying Middle Devonian Fort Simpson Group will provide the primary seal with respect to preventing leakage to the surface. The Mississippian-age Banff Formation, a carbonate formation that directly overlies the Devonian section in the northern portion of the Western Canadian Sedimentary Basin, is considered regionally to be an aquitard, thereby providing an additional seal between the target injection zones and the surface. Finally, the shales of the Cretaceous-age lower Fort St. John Group provide yet another layer of protection from leakage to the surface.

To gain a thorough understanding of the sealing capabilities of the Fort Simpson and Muskwa Shales, three samples were taken from cap rock intervals of the C-61-E test well core in January 2011 and delivered to the EERC shortly thereafter. Sample intervals were chosen by Dr. Ernie Perkins at a meeting of the geological team for the Fort Nelson project and are thought to represent a transition zone from the carbonate-rich reservoir into organic-rich shales with decreasing carbonate content. Table 1 shows the sample depths with their unique identification numbers as assigned by the EERC. The interval tags TH-1, T-1, and T-3 are used throughout this document to reference the samples.

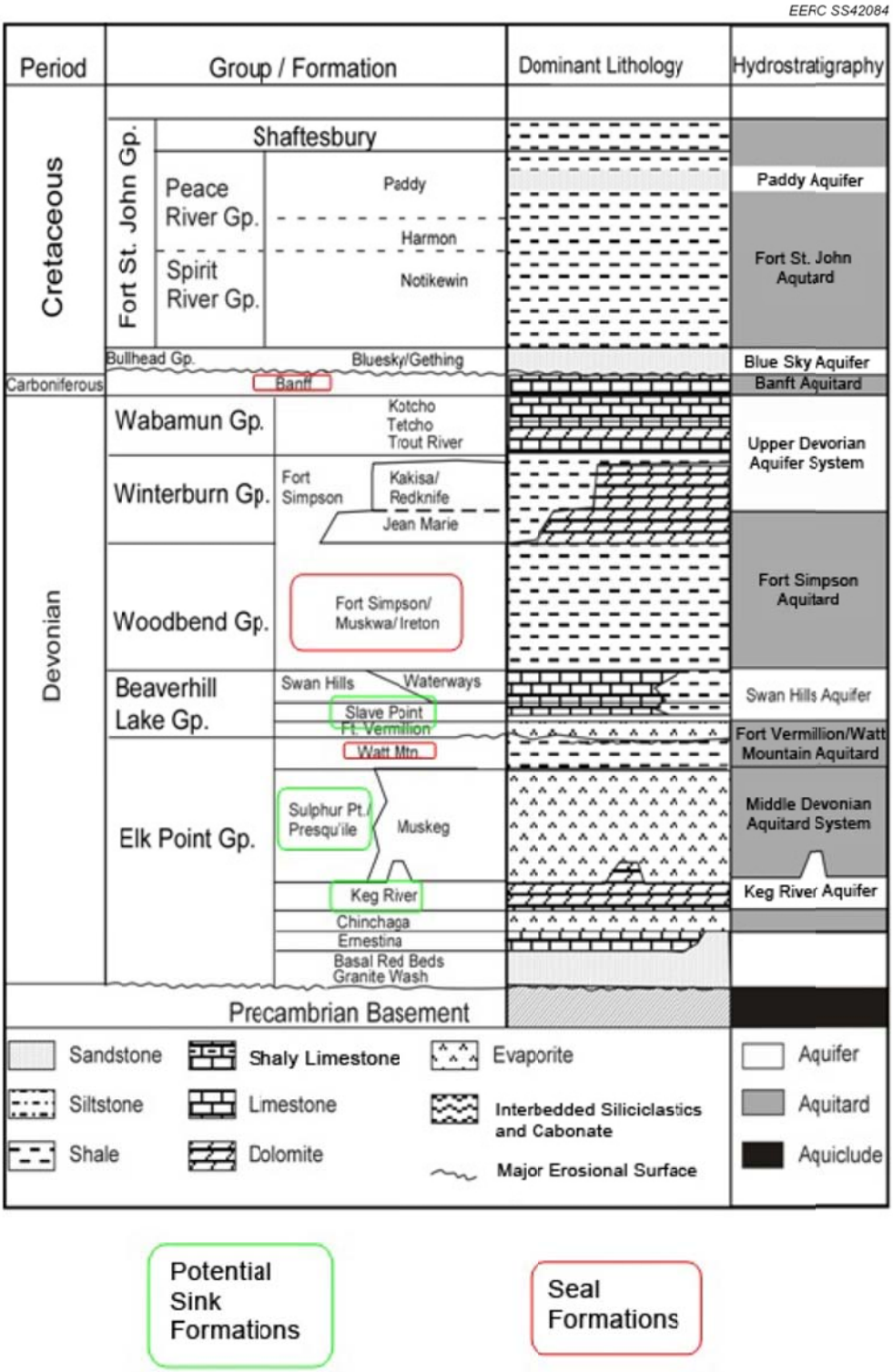

Figure 1. Stratigraphic and hydrostratigraphic delineation and nomenclature as well as general lithology for the northern part of the Alberta Basin, including northeastern British Columbia (from Gorecki and others, 2010).

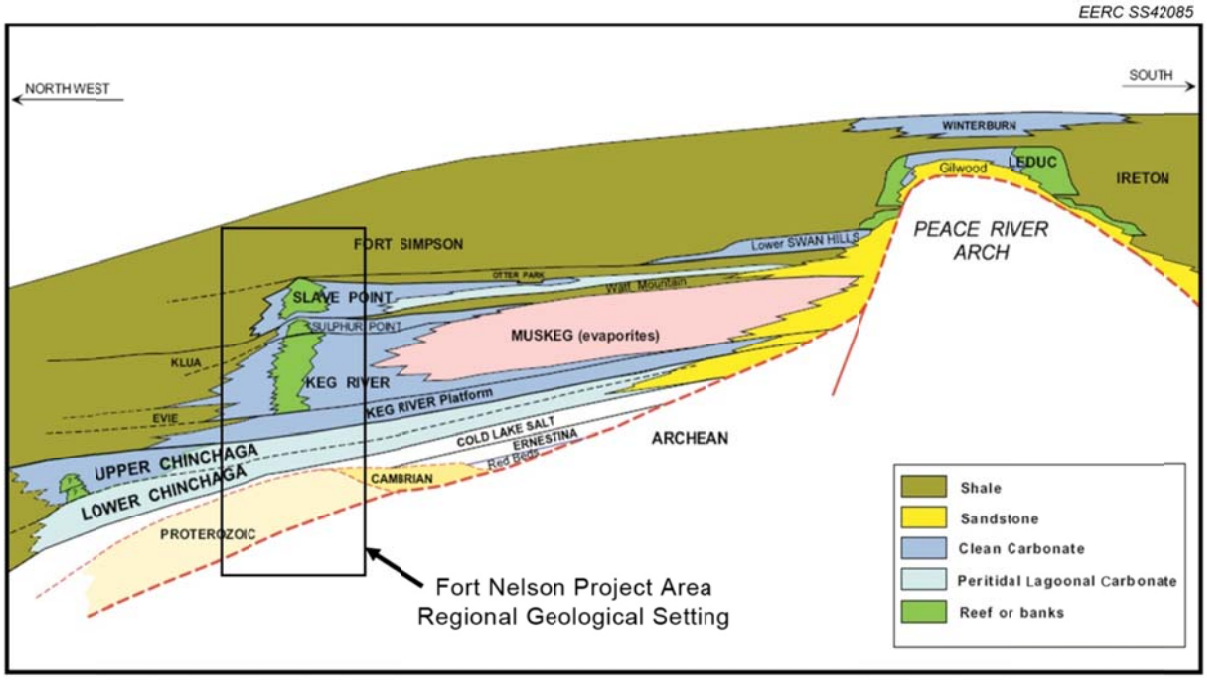

Figure 2. Stratigraphic architecture of the Middle Devonian formations in the Fort Nelson area, northeastern British Columbia (from Gorecki and others, 2010).

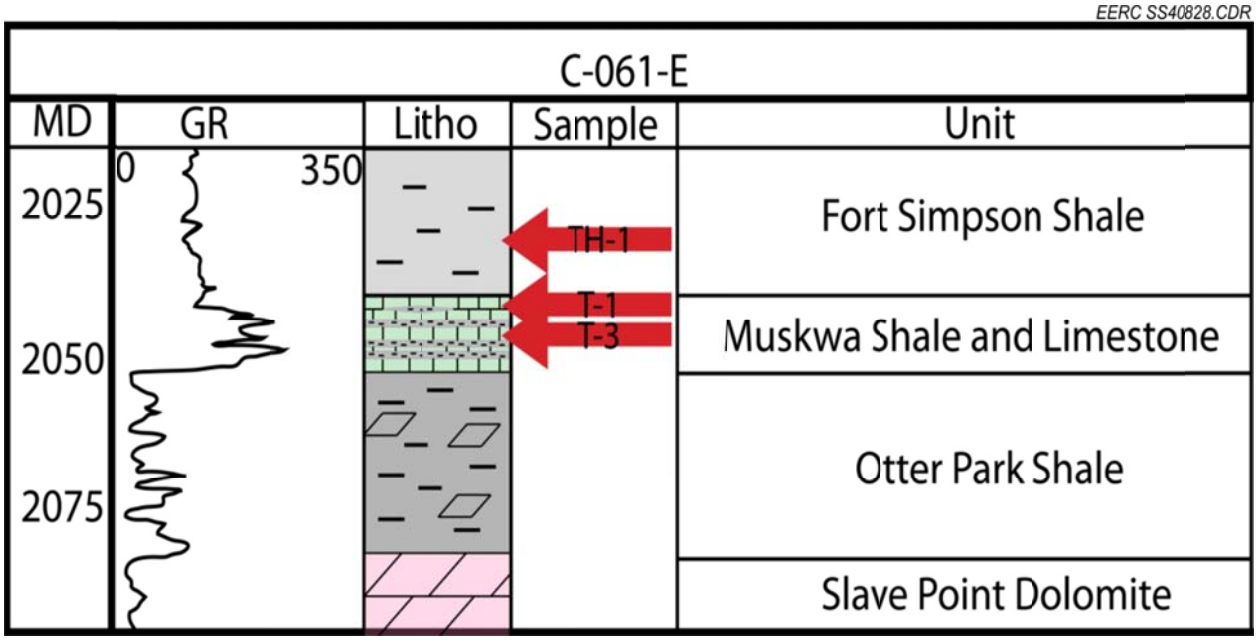

Figure 3. Gamma and lithology logs from Well C-061-E, with marked sample locations from the Fort Simpson and Muskwa Formations.

Table 1. Depth and Identification Information for Fort Nelson Cap Rock Samples

Depth, meters	Formation	Sample Designation	NMARL[1] No.	AGL[2] No.
2030.04	Fort Simpson	TH-1	10-0209	1663-019-02
2042.11	Muskwa	T-1	10-0208	1663-019-01
2045.75	Muskwa	T-3	11-0210	1663-019-03

[1] Natural Materials Analytical Research Laboratory.
[2] Applied Geology Laboratory.

It is expected that rocks in the area represent a typical shallow marine shelf setting that experienced a short-term marine regression, resulting in nearshore deposition of Muskeg salts in a restricted setting, followed by a larger-scale transgressive event. The deeper water was sufficient to bury the system in shale and organic material, which was preserved by anoxic conditions (Figure 4). High-salinity fluids were later expelled from the carbonate reefs during early-period compaction (and possibly later during hydrocarbon generation), leading to secondary mineralization surrounding the reservoir.

In order to facilitate a geochemical evaluation to be performed by Dr. Perkins, testing of these cap rock samples was performed at the EERC. Laboratory activities focused on quantification of mineral phases and elemental compositions, sample morphology and diagenesis, and rock properties.

This data set will be used to fully characterize cap rocks, with the goal of understanding potential rock–injected fluid reactions that may arise because of a variety of gas compositions that may exist over the lifetime of the Fort Nelson CCS project.

SUMMARY OF TESTING

Testing was conducted to collect a suite of mineralogic and lithologic data from the core samples provided (Figure 5). The testing was designed to minimize sample handling and, at the same time, produce the range of desired test methods. The analyses performed involved a suite of techniques that each provide their own unique view of the sample and output data.

- **Bulk mineralogy:** X-ray diffraction (XRD) techniques were employed on powdered specimens using a Bruker D8 Advance apparatus to attain bulk mineralogy.

- **Trace element detection:** X-ray fluorescence (XRF) techniques were employed on sintered, powdered specimens. Elemental signatures were collected and analyzed as weight percentages of oxide phases (if applicable) or anionic species.

- **Petrographic analysis**: Samples were mounted, cut, and polished to ~30 micrometers in thickness using water as the cutting fluid. Sections were analyzed and photographed using a petrographic microscope.

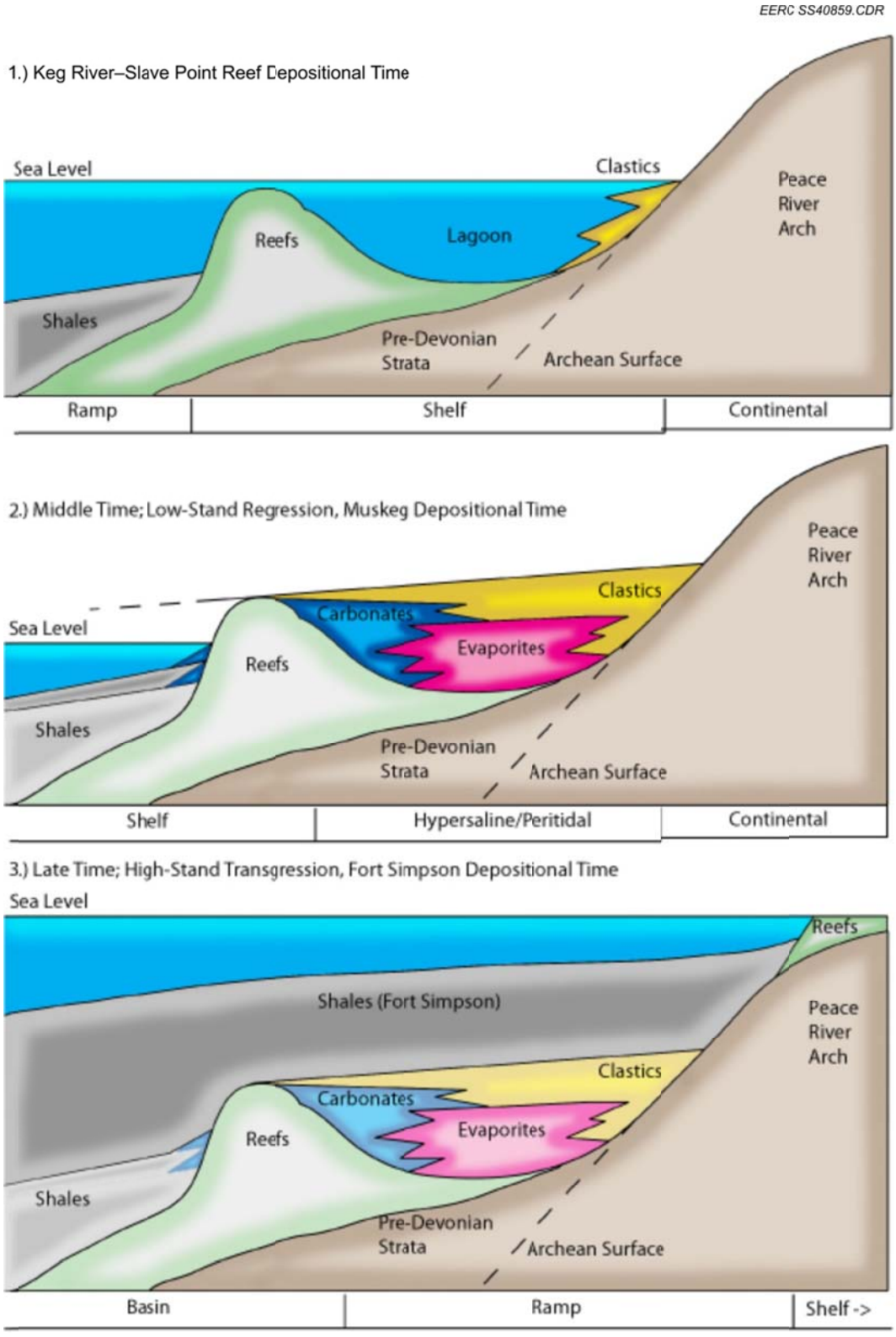

Figure 4. Illustration depicting the depositional history of the Keg River, Slave Point, and Fort Simpson Formations in the Fort Nelson area.

Figure 5. Photographs of Fort Nelson cap rock samples as received. These samples represent three cap rock intervals present in the Fort Nelson area.

- **QEMSEM** (quantitative elemental mapping using scanning electron microscopy): QEMSEM was used to collect backscatter electron and energy-dispersive spectroscopy (EDS) data two-dimensionally across a sample surface. This technique provides information pertaining to grain shape, mineralogy, location, and situation in the sample.

- **SEM**: High-resolution backscatter electron images were collected using a scanning electron microscope. EDS was also employed to examine specific points for elemental attributes, which aids in mineralogical identification.

- **CHN/S**: A carbon–hydrogen–nitrogen/sulfur (CHN/S) analyzer was used to determine the elemental prevalence of carbon, hydrogen, and sulfur within the sample.

- **Surface area**: A surface area analyzer was employed to measure a pulverized sample's surface area using gas adsorption.

- **Skeletal density**: Also known as grain density, skeletal density was measured using a helium pycnometer. The device measures the reduction of gas volume in the sample chamber caused by the presence of the rock sample.

- **ICP–MS/AES (**inductively coupled plasma–mass spectroscopy/atomic emission spectroscopy)**:** Elemental concentrations were measured for 32 trace metals, including rare earth, transition, lanthanides, and actinides.

ANALYTICAL RESULTS

Bulk Mineralogy by XRD

XRD was used to detect and identify crystalline phases of the shale samples provided for this evaluation.

For phase identification and Rietveld quantitative phase analysis (QPA), samples are prepared by reducing the specimen in a percussion mill followed by grinding into a powder using a micronizing mill. The sample is then dried and prepared as a randomly oriented powdered XRD sample. Crystalline phases are first identified using an automated search. After this, a Rietveld analysis is performed using whole-pattern general least-squares refinement to quantify mineral constituents.

For clay analysis, a decantation method first separates clay from silt. An oriented aggregate sample is made from the clay fraction to force platelike particles to lie flat, allowing the incident and diffracted beams to strongly interact with the [0 0 n] planes within the clay phases. XRD analysis of these low-angle reflections allows the direct observation of the spacing between these planes. The degree to which changes in spacing occur after the sample absorbs ethylene glycol is used to determine whether the clay has a smectite component. For a high concentration of clay sample, it is also possible to identify mixed-layer clays and to determine the ratio between illite group and smectite group layers by following procedures similar to U.S. Geological Survey (USGS) methodology (Środań, 1980; U.S. Geological Survey, 2001). The glycolation methodology flow chart that defines end member products is presented in Figure 6.

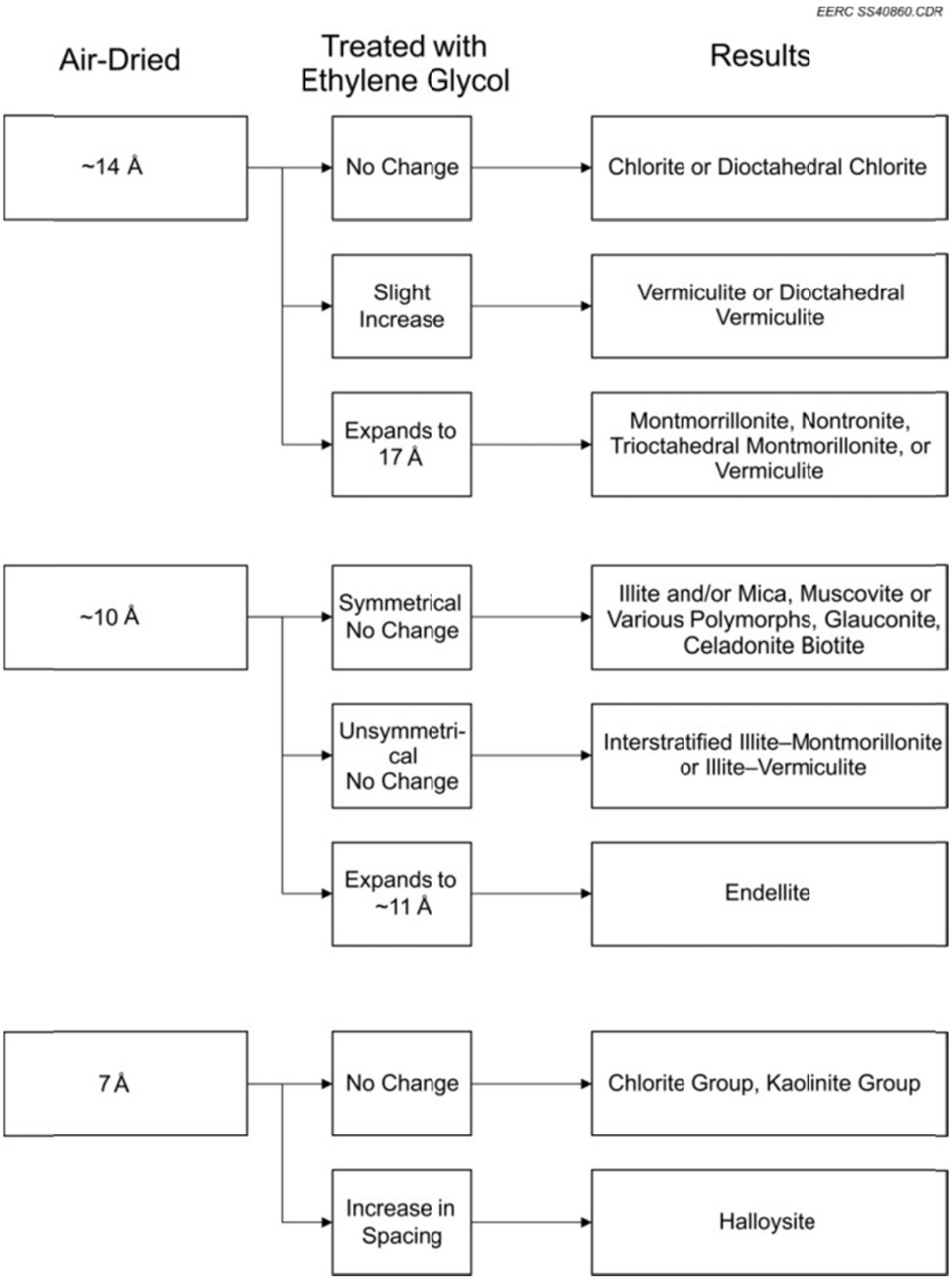

Figure 6. Flow chart showing defined clay assemblages identified through oriented glycolation methods.

For QPA, the Rietveld method is used to reduce the difference between a calculated diffraction pattern and the experimental data. Effects that normally detract from the quality of information from semiquantitative XRD, such as preferred orientation, instrument aberrations, and peak overlap can be accounted for using this method. Quartz was measured in higher quantities than were found through other methods (SEM, QEMSEM, XRF, and thin-section analysis). XRD is selective in measuring only phases that are crystalline. Chemical phases without long-range structure or comprising particles below several nanometers in size will appear amorphous and not yield a significant diffraction pattern. These phenomena are expected to affect clay detection and result in underestimation.

Key Observations

Relative weight percentages and XRD spectra were determined for prominent minerals in each sample and are reported in Table 2 and Figure 7. Quartz and clay were found to be the most common phases in these samples, followed by dolomite and ankerite, which were only prevalent in Sample T-3. Pyrite was a common accessory mineral in all three intervals, but was least common in Sample T-3. The remainder of detected phases represents a combination of clastic and chemical species.

- Nonswelling illite clay is thought to be the dominant clay type in the examined samples.
- Concentrations of swelling clays were found to be below detectable limits.
- Additional spectral images including glycolation scans are presented in Appendix A.

Table 2. Relative Weight Percentages of Identified Mineral Phases in Each Sample

	TH-1, 11-0209	T-1, 11-0208	T-3, 11-0210
Illite	47.0	46.2	21.6
Pyrite	7.0	6.5	3.5
Quartz	41.6	40.9	31.0
Sanidine $Na_{0.56}$	2.0	2.5	0.6
Anhydrite	0.0	0.0	0.0
Ankerite $Fe_{0.55}$	0.8	2.0	16.1
Dolomite	1.0	0.7	25.0
Ankerite $Fe_{0.7}$	0.0	0.0	1.9
Dolomite Disordered	0.0	0.0	0.0
Muscovite-2M1	0.4	0.5	0.2
Kaolinite (BISH)	0.0	0.0	0.0
Siderite	0.3	0.7	0.0
Goodness of Fit	1.67	1.77	1.47
R_{exp}	9.66	9.53	9.30

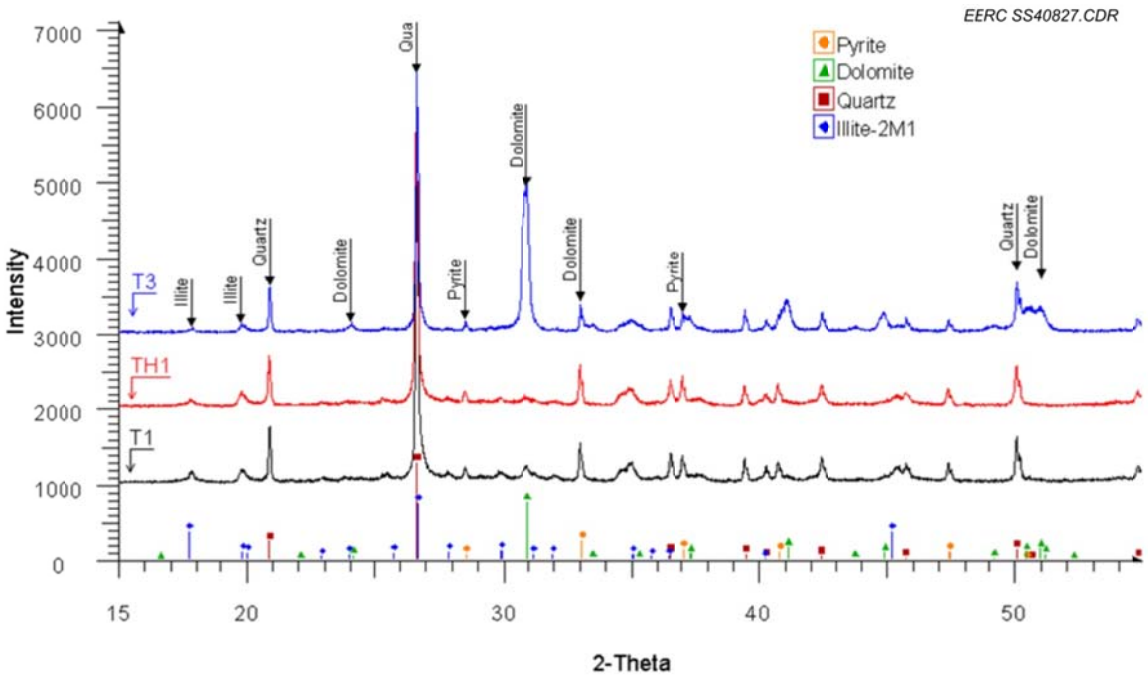

Figure 7. XRD patterns for Fort Nelson cap rock samples with annotated peaks for prevalent minerals detected through analysis.

- Other than quartz/clay portions, prevalence of other detected minerals is highly agreeable to results derived from QEMSEM/thin-section analysis.

- XRD results are thought to overestimate quartz and underestimate clay.

- Quartz was measured in higher quantities than were found through other methods (SEM, QEMSEM, XRF, and thin-section analysis) and is thought to be a product of oriented-aggregate sample preparation. This method of sample preparation settles the powdered sample onto a filter paper where less buoyant materials (pyrite, quartz, etc.) will be deposited before suspended clays, possibly causing preferential sampling of quartz present in the sample.

- Additional clay may have been lost in the amorphous background because of the small crystallite size.

Trace Element Analysis by XRF

XRF is a technique that provides the bulk elemental composition of samples. The device allows semiquantitative determinations to be made for elements with atomic numbers of 6 through 92 (carbon through uranium), with accuracies that can be attained to the ppm level (typical reporting to 0.1 wt%). Although XRF by itself cannot distinguish elemental arrangements, it excels at detecting products of trace minerals, elemental replacement, and small concentrations of elements.

Samples TH-1 and T-1 were processed through a typical routine that quantitatively analyzes 14 elements (reported as oxide weight percentages). Sample T-3 had a significant amount of material that was not included in ordinary analysis, and an additional 12 elements were semiquantitatively collected.

Only two elements were subject to shared analysis between XRF and ICP–MS, these being titanium and manganese. Titanium concentrations were found to be in agreement, with titanium decreasing with depth. Manganese concentrations are in disagreement between the two devices, with XRF reporting high manganese in Sample T-1, while ICP–MS methods detected this interval to have the lowest of the three samples. The cause of this disagreement is unknown. Additional semiquantitative analysis of T-3 overlapped nine elements with ICP–MS testing. Results appear to be in agreement for arsenic, zinc, copper, nickel, manganese, vanadium, and titanium. Discrepancies are apparent between the two device's measurements of chromium and yttrium. It is difficult to diagnose the cause of this difference, although it is expected that small sample size and low concentrations of these elements may have eluded XRF analysis.

Key Observations

Results of XRD testing are presented in Tables 3 and 4. The following observations were noted while analyzing results of XRF testing on Fort Nelson cap rock samples:

- Samples TH-1 and T-1 had low volumes (less than 2%) of unknown phases.
- Because of a high amount of unknown phases (9.5%) in Sample T-3, additional processing resulted in semiquantitative relative weight percentages of each phase present. Carbon was found to be a significant phase in this sample.
- Elemental signatures were highly similar between Samples TH-1 and T-1. A notable difference was observed, however, in manganese content.
- Significantly higher calcium and magnesium levels were detected in Sample T-3, indicating a higher concentration of dolomite. The previously noted significant carbon phase in this sample also supports this finding.
- A variety of trace metals are apparent in the samples, suggesting continental influx and/or hydraulic enrichment.

Table 3. Quantitative Common Oxide Weight Percentages for Fort Nelson Samples

	SiO_2	Al_2O_3	Fe_2O_3	TiO_2	P_2O_5	CaO	MgO	Na_2O	K_2O	SO_3	BaO	SrO	MnO	Cl	Total
TH-1	64.80	19.01	5.05	0.66	0.07	0.43	1.47	0.29	4.51	1.88	0.15	0.02	0.01	0.03	98.37
T-1	62.46	18.86	5.40	0.64	0.10	1.13	1.81	0.28	4.75	2.49	0.14	0.01	1.78	0.03	99.88
T-3	47.38	8.61	3.50	0.40	0.07	18.21	7.48	0.10	2.58	2.17	0.08	0.02	0.11	0.03	90.73

Table 4. Semiquantitative Report of Detectable Phases in Sample T-3

No.	Component	Result, wt%	Detection Limit, wt%
1	CO_2	17.0000	0.10406
2	F	0.1810	0.07410
3	Na_2O	0.1320	0.01012
4	MgO	8.0900	0.00990
5	Al_2O_3	8.9200	0.00685
6	SiO_2	37.2000	0.00882
7	P_2O_5	0.0874	0.00144
8	SO_3	3.3400	0.00290
9	Cl	0.0202	0.00243
10	K_2O	2.3900	0.00241
11	CaO	17.1000	0.00474
12	TiO_2	0.4350	0.00724
13	V_2O_5	0.0213	0.00689
14	Cr_2O_3	0.0137	0.00393
15	MnO	0.1070	0.02249
16	Fe_2O_3	3.1400	0.00332
17	NiO	0.0085	0.00175
18	CuO	0.0052	0.00146
19	ZnO	0.0030	0.00123
20	As_2O_3	0.0023	0.00119
21	Rb_2O	0.0079	0.00078
22	SrO	0.0164	0.00080
23	Y_2O_3	0.0064	0.00413
24	ZrO_2	0.0140	0.00084
25	BaO	0.0961	0.01857
26	C	1.6900	–

Petrographic Analysis

Optical petrography is a geologic technique that utilizes thin (approximately 30 micrometers thick) polished sections of rock to differentiate mineralogy and fabric within the sample. This type of analysis is often able to identify common mineral assemblages and estimate their prevalence as well as identify any microscopic structures or fractures present in the sample. Pore sizes may be measured and defined, and diagenetic events (including pore creation) may be inferred.

Thin sections of Samples TH-1, T-1, and T-3 were created using a standard thin-section mill to cut and grind the epoxy-mounted rock specimens. Samples were analyzed with a petrographic microscope utilizing plane-polarized, cross-polarized, and reflected light. Photomicrographs of the finished thin sections and complete descriptions are provided in Appendix B. Annotated photomicrographs showing representative areas of each interval are shown in Figures 8–10.

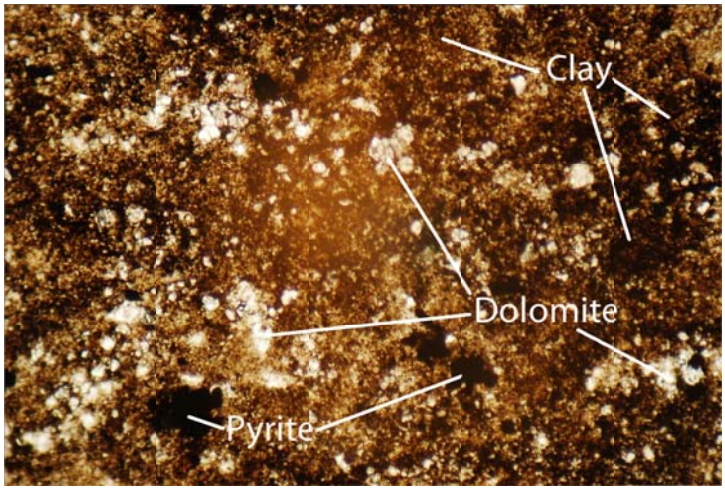

Figure 8. Photomicrograph of TH-1, plane-polarized light, 100× magnification.

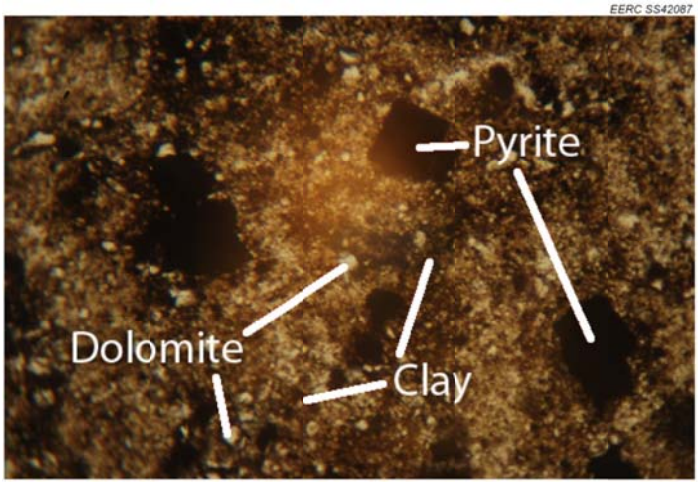

Figure 9. Photomicrograph of T-1, plane-polarized light, 100× magnification.

No dyes were used for thin-section production, which may be applied for various purposes such as carbonate typing or simplified porosity identification. As such, all carbonates were identified as dolomite based on observable rhombahedral shape. This was validated as dolomite in subsequent analyses of these samples. No point counts were performed on thin sections, as QEMSEM and scanning electron microscope data provide higher accuracy and precision in their measurements.

No porosity was observed during thin-section analysis, which is in disagreement with porosity measurements obtained during skeletal density measurements. This impasse is the result of the very fine microporosity in the samples, which, even at high magnification, does not become apparent in a ~30-µm-thick thin section. This observation is supported by high-magnification scanning electron microscope images showing fine pore structure of the rock samples.

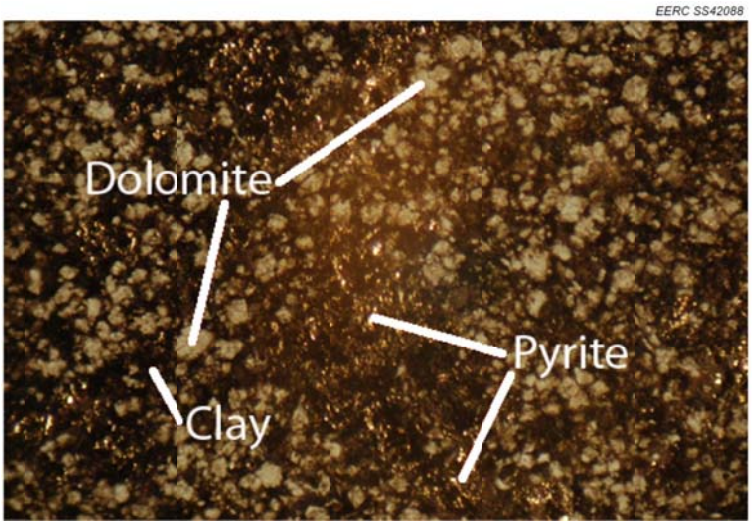

Figure 10. Photomicrograph of T-3, reflected light, 40× magnification.

Sample TH-1 lithologically comprises consolidated shale/mudstone. Thin sections are approximately 75% clay and 10% pyrite, with 15% fine-grained sparry carbonate. Grains are very fine-textured with the exception of interclasts, and the sample contains no visible porosity. Carbonate interclast growth is diagenetic. No microstructures were observed, and the sample is fairly homogeneous. Rare dolomite-cemented microfractures were observed. Dolomite clasts are euhedral to subhedral, and pyrite is subhedral to anhydral. Both mineralization varieties are of variable size. The sample likely contains low levels of organic material. Rock material was interpreted to have been originally deposited in a deep restricted marine setting followed by hypersaline influx postdepositionally.

Sample T-1 is a slightly mineralized, consolidated shale/mudstone. The section is approximately 75% clay, 15% sparry dolomite interclasts, and 10% pyrite, with trace quartz (silt) grains. The sample is very fine-grained, with the exception of the euhedral/subhedral dolomite and subhedral–anhedral pyrite clasts, which are secondary formations. The sample contained no visible porosity. No microstructures were observed, and the sample is fairly homogeneous, with the exception of scattered/loosely bedded pyrite growths. The sample likely contains low levels of organic material. The sample is thought to have been originally deposited in an anoxic, deep, restricted marine environment, followed by hypersaline influx postdepositionally.

The T-3 interval comprised argillaceous sparry dolomite. The section is approximately 70% coarse dolomite grains with significant clay (20%) and traces of silt (5%) and pyrite (5%). The sample is fairly homogeneous, with no preferential bedding or microstructure and no visible porosity. Dolomite clasts appear euhedral to anhedral and are of similar size. Pyrite varies in size and is anhedral to subhedral, with rare euhedral crystals. This rock has been highly impacted by diagenetic activity. T-3's carbonate fabric is classified as a sparite/dismicrite according to the Folk classification system and a packstone by the Dunham system. The interpreted depositional environment for this interval is restricted marine, followed by diagenetic hypersaline influx.

Key Observations

All three specimens represent various tight cap rock units from the Fort Nelson area. The first two intervals were very similar, containing high percentages of clay, with variable pyrite, silt and fine-grained carbonate, while the third interval contained a much higher degree of sparry carbonate growth (Tables 5 and 6). No microstructure was visible in any of the sections. These results confirm 1) the Fort Simpson Shale will provide a significant barrier to flow and 2) the Muskwa Formation warrants additional study to determine the flow characteristics and potential for reactivity between injected CO_2 and carbonates contained within the shale matrix. Other observations included the following:

- Samples TH-1 and T-1 were observed to be remarkably similar, with only minor differences noted in pyrite crystalline behavior and size. Sample T-3 was different in that scattered carbonate growth was much more common throughout the sample.

- No porosity was observed in any of the sections.

- Observations are consistent with the geological interpretation of an offshore restricted marine environment that has received postdepositional dolomitization seen to increase with depth, likely because of enriched water exiting the underlying Slave Point carbonates.

- Pyrite growth is more apparent in the clay-rich TH-1 and T-1, likely caused postdepositionally by enriched water moving through the reducing organic shales.

- Results of optical mineralogy analysis are in agreement for major phases observed in QEMSEM and SEM data. Results are in agreement with XRD-derived bulk mineralogy in non-clay/quartz phases.

Table 5. Mineralogical Estimates Derived Through Thin-Section Analysis

Sample	Clay/Silt, %	Carbonate, %	Pyrite, %	Quartz
TH-1	75	15	10	–
T-1	75	15	10	Trace
T-3	20	70	5	5%

Table 6. Rock Fabric Descriptions Related to Grain, Pore, and Clay Characteristics, Based on Thin-Section Analysis

Sample	Grain Size	Texture	Porosity Est.	Uniformity
TH-1	Very Fine	Anhedral–subhedral	None observed	Well, except for pyrite
T-1	Very Fine	Anhedral–subhedral	None observed	Well, except for pyrite
T-3	Fine	Anhedral–euhedral	None observed	Well, except for pyrite

QEMSEM Analysis

QEMSEM is a specialized scanning electron microscope technique that allows for acquisition of high-resolution backscatter and EDS scans of a polished sample surface. Data are collected and processed through software that allows the user to define modeled mineralogic phases based on collected elemental and back-scatter signatures. The device is used in the mining industry to characterize the size, shape, and concentration of product in ore; however, the two-dimensional mapping capability has found new uses in geochemistry, kinetics, and characterization.

Rough samples were prepared by suspension in epoxy, which was allowed to harden prior to slabbing a fresh face using a diamond-impregnated steel saw, with IsoCut® fluid as the cutting medium. Samples were polished using a progressively fining diamond–alcohol suspension fluid. The samples were coated with a thin layer of gold to prevent electron charging in the microscope. Scans collecting electron backscatter and EDS were performed at 15 μm resolution across the entire polished surface.

Mineral assemblages were decoded from elemental signatures and were quantified across the sample surface, as shown in Table 7. Color-coded photomicrographs of each QEMSEM sample representing the detected mineral contents are shown in Figures 11–13. Epoxy surrounding the samples has been removed from quantification, while epoxy surrounded by the sample was retained. Removed epoxy quantifications include the separation feature in Sample T-1.

Porosity was not observed in any of the samples except for microfractures. This is in disagreement with SEM and skeletal density measurements and is the result of porosity being of finer size than the 15-μm scan resolution. Because of the small pore size and relatively high scan resolution, the device is able to detect enough of the polished rock surface to register it as rock, rather than inference caused by the pores.

Sample TH-1 is primarily illite clay (76%), with silt-sized quartz grains (7%) and minor kaolinite (6%) scattered throughout the muddy fabric. Pyrite (4%) and dolomite (2%) are prevalent thoughout the sample as small inclusions that are primarily subhedral, with rare euhedral crystals. Thin bedding is observable in QEMSEM imagery as laminations of quartz and porous bedding planes, concentrated in the upper half of the sample. Trace apatite, barite, and sphalerite were also detected.

Sample T-1 comprises primarily illite clay (75%), with silt-sized quartz grains (6%) and minor kaolinite (7%) to form the muddy rock fabric. Pyrite (8%) is concentrated across the sample in a band; however, a small amount is dispersed through the sample as small crystals. The size and concentration of dolomite is reduced from the lower intervals, only present as 1% of this sample. Trace amounts of apatite and barite were also detected. Microfractures across the sample are not laminar, possibly indicative of cross-bedding, although quartz bedding is not observable in this sample.

Table 7. Quantitative Mineral Assemblages Present in QEMSEM Samples

Interval	Illite	Kaolinite	Quartz	Dolomite	Pyrite	Other	Unidentified
TH-1	76	6	7	2	4	2	3
T-1	75	7	6	1	8	1	2
3	16	4	13	46	4	10	7

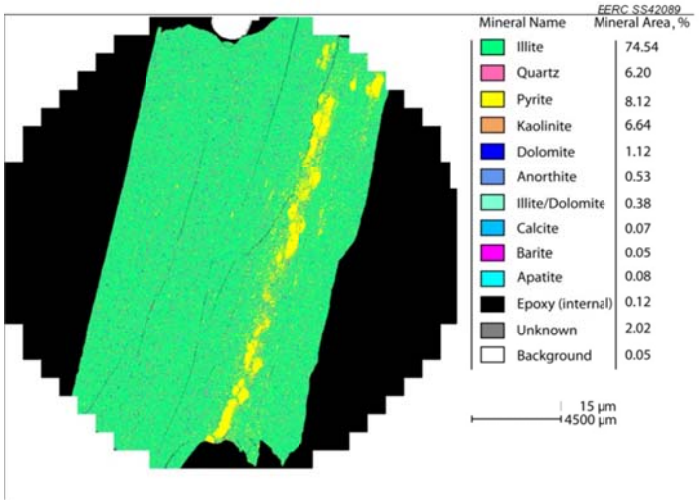

Figure 11. QEMSEM image of the TH-1 interval. Groundmass consisting of illite clay (green) with quartz (pink) and dolomite (blue) should be noted. A dominating band of pyrite (yellow) cuts across the sample. The sample contains several microfractures (black – epoxy) which possibly indicate fine-scale cross-bedding.

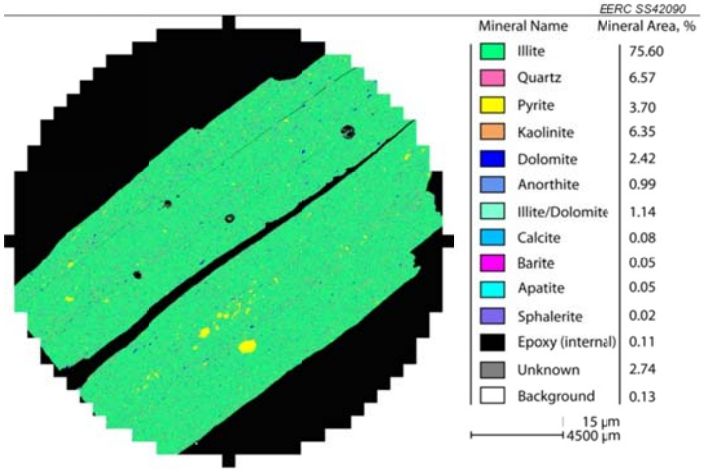

Figure 12. QEMSEM image of the T-1 interval. Groundmass consisting of illite clay (green) containing quartz (pink) and dolomite (blue) should be noted. The sample contains inclusions of pyrite (yellow). Microfractures (black – epoxy) may indicate laminar bedding plains across the sample.

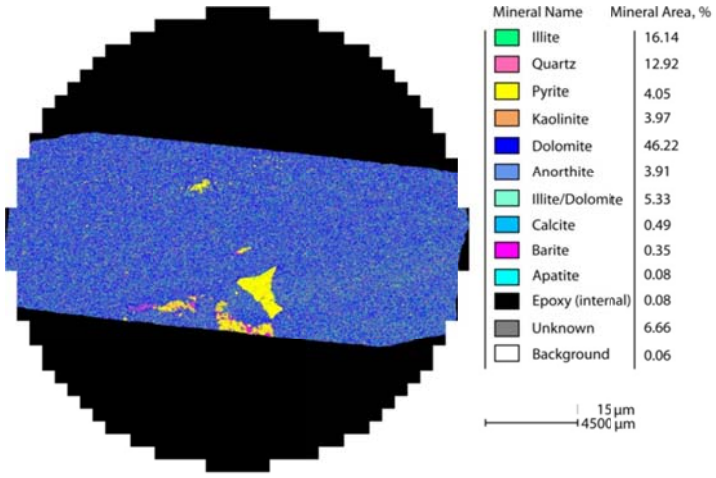

Figure 13. QEMSEM image of the T-3 interval. This sample contains significant dolomite (blue) with mixed argillaceous material. Pyrite (yellow) and barite (magenta) are possibly replacing fossiliferous material in the middle of the sample or filling irregular vuggy porosity. No microfractures or observable bedding are present in the sample.

Sample T-3 is observably different than the other two examples, comprising primarily dolomite (46%), with a high percentages of argillaceous, dispersed illite (16%), silt-sized quartz (13%), and kaolinite (4%). Large and small inclusions of pyrite (4%) appear to be replacing possibly fossiliferous material in conjunction with associated barite and apatite (trace). This sample contains a significant portion of unidentified material (7%). No microfractures or observable bedding are present across the sample.

Key Observations

The following observations were made during QEMSEM analysis of the Fort Nelson cap rock samples:

- No porosity (other than microfractures) was found in any of the samples.
- Illite clay (potassium-rich) was the prevalent groundmass of Samples TH-1 and T-1.
- Dolomite was the most common mineral in Sample T-3, but the rock mass remains highly argillaceous.
- Sample TH-1 appears to have thin laminar bedding. The bedding in T-1 appears to be less linear, possibly indicating fine-scale cross-bedding.
- Sample T-3 has the highest concentration of "uncommon" phases, such as barite and apatite, as well as the most unidentified phases.

- QEMSEM results are consistent with mineralogical estimations made through thin-section analysis and are supported by SEM data. XRD is in reasonable agreement for non-clay/quartz phases.

SEM Reporting

Scanning electron microscopes are used extensively to capture detailed images at high magnification. Rather than using transmitted or reflected light, as in typical optical microscopy, scanning electron microscopes use an electron beam that bombards the surface of the sample, resulting in several sensory phenomena, foremost being backscatter electrons. By scanning the beam across a surface, high-resolution images may be captured that correlate to the density of the viewed object.

An additional phenomenon arises when electrons are absorbed by struck atoms, which releases a characteristic x-ray unique to the atom's atomic number. By collecting and analyzing the x-ray wavelengths, atomic signatures can be collected through a process known as EDS.

SEM was performed on both polished and fractured sample fragments. Prior to scanning, a thin coat of carbon or gold was applied to the sample to prevent electrical charging of the surface. Backscatter electron-based images were captured at high magnification of the surface in conjunction with EDS measurements. Descriptions of key observations are presented in this portion of the document, with additional high-magnification backscatter electron images, EDS point count data, and additional descriptions presented in Appendix C.

For Sample TH-1, the sample fabric contains high concentrations of microporous silt and potassium-rich clay. Rare fossil and chemically deposited material comprising apatite is present in the sample as well as scattered accumulations of subhedral, radial (variable marcasite), and framboidal pyrite. Dolomite recrystallized zones appear to contain significant portions of iron, possibly indicative of ankerite alteration. Rare accumulations of titanium were also observed in the sample (Figure 14).

For sample T-1, potassium- and magnesium-rich clay constitutes a majority of the sample fabric, with trace amounts of iron and titanium present. Pyrite and, possibly, marcasite accumulations are obvious as bright zones in any frame of the sample and consist of framboidal, radial, occasionally globby, and subhedral cubic forms. Dolomite recrystallization in the sample is zonal and appears to favor more porous areas with higher concentrations of quartz than the typical clay-rich accumulation. Rare porous fossiliferous material was observed comprising apatite (Figure 15, Tables 8 and 9).

Sample T-3 comprised primarily microporous dolomite and argillaceous dolomite, with accumulations of pyrite and a significant portion of barite. Pyrite exists as both subhedral-to-anhedral fine-grained inclusions to large recrystallized zones, showing both cubic and radial forms. Rarely, pyrite accumulations were observed to contain inclusions of barite (Figure 16, Tables 10 and 11).

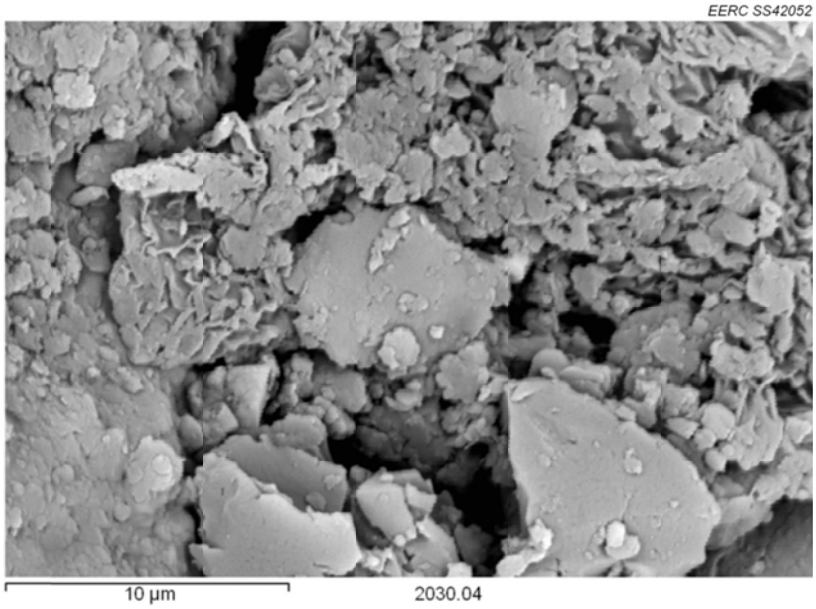

Figure 14. Fracture-mounted photomicrograph of Sample TH-1 at 5000× magnification. This sample shows microporous, disoriented clay particles.

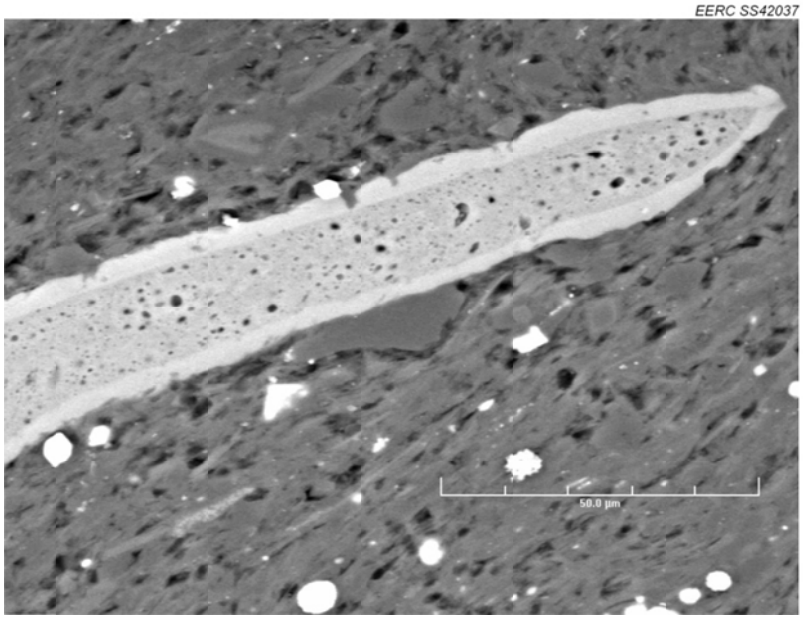

Figure 15. Electron backscatter micrograph of polished section of Interval T-1 taken at 750× magnification. This image depicts fossiliferious material comprising porous apatite (center) surrounded by a microporous silty shale groundmass. Fine-grained pyrite/marcasite is present throughout the sample as bright accumulations.

Table 8. Elemental Compositions at Probed EDS Locations for Figure 15, Sample T-1, as relative percentage

Tag	Na	Mg	Al	Si	P	S	Cl	K	Ca	Ti	Fe	Ba
1	0.00	18.69	0.74	2.74	0.20	0.08	0.00	0.39	58.14	0.00	19.02	0.00
2	0.00	0.58	10.15	76.85	0.00	0.50	0.00	9.74	0.88	0.09	1.20	0.00
3	0.00	0.04	5.12	86.45	0.24	0.00	0.00	6.29	1.06	0.00	0.59	0.20
4	0.00	0.00	0.10	0.92	32.81	0.00	0.00	0.12	66.01	0.00	0.03	0.00
5	0.00	0.00	0.18	1.19	32.04	0.00	0.00	0.14	66.45	0.00	0.00	0.00
6	0.09	0.00	0.05	0.52	32.61	0.00	0.00	0.12	66.54	0.00	0.07	0.00
7	0.00	0.00	0.00	0.44	32.80	0.00	0.10	0.06	66.60	0.00	0.00	0.00
8	0.00	0.00	0.63	95.95	0.39	0.00	0.00	2.70	0.21	0.00	0.11	0.00
9	0.00	0.00	4.52	88.54	0.00	0.00	0.00	5.39	0.00	0.81	0.74	0.00
10	0.00	0.00	4.71	88.32	0.00	0.00	0.00	5.99	0.00	0.33	0.65	0.00

Table 9. Mineralogical Interpretation of Probed EDS Locations for Figure 15, Sample T-1

Tag	Mineralogical Interpretation	Tag	Mineralogical Interpretation
1	Ankerite	6	Apatite
2	Illite	7	Apatite
3	Illite	8	Illite
4	Apatite	9	Illite
5	Apatite	10	Illite

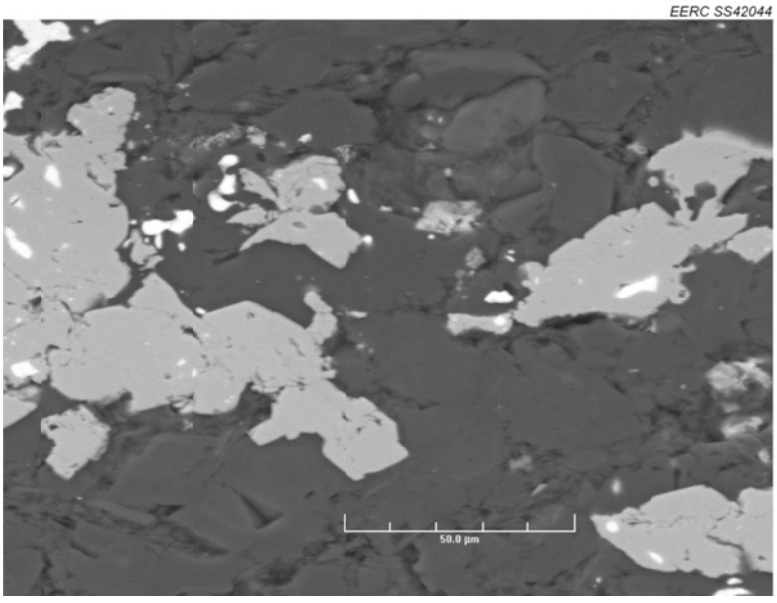

Figure 16. Electron backscatter micrograph of T-3 taken at 750× magnification. This image shows argillaceous dolomite (dark, rough surface), with secondary accumulations of subhedral to anhedral pyrite (gray) containing bright white inclusions of barite.

Table 10. Elemental Compositions at Probed EDS Locations for Figure 16, Sample T-3, as relative percentage

Tag	Na	Mg	Al	Si	P	S	Cl	K	Ca	Ti	Fe	Ba
1	0.00	25.08	0.32	1.65	0.29	0.41	0.00	0.14	70.47	0.00	1.65	0.00
2	0.00	27.27	0.00	0.58	0.50	0.12	0.00	0.00	70.43	0.00	1.09	0.00
3	0.00	30.16	0.13	0.29	0.41	0.15	0.00	0.00	67.63	0.00	1.22	0.00
4	0.00	0.00	0.00	0.30	0.24	54.14	0.10	0.00	0.05	1.48	43.69	0.00
5	0.00	0.00	0.00	8.89	0.05	16.91	0.00	0.00	0.03	9.17	1.11	63.85
6	0.00	0.00	0.00	0.03	0.33	53.97	0.22	0.00	0.08	1.55	43.80	0.00
7	0.01	0.00	0.00	0.04	0.10	30.05	0.00	0.00	0.00	6.89	14.83	48.08
8	0.00	0.00	0.00	0.59	0.00	28.67	0.00	0.00	0.00	7.46	12.22	51.06
9	0.00	25.68	0.87	3.01	0.68	0.31	0.09	0.42	67.94	0.00	1.00	0.00
10	0.00	27.13	0.21	0.62	0.48	0.12	0.00	0.00	69.61	0.00	1.83	0.00

Table 11. Mineralogical Interpretation of Probed EDS Locations for Figure 16, Sample T-3

Tag	Mineralogical Interpretation	Tag	Mineralogical Interpretation
1	Dolomite	6	Pyrite
2	Dolomite	7	Barite
3	Dolomite	8	Barite
4	Pyrite	9	Dolomite
5	Barite	10	Dolomite

Key Observations

The following observations were made while analyzing Fort Nelson cap rock samples under SEM:

- SEM data were found to be integral to describing the fine-scale microporosity in the samples. Porosity observed through SEM techniques explains measurements of surface area and skeletal density testing that were not found from thin-section or QEMSEM methods.

- SEM data found barite within pyrite masses, which is also seen with QEMSEM.

- Fracture-mounted images show chaotic clay bedding and three-dimensional images of crystallography and complex structures.

- Iron sulfide is seen in framboidal, cubic, and radial (marcasite) forms. Framboidal pyrite structures are often biogenically controlled (Kamamura, 2002).

CHN/S Analysis

CHN analyzers specialize in providing quantification of carbon, hydrogen, and nitrogen which are present in the sample. The device measures both elemental and ionic content, meaning that carbon is detected both as elemental carbon and the carbon portion of carbonate, if present. An additional module provides independent sulfur measurement capabilities to determine the total sulfur content of the sample.

In this study, total carbon, hydrogen, and sulfur were measured in each specimen (Table 12). Nitrogen was not measured and is expected to be a minor phase outside of detectable limits, as nitrogen does not incorporate into common rock-building minerals; instead, it is typically found in unaltered organic compounds, which are not present in these samples.

Carbon, hydrogen, and sulfur are common in rock-forming minerals, being present in carbonate, sulfate, sulfite, and sulfide salts as well as metal hydroxides. Aside from minerals and preserved organic material, hydrocarbons and hydrocarbon residues are known to accumulate CHN/S material.

Sulfur contents derived through this method were approximately four times higher than were observed through XRF testing. Calculations based on pyrite (FeS_2) content, which was the only major sulfur-containing mineral detected, yielded results approximately half of CHN/S analysis for QEMSEM values. Pyrite contents from XRD data calculated values approximately equal to CHN/S results for Samples T-1 and T-3 and showed greater sulfur concentration in Sample TH-1 than CHN/S. Sulfur content data remain inconclusive, as no clear trends or agreement in data could be attained. Sulfur in the cap rock system should be considered heterogeneous on a fine scale (observed in thin section, QEMSEM, and SEM), and may exist in the range of 0.5% to 3.7%. A plot of sulfur content data is presented in Figure 17.

Key Observations

Results from testing show that samples have variable contents of carbon, hydrogen, and sulfur, specifically:

- Carbon was significantly higher in Sample T-1 than in the other samples.
- Sample T-3 had significantly more carbon than TH-1. The high content of T-3 is in part due to the high carbonate content of the sample.

Table 12. Results of CHN/S Analysis

Sample	% Carbon	% Hydrogen	% Sulfur
TH-1	1.67	0.27	3.14
T-1	27.6	0.28	3.60
T-3	8.28	0.07	2.07

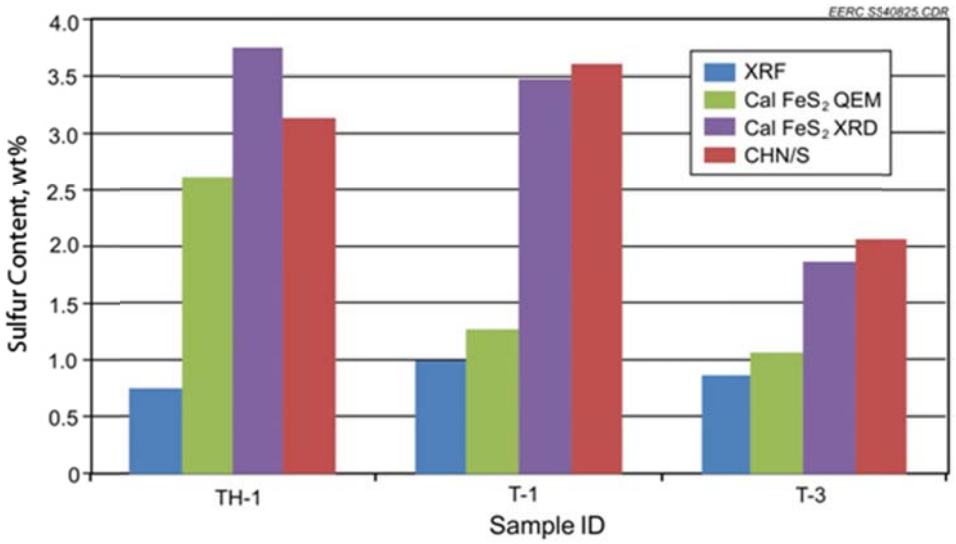

Figure 17. Results of sulfur analysis derived through XRF and CHN/S and calculated from pyrite contents derived from QEMSEM and XRD data.

- Hydrogen content was nearly equivalent in Samples TH-1 and T-1 but decreased sharply in Sample T-3.

- Sulfur increases slightly from Sample TH-1 to Sample T-1. Sample T-3 has the lowest concentration of sulfur. Sulfur content is thought to be a product of pyrite/marcasite content.

- Despite sample proximity and similarities in appearance, carbon, hydrogen, and sulfur contents show that heterogeneity still exists in the system.

- Sulfur contents found through total sulfur testing were higher than XRF measurements and from calculated pyrite concentrations derived through QEMSEM. Sulfur contents from XRD pyrite concentrations were close to CHN/S values; however, higher values for sulfur were observed in Sample TH-1.

Surface Area

A surface area analyzer was used in this study to measure total surface area of a sample in an effort to better understand reactive area and surface area-related attributes. The surface area of granulated and powdered solids or porous materials is measured by determining the quantity of gas that adsorbs as a single layer of molecules on the sample and is reported in square meters of coverage corrected to 1 gram of sample. These data have use in kinetics, as high surface areas can experience much faster and more dramatic reactions than tight crystalline materials.

Surface area correlates strongly to particle size and shape where small platelike clay particles tend to have higher surface area than more three-dimensional silt or dolomite portions. Carbon within a sample can be present in structures with a variety of surface areas and may

highly impact measurements. Surface area is used directly in chemical kinetics and may also be used to describe more abstract properties such as degree of cementation. Surface area measurements are reported in Figure 18 and Table 13.

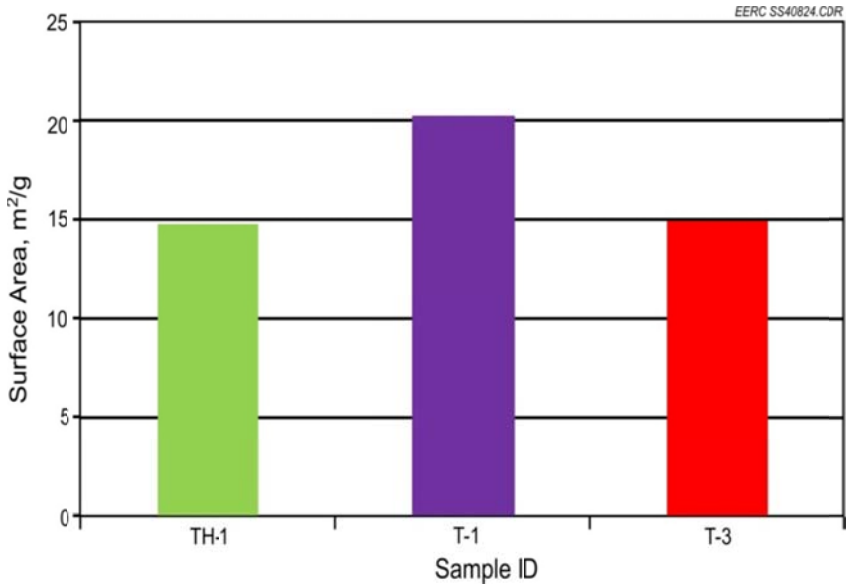

Figure 18. Comparison of results of surface area testing for Fort Nelson cap rock samples.

Table 13. Results and Calculations from Surface Area Measurements for Fort Nelson (C-61-E/94-J-10) C1-49528

Pulverized TH1 Depth 2030.04 m					
Sample	Monsorb Reading, m^2	Avg. Reading, m^2	Sample Weights	grams	Surface Area, m^2/g
1	10.82	10.82	Sx + tare:	11.4496	14.66
2	10.82		Tare:	10.7115	
3	10.81		Sx:	0.7381	
Pulverized T1 Depth 2042.11 m					
Sample	Monsorb Reading, m^2	Avg. Reading, m^2	Sample Weights	grams	Surface Area, m^2/g
1	12.28	12.28	Sx + tare:	11.6438	20.16
2	12.27		Tare:	11.0346	
3	12.28		Sx:	0.6092	
Pulverized T3 Depth 2045.75 m					
Sample	Monsorb Reading, m^2	Avg. Reading, m^2	Sample Weights	grams	Surface Area, m^2/g
1	9.73	9.73	Sx + tare:	11.3491	14.82
2	9.73		Tare:	10.6927	
3	9.74		Sx:	0.6564	

Key Observations

Results indicate the following:

- With respect to surface area, Sample T-1 has significantly more than Samples TH-1 and T-3. This is likely because of a significant amount of preserved porosity, including fossil fragments.

- Samples TH-1 and T-3 reported similar values, with slightly more surface area being observed in Sample T-3. This is unexpected because mineralogy differs greatly between the two samples. The discrepancy may be because of clay particle size differences in the samples.

- Results are in agreement with skeletal density measurements that show similar trends; in particular, the similarity of total density of Samples TH-1 and T-3 and the lower total density that indicates higher porosity in Sample T-1.

Skeletal Density

Densities of whole and crushed samples were determined using a helium pycnometer. This multivolume pycnometer determines the skeletal density by measuring the reduction of gas volume in the sample chamber caused by the presence of the research sample. Skeletal density correlates strongly with mineralogy and can help define pore volume within the sample. Through repeated testing of a crushed sample, an understanding can be gained regarding the isolation or connection relationship in the pore structure, as disaggregated samples provide access approaching the entire porous network.

The resulting density measurements (Table 14) have strong ties to mineralogy. Quartz, for example, has a known density of 2.62 g/cm³, whereas metal salts such as pyrite can have densities over 5.0 g/cm³ (Ralph and Chau, 2011). Observed densities of 2.7 to 2.8 suggest concentrations of clay (density ~2.75 g/cm³) and dolomite (density ~2.84 g/cm³) in these samples. Measured skeletal densities agree well with mineralogical contents determined by XRD, SEM, QEMSEM, and optical petrography.

Differences in density between whole and crushed specimens were performed to show the influence of pore space in the sample (Figure 19). Whole samples shelter ineffective porosity from the measurement and, overall, lead to showing lower density (i.e., higher volume with the same weight). Crushing a sample effectively removes any pore space that would have been present in the sample and shows the maximum attainable density of the material.

Key Observations

- Sample TH-1 shows very little difference between whole vs. crushed results. This sample is thought to have the most consistent fabric, despite heterogeneous pyrite.

- Sample T-3 has a much higher degree of ineffective porosity, likely because of the highly cemented fabric.

Table 14. Measurements and Calculations Performed for Skeletal Density Values

	TH-1 Crushed	TH-1 Whole	T-1 Crushed	T-1 Whole	T-3 Crushed	T-3 Whole
Mass, g	1.5719	4.8518	1.5387	5.0706	1.5387	4.227
Grain Volume, cm^3	0.5748	1.7766	0.5466	1.9174	0.5466	1.5496
Grain Density, g/cm^3	2.73469	2.730947	2.815038	2.644519	2.815038	2.727801
+Uncertainty	2.71784	2.715906	2.797458	2.628168	2.797458	2.722028
–Uncertainty	2.751751	2.746155	2.832841	2.661074	2.832841	2.733598

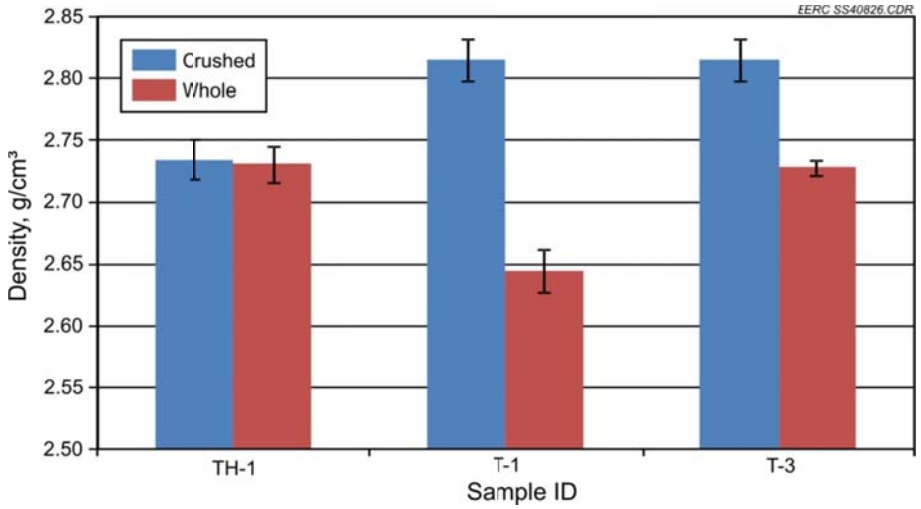

Figure 19. Skeletal density testing of whole (blue) and pulverized (red) test samples.

- Sample T-1 has a large difference in density found between whole and crushed tests. This is thought to be a result of disconnected porosity that formed as a result of pyrite and dolomite cementation.

- Samples T-1 and T-3 have very similar densities from crushed samples of approximately 2.81. This value is consistent with mineralogy high in illite and dolomite, measured through the various methods employed. Dense pyrite is also a significant factor in these samples.

- Sample TH-1 has a significantly lower density ~2.73. This is because of lower concentrations of pyrite and dolomite in the sample and remains consistent with measured mineralogy.

- Mineralogy-based density calculations using measured concentrations of mineral assemblages and estimated densities are shown to slightly overestimate skeletal density for these samples. This may be because of small overestimations of heavy, high-

visibility minerals or an underestimation of lighter phases present in clays, metals, and/or carbonates.

ICP–MS

MS is a type of destructive analysis that detects ionic energy at very high resolution. This type of analysis often is able to analyze trace constituents down to 1 part per trillion. For this analysis, rock samples were completely dissolved through mixed-acid digestion and run through the ICP–MS unit. The ICP ionized the liquefied stream, and ionic energy measurements were collected for 38 elements representing rare-earth, transition, lanthanide, and actinide groups. Thirty-one of these elements were compared with reported data for simultaneously processed RGM-1 standard reference material (Table 15). The remaining seven were not reported for RGM-1 standard reference material, so the standard error in detection for these phases is unknown. Semiquantitative analysis was still possible, however, and is reported in Table 16.

Clay-rich intervals of the Fort Simpson and Muskwa Shales showed higher trace element concentrations than the heavily dolomitized sections of the Muskwa Formation. Manganese is an exception to this, as it is a common replacement element in dolomites. Specifically, the shale samples had higher concentrations in 23 out of 27 elements, suggesting that clays have trapped significantly higher amounts of trace elements than the carbonate-rich units. The trace metal content of clay samples is thought to be the result of a combination of classic sedimentary accumulation from continental sources or of enriched water traveling through reducing organic carbon-rich units.

Trace element contents found through this method present a broad spectrum view of geochemical contents of the Fort Nelson cap rock samples. Some trace elements were detected in quantities sufficient to serve as natural tracers. This use is highly dependent on formation fluid sample quality and will require additional fluid analysis in both reservoir and monitoring lithologies.

Table 15. Trace Elements Measured During ICP–MS Analysis Against RGM-1 Standard

Yttrium	Lead	Copper	Lanthanum	Vanadium
Chromium	Antimony	Cerium	Cobalt	Beryllium
Neodymium	Manganese	Titanium	Scandium	Dysprosium
Gadolinium	Samarium	Ytterbium	Arsenic	Europium
Zinc	Thorium	Nickel	Lutetium	

Table 16. Trace Elements Measured During ICP–MS Analysis that Had No Values Reported for Standard RGM-1

Selenium	Promethium	Cadmium	Terbium
Holmium	Erbium	Thulium	

Key Observations

Results of ICP–MS testing are shown in Figures 20 and 21 and Tables 17 and 18. Specific observations while analyzing ICP–MS data include the following:

- 28 of the 31 measured elements were detected on the 0.5–1200-µg/g scale within all samples. Promethium, thulium, and holmium were not detected in at least one of the samples (less than 0.5 µg/g).

- Comparatively, TH-1 had the highest concentrations of 12 elements, followed closely by T-1, which had high concentrations of 11 elements. Sample T-3 only had higher concentrations of four elements (Gd, Mn, Dy, and Y).

- Only two elements had shared analysis with XRF testing, titanium and manganese. Titanium results appear to agree between the two methods; however, discrepancies exist in the manganese measurements.

- Sample T-3 received additional XRF testing, which covered nine of the same elements: arsenic, zinc, copper, nickel, manganese, vanadium, titanium, yttrium, and chromium. These were found to be in agreement, with the exception of yttrium and chromium, which is thought to be an error in XRF analysis because of small sample size and low elemental concentration.

- Metals, including toxic species (lead, cadmium, arsenic, etc.), are present within cap rock intervals. Geochemical modeling should be performed to assess and ensure that mobilization of metallic species does not have potential impact on water resources.

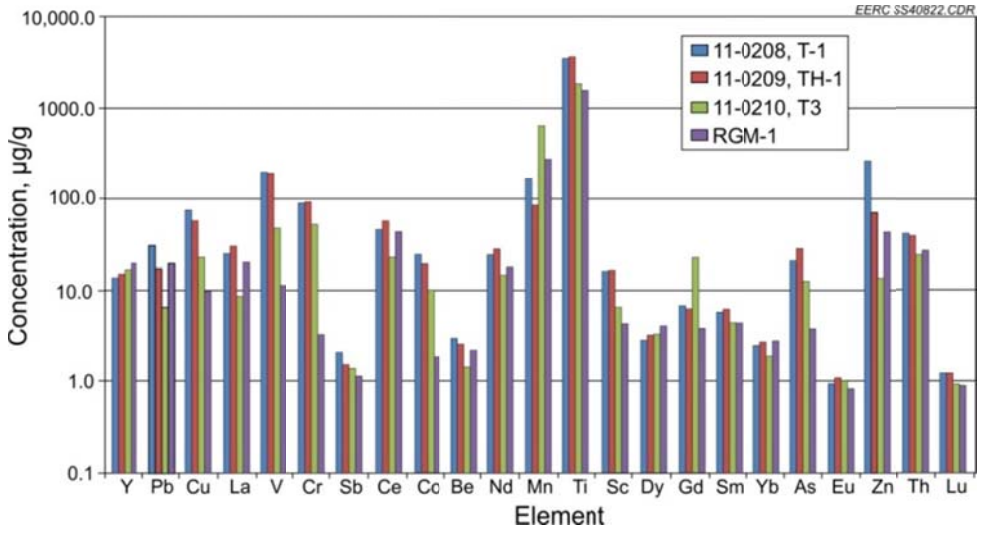

Figure 20. Results of trace element analysis comparing Samples TH-1, T-1, and T-3 with Glass Mountain rhyolite (RGM-1).

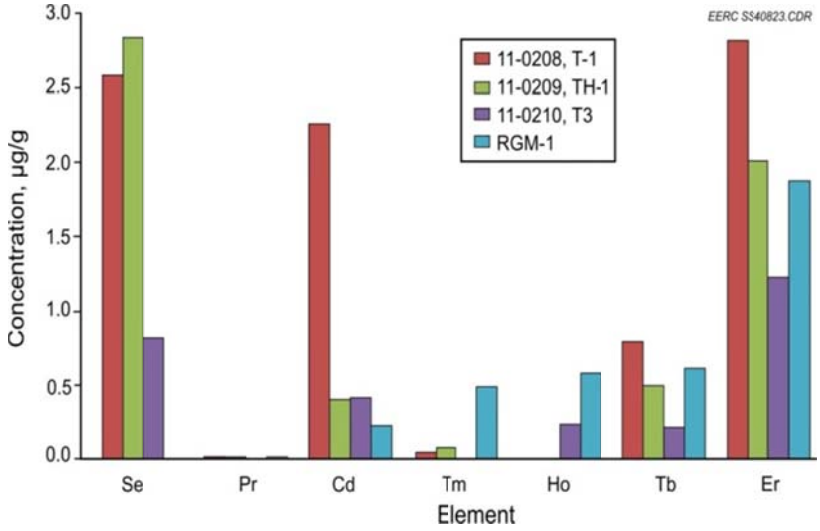

Figure 21. Results of trace element analysis for Samples TH-1, T-1, and T-3 for elements not reported in RGM-1 sample literature.

Table 17. Concentrations of ICP–MS Measured Trace Elements for Metals with RGM-1 Standard, µg/g

Sample	Y	Pb	Cu	La	V	Cr	Sb	Ce
TH-1	15.089	17.456	57.761	30.671	197.633	92.604	1.524	57.949
T-1	13.541	31.058	76.789	24.920	201.983	92.068	2.067	46.950
T-3	17.221	6.683	22.779	8.683	47.609	52.740	1.406	23.392

	Co	Be	Nd	Mn	Ti	Sc	Dy	Gd
TH-1	19.231	2.584	28.412	85.888	3660.750	16.489	3.156	6.223
T-1	24.400	3.022	24.655	167.044	3473.088	15.779	2.814	6.862
T-3	10.010	1.458	14.490	656.949	1886.297	6.449	3.279	22.255

	Sm	Yb	As	Eu	Zn	Th	Lu	Ni
TH-1	6.262	2.692	28.600	1.105	70.750	39.714	1.237	117.949
T-1	5.817	2.502	20.774	0.925	266.667	41.992	1.251	101.794
T-3	4.497	1.874	12.527	1.009	13.528	24.354	0.946	39.125

Table 18. Concentrations of ICP–MS Measured Trace Elements for Metals Without RGM-1 Standard, µg/g

Sample	Se	Pr	Cd	Tm	Ho	Tb	Er
TH-1	2.840	0.0119	0.400	0.076	ND	0.497	2.022
T-1	2.587	0.004	2.257	0.043	ND	0.788	2.842
T-3	0.816	ND	0.412	ND	0.229	0.218	1.236

SUMMARY

Petrographic assessment was performed on primary cap rock samples from the Fort Nelson demonstration project reservoir. Three samples from Well C-61-E/94-J-10 representing the Fort Simpson Shale and Muskwa Formation were characterized, with emphasis on geochemical stability, mineralogy, and rock properties pertinent to geochemical assessment. Ten separate analyses were conducted in order to collect properties, provide supporting data, correlate findings, and provide illustrations and explanations of results. Specifically, testing included the following:

- XRD for bulk mineralogy
- XRF for trace element analysis
- Petrographic analysis via thin section for mineralogy and rock fabric descriptions
- QEMSEM for mineralogical mapping
- SEM with EDS for mineralogical identification and rock fabric descriptions
- CHN/S measurements for elemental composition information
- Surface area to determine reactive surface
- Skeletal density to support mineralogy and examination of total vs. effective porosity and degree of cementation
- ICP–MS to examine trace element abundance

Paleoenvironmental interpretation based on rock mineralogy and fabric suggests that Keg River, Sulphur Point, and Slave Point reef complexes were deposited along a shallow shelf extending onto the flooded continental shelf. Brief marine regressions caused the back-reef environment to fill with siliclastic carbonate debris and evaporite deposits (Meijer Drees, 2008). Continental influx persistently provided clastic sediments to the system, which accelerated following a large-scale marine transgression that covered the area, resulting in the deposition of organic-rich marine shales including the Fort Simpson.

Illite group clay-rich cap rock samples contain inclusions of secondary dolomite and pyrite which are thought to be the result of enriched water moving through the system during lithification and/or hydrocarbon maturation. In some cases, these inclusions now outnumber the volume of autochthonous rock. Small portions of barite, calcite, silt-sized quartz, fossiliferous apatite, and lithic fragments were also detected through analysis. Sample porosity was difficult to visualize and practically inexistent on a macro/meso scale. SEM techniques proved invaluable to observing the porous structure of these rocks.

Selected intervals are consistent with published formation descriptions in the Fort Simpson and Muskwa Formations, although dolomitized portions of the Otter Park Formation underlying the Muskwa are expected to have formation characteristics similar to Sample T-3. The cap rock intervals were shown to contain tight, partially mineralized collections of stable minerals with low porosity and small pore throat diameter. No leakage pathways were observed in the submitted samples, and all three are expected to provide significant resistance to vertical migration of injected nonmiscible fluids. Geochemical and mechanical modeling and simulation are required to validate and confirm cap rock–fluid interactivity with injected fluids under reservoir conditions.

REFERENCES

Gorecki, C.D., Sorensen, J.A., Klapperich, R.J., Holubnyak, Y.I., Hamling, J.A., Bremer, J.M., Smith, S.A., Steadman, E.N. and Harju, J.A., 2010, Fort Nelson test site – site characterization, modeling, and monitoring plan: Plains CO_2 Reduction (PCOR) Partnership Phase III, Task 9, Deliverable D52, for U.S. Department of Energy National Energy Technology Laboratory Cooperative Agreement No. DE-FC26-05NT42592, EERC Publication 2011-EERC-08-06, Grand Forks, North Dakota, Energy & Environmental Research Center, September.

Kamamura, K., 2002, Growth process of framboidal pyrite in deep-sea sediments, sediments, clastic: processes, petrology and provenance [abs.]: Geological Society of America Paper No. 89-6.

Meijer Drees, N.C., 2008, Devonian Elk Point Group of the Western Canada Sedimentary Basin Geological Atlas of the Western Canada Sedimentary Basin, Chapter 10, Alberta Geological Survey.

Ralph, J., and Chau, I., 2011, Mineralogy Database: www.mindat (accessed July 2011).

Środań, J., 1980, Precise identification of illite/smectite interstratifications by x-ray powder diffraction: Clay and Clay Minerals, v. 28, no. 6, p. 401–411.

U.S. Geological Survey, 2001, A laboratory manual for x-ray powder diffraction: U.S. Geological Survey Open-File Report 01–041 http://pubs.usgs.gov/of/2001/of01-041/ htmldocs/methods.htm (accessed August 2011).

APPENDIX A

BULK MINERALOGY XRD SCANS

Table A-1. Relative Weight Percentages of Identified Mineral Phases in Each Sample Determined by X-Ray Diffraction

	TH-1, 11-0209	T-1, 11-0208	T-3, 11-0210
Illite	47.0	46.2	21.6
Quartz	41.6	40.9	31.0
Dolomite	1.0	0.7	25.0
Pyrite	7.0	6.5	3.5
Ankerite	0.8	2.0	18.0
Sanidine $Na_{0.56}$	2.0	2.5	0.6
Muscovite 2M1	0.4	0.5	0.2
Siderite	0.3	0.7	0.0
Kaolinite (BISH)	0.0	0.0	0.0
Anhydrite	0.0	0.0	0.0
Goodness of Fit	1.67	1.77	1.47
Rexp	9.66	9.53	9.30

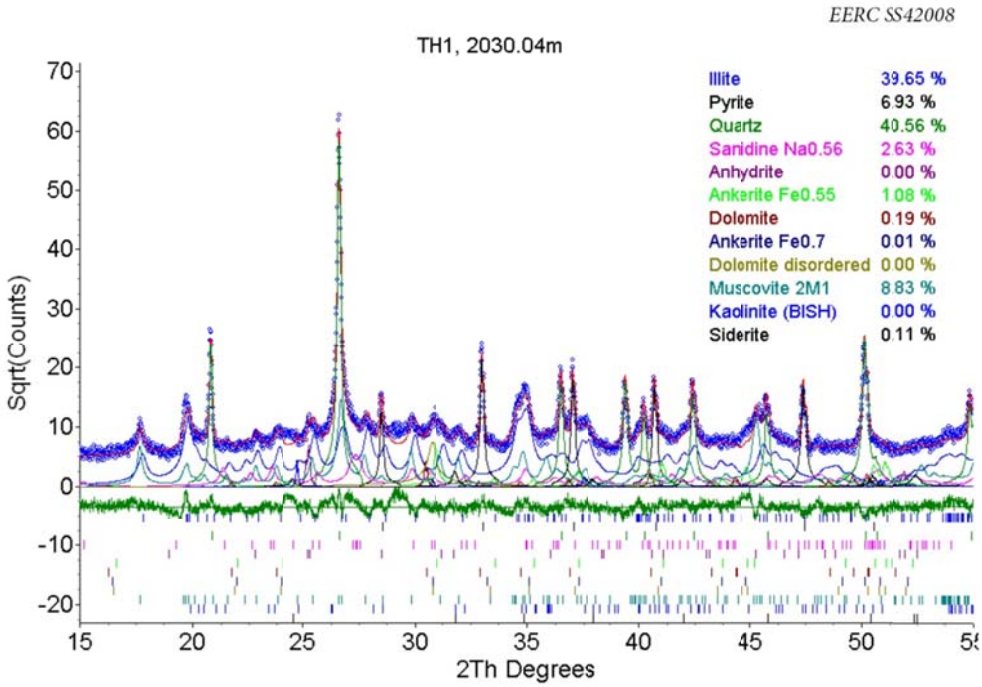

Figure A-1. Spectrographic scan and mineralogical phase identification of Sample TH-1 through Rietvelt refinement. The measured and modeled curves are displayed as well as model constituents and their individual peak spacing. This sample reported high contents of illite and quartz, with minor pyrite.

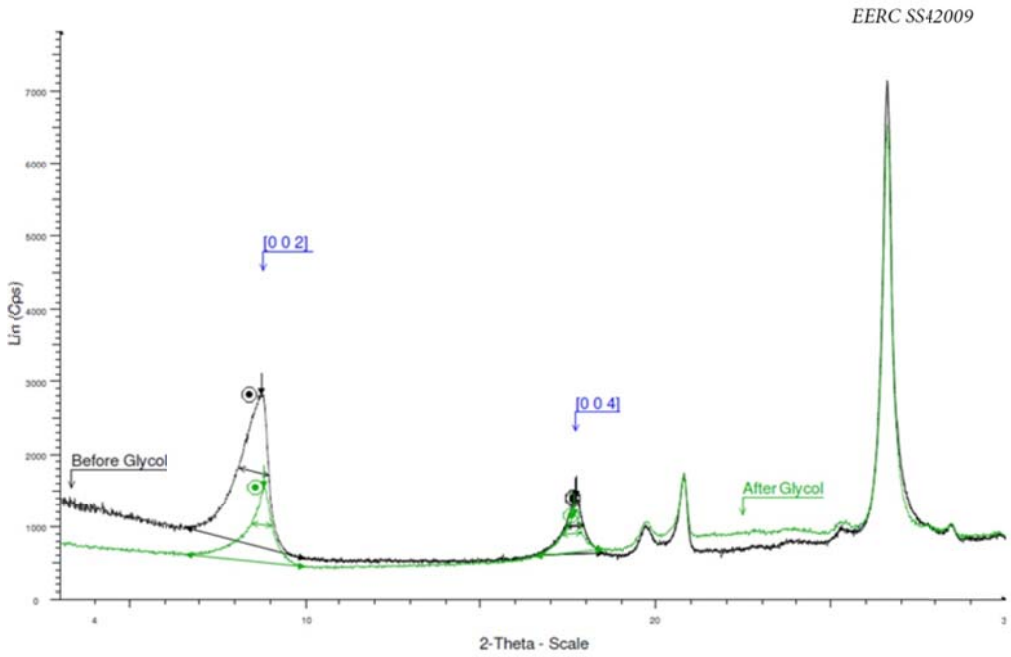

Figure A-2. Prior- and post-glycolation scans of Sample TH-1 showing low-angle peak behavior and swelling reaction due to glycol exposure.

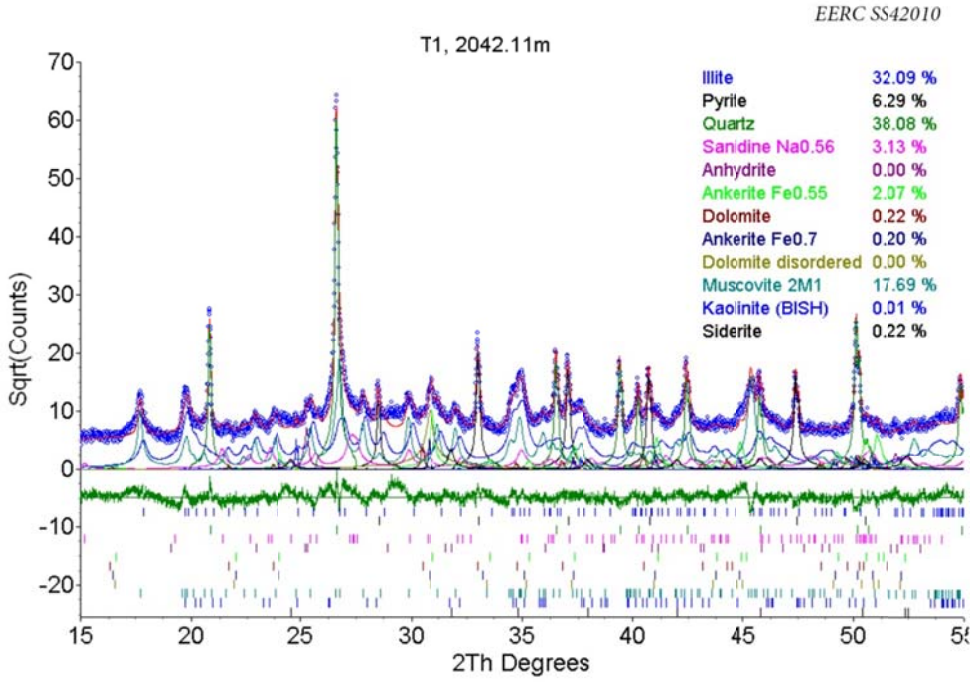

Figure A-3. Spectrographic scan and mineralogical phase identification of Sample T-1 through Rietvelt refinement. The measured and modeled curves are displayed as well as model constituents and their individual peak spacing. This sample reported high contents of illite and quartz, with minor pyrite.

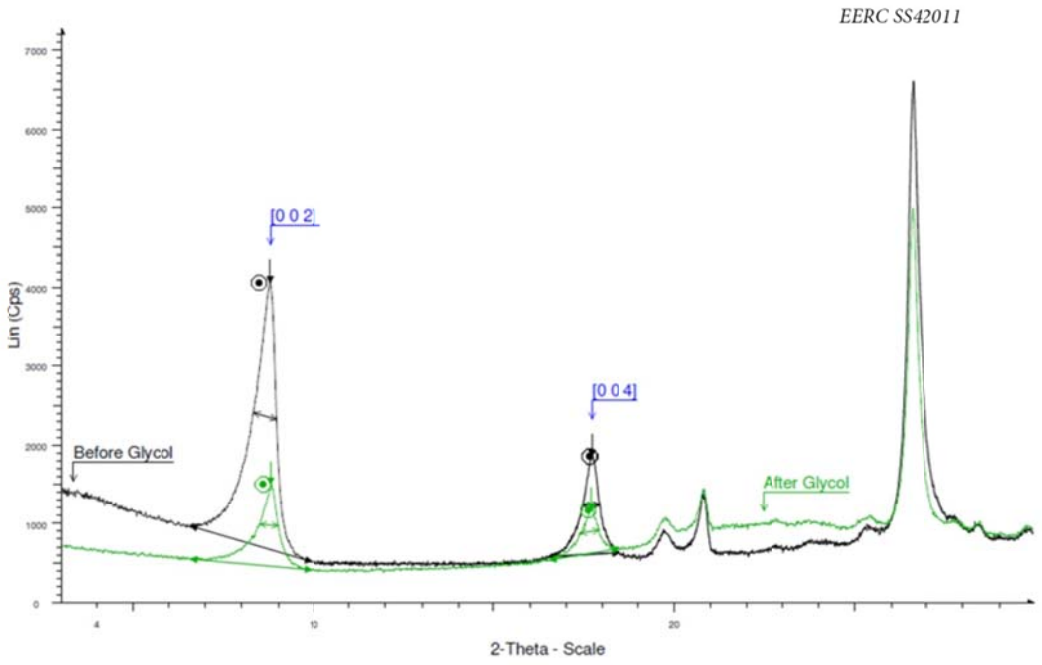

Figure A-4. Prior- and post-glycolation scans of Sample T-1 showing low-angle peak behavior and swelling reaction due to glycol exposure.

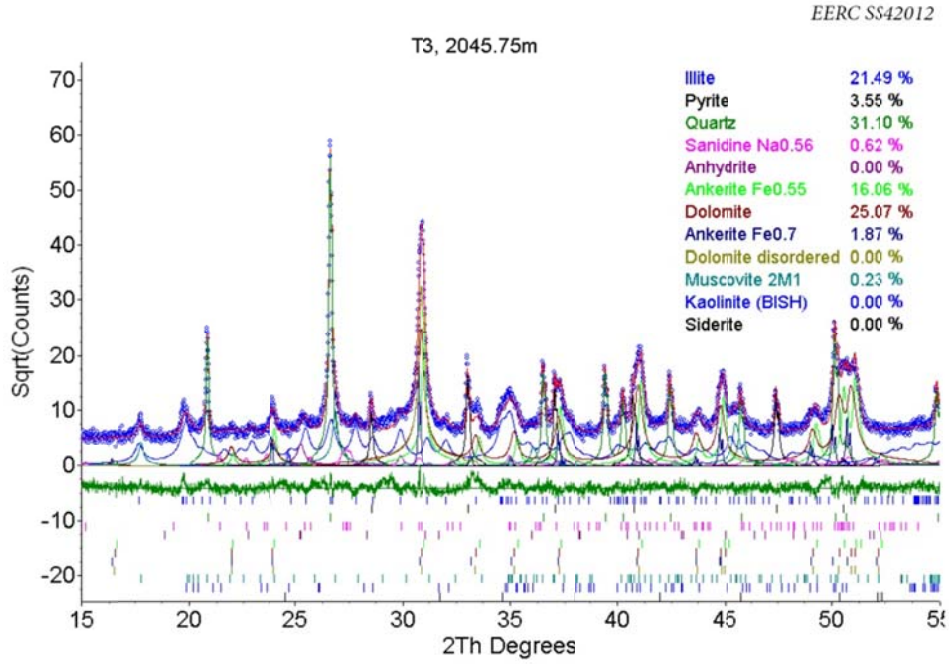

Figure A-5. Spectrographic scan and mineralogical phase identification of Sample T-3 through Rietvelt refinement. The measured and modeled curves are displayed as well as model constituents and their individual peak spacing. This sample reported significant portions of illite, quartz, dolomite, and ankerite, with minor pyrite.

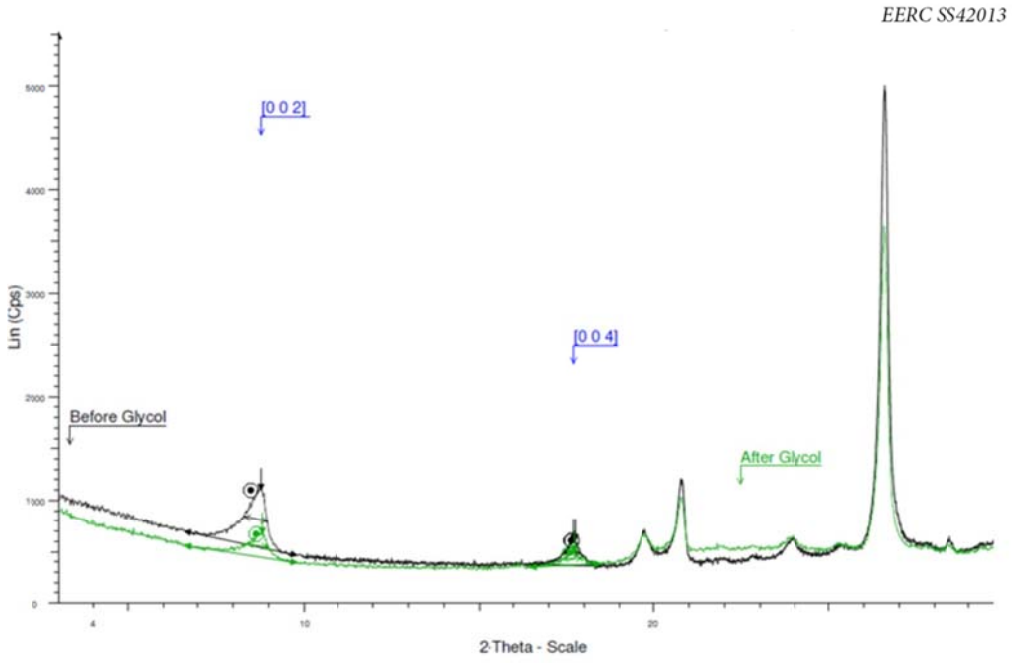

Figure A-6. Prior- and post-glycolation scans of Sample TH-3 showing low-angle peak behavior and swelling reaction due to glycol exposure.

APPENDIX B

PETROGRAPHIC THIN SECTIONS

Table B-1. Sample TH-1, 2030.04 meters

Assemblage	Percentage	Comments
Clay/Silt	75	No observable porosity
Carbonate	15	Subhedral to euhedral
Pyrite	10	Subhedral/anhedral

Sample TH-1 is very fine-grained, poorly sorted, well-consolidated shale that is dark charcoal gray to black. Thin-section analysis estimated that the rock is composed primarily of clay (75%) spread throughout the sample, with scattered accumulations of dolomite (15%) and pyrite (10%). No apparent porosity or fossil assemblages were encountered during analysis (Figures B-1 and B-2).

Table B-2. Sample T-1, 2042.11 meters

Assemblage	Percentage	Comments
Clay/Silt	75	No observable porosity
Carbonate	15	Subhedral
Pyrite	10	Subhedral to euhedral

Sample T-1 is a very fine-grained, poorly sorted, well-consolidated shale that is dark charcoal gray to black. A thin-section sample produced from the interval showed high concentrations of clay (75%) spread throughout the sample, with scattered subhedral dolomite (15%) and subhedral to euhedral pyrite (10%). No porosity or fossil assemblages were observed in this sample, which, other than the increased crystal structure in pyrite, appears identical to the TH-1 interval (Figures 3 and 4).

Table B-3. Sample T-3, 2045.75 meters

Assemblage	Percentage	Comments
Clay/Silt	25	No observable porosity
Carbonate	70	Subhedral
Pyrite	5	Anhedral

The T-3 interval is a very fine-grained, poorly sorted, well-consolidated and cemented shale that is black in color. The rock contains digenetic subhedral dolomite (70%), which has become the dominant phase in the sample. A significant percentage of clay (25%) is present in the sample, with approximately 5% pyrite. No porosity or fossil assemblages were observed in this sample (Figures 5-7). Despite high carbonate content, the sample appears very similar to the previous intervals in hand specimen.

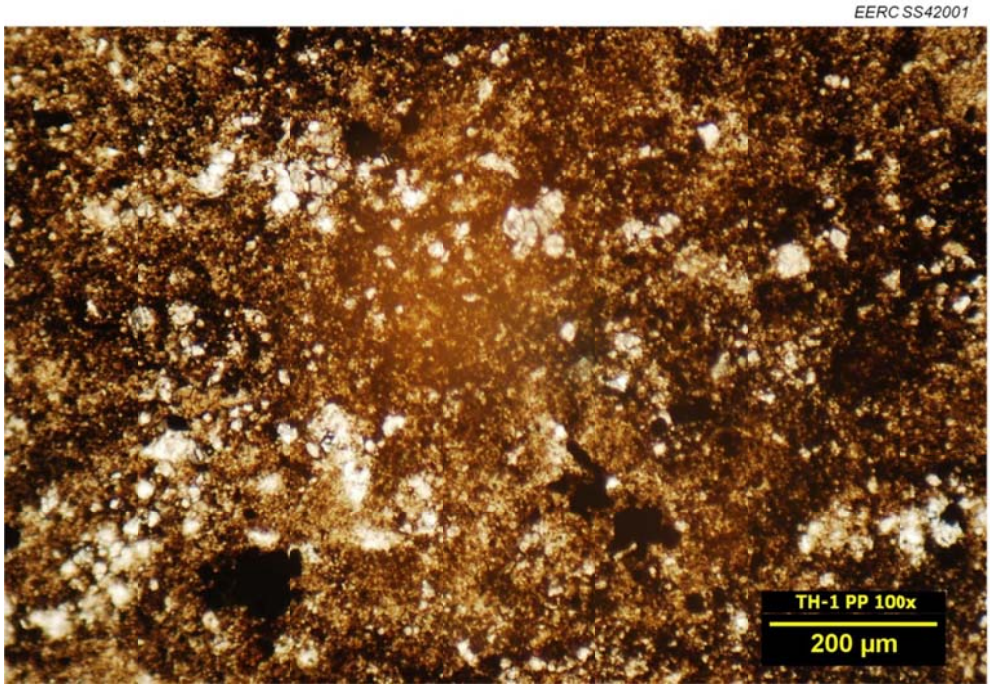

Figure B-1. Photomicrograph of TH-1, plane-polarized light, 100× magnification.

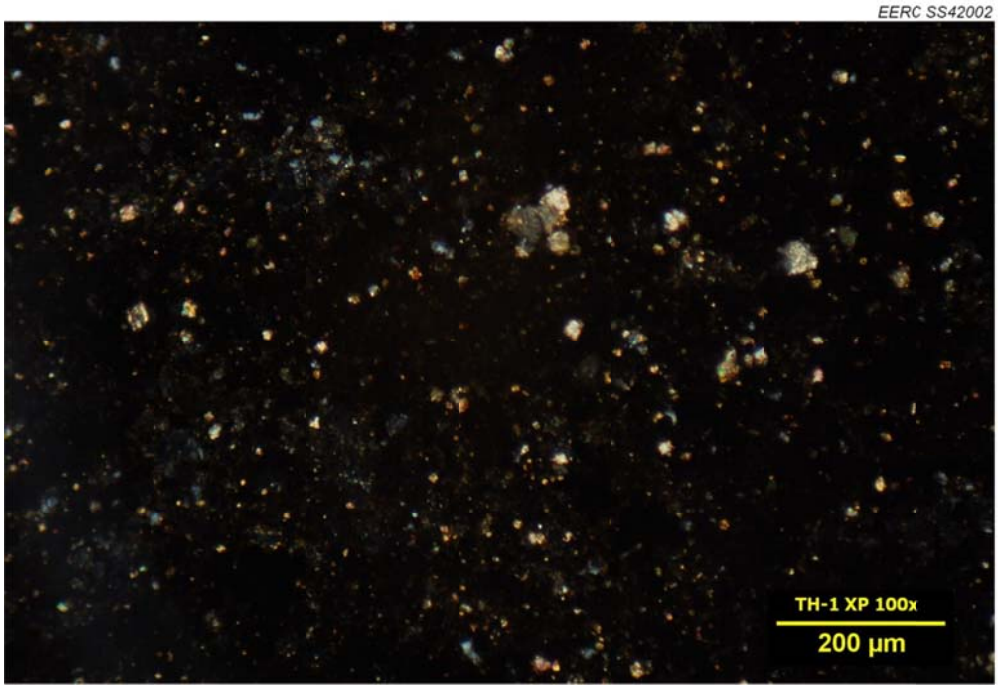

Figure B-2. Photomicrograph of TH-1, cross-polarized light, 100× magnification.

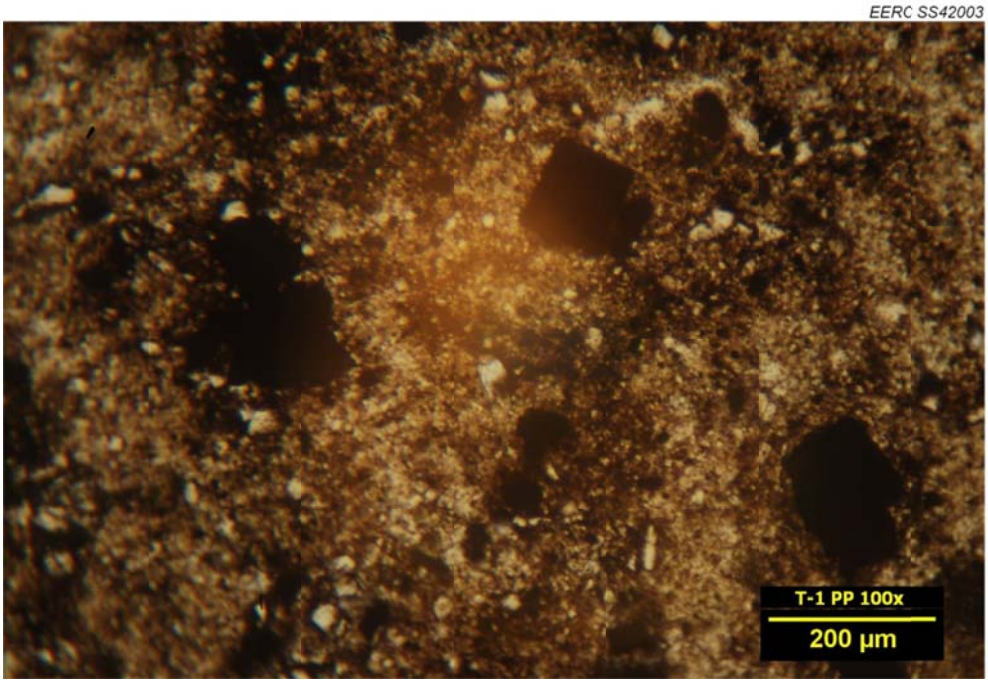

Figure B-3. Photomicrograph of T-1, plane-polarized light, 100× magnification.

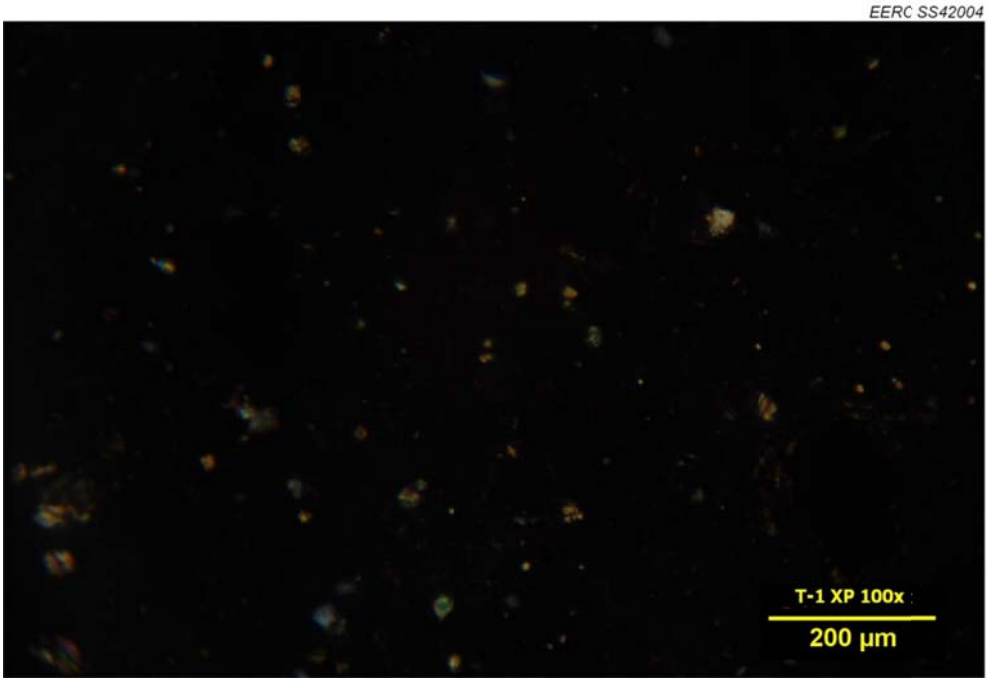

Figure B-4. Photomicrograph of T-1, cross-polarized light, 100× magnification.

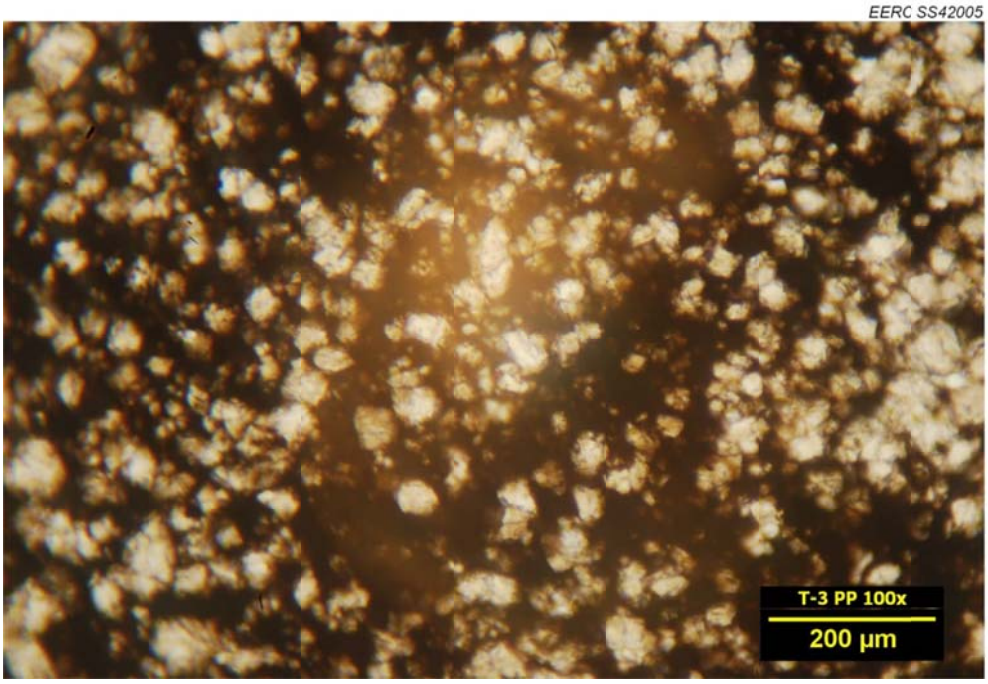

Figure B-5. Photomicrograph of T-3, plane-polarized light, 100× magnification.

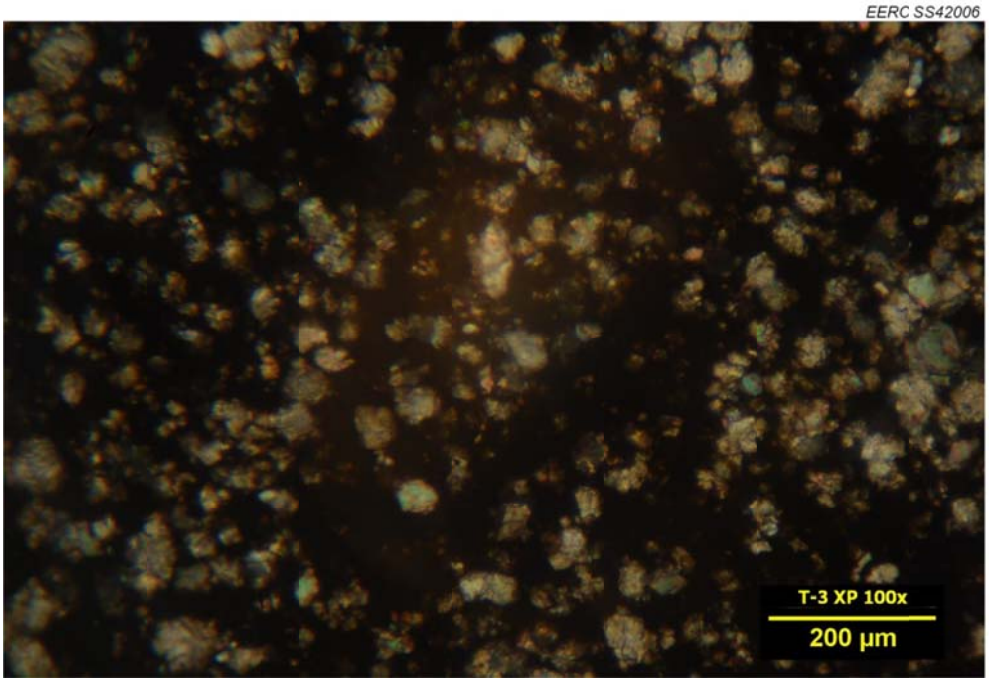

Figure B-6. Photomicrograph of T-3, cross-polarized light, 100× magnification.

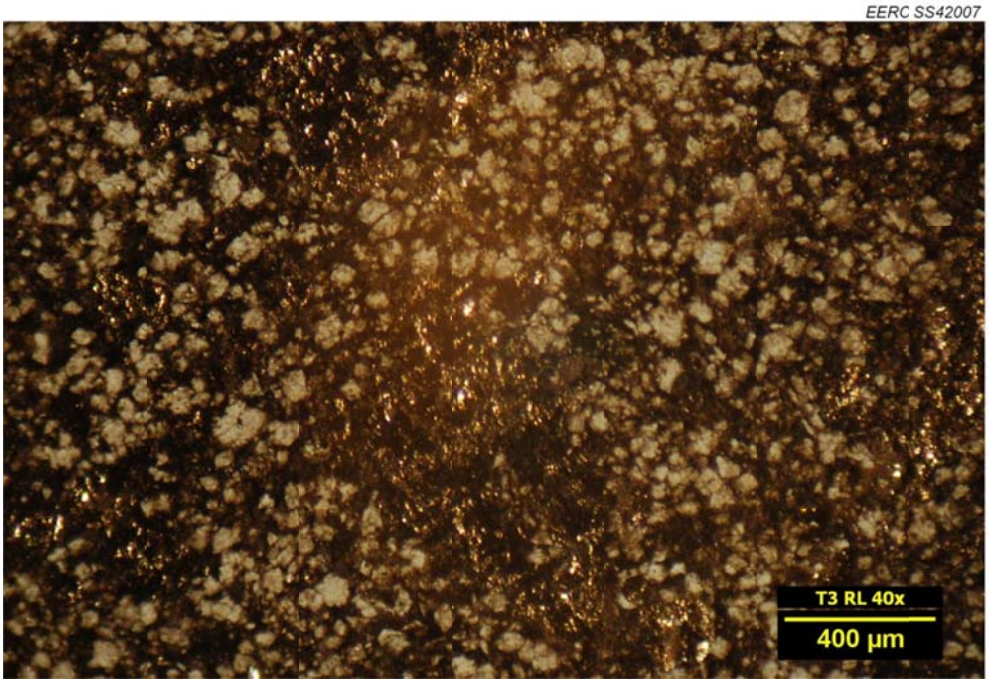

Figure B-7. Photomicrograph of T-3, reflected light, 40× magnification. Gold-colored reflective areas are high in pyrite, darker areas are primarily clay, and light areas are carbonates.

APPENDIX C

SCANNING ELECTRON MICROSCOPY (SEM)

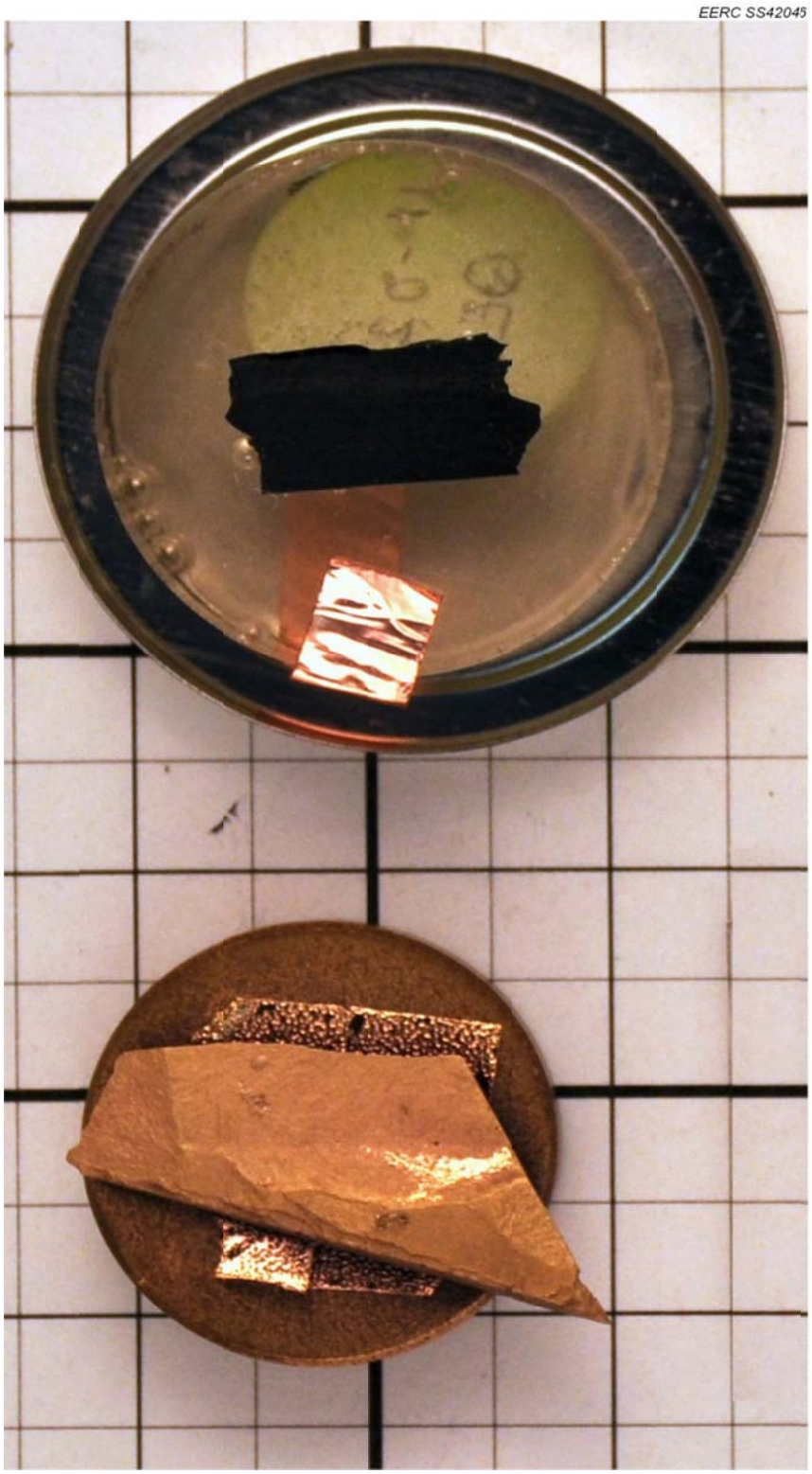

Figure C-1. Photograph of the TH-1 interval specimens after experiment. The polished epoxy-mounted sample (above) was used for SEM–EDS and QEMSEM, and fractured, gold-dusted SEM sample (below) was used for SEM imagery.

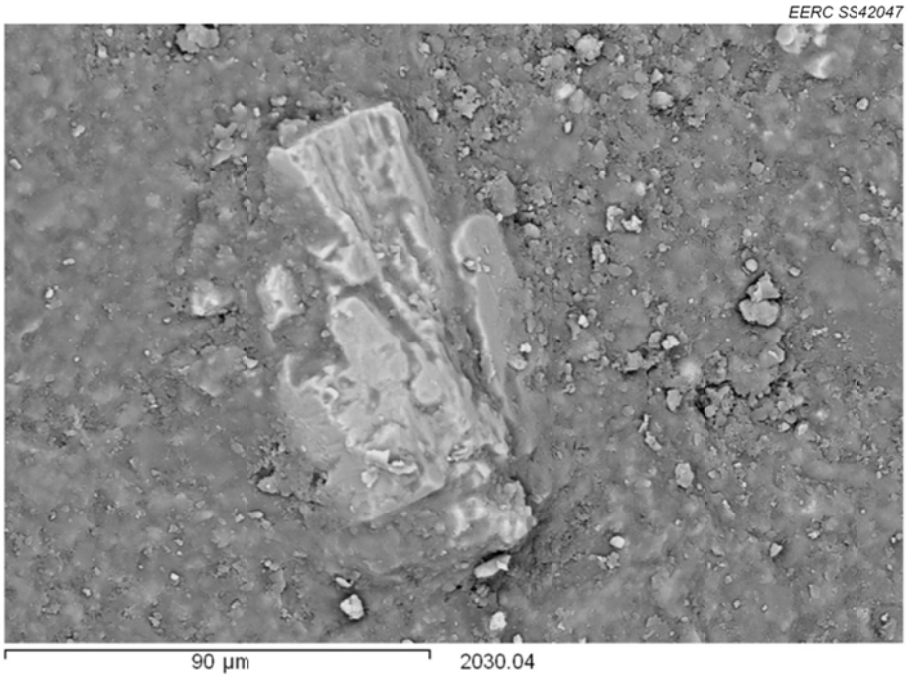

Figure C-2. SEM photomicrograph of TH-1, fractured, 750× magnification, showing pyrite growing out of the primarily illite matrix.

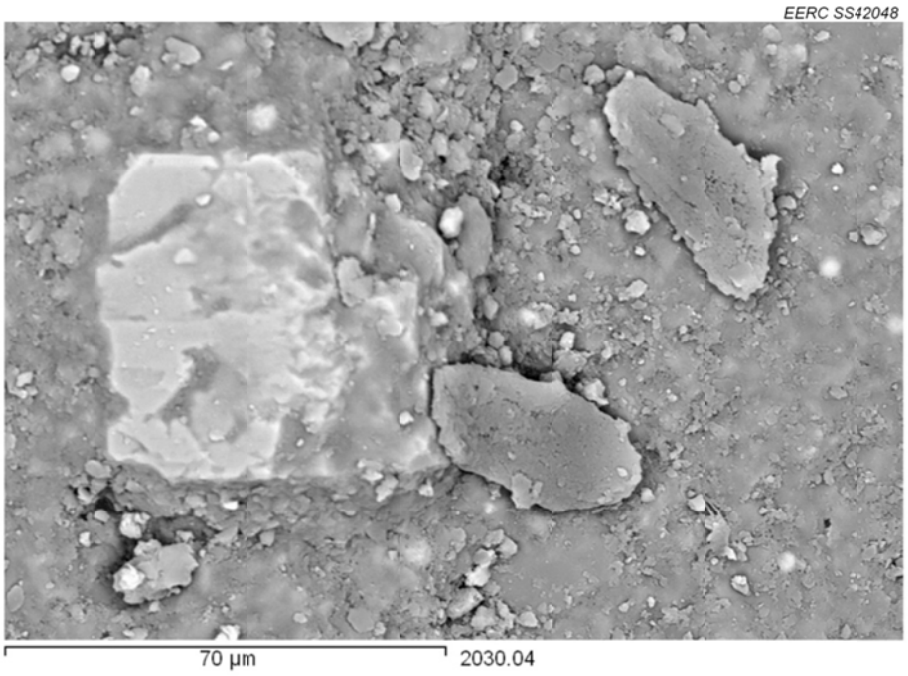

Figure C-3. SEM photomicrograph of TH-1, fractured, 1000× magnification, showing pyrite growing out of an illite matrix.

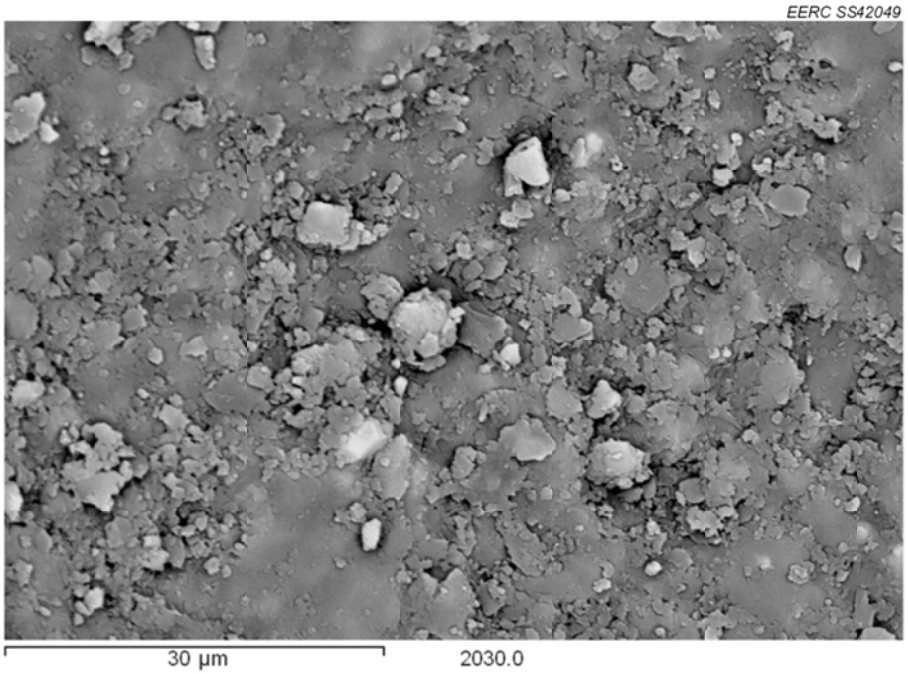

Figure C-4. SEM photomicrograph of TH-1, fractured, 2000× magnification, showing primarily illite clay.

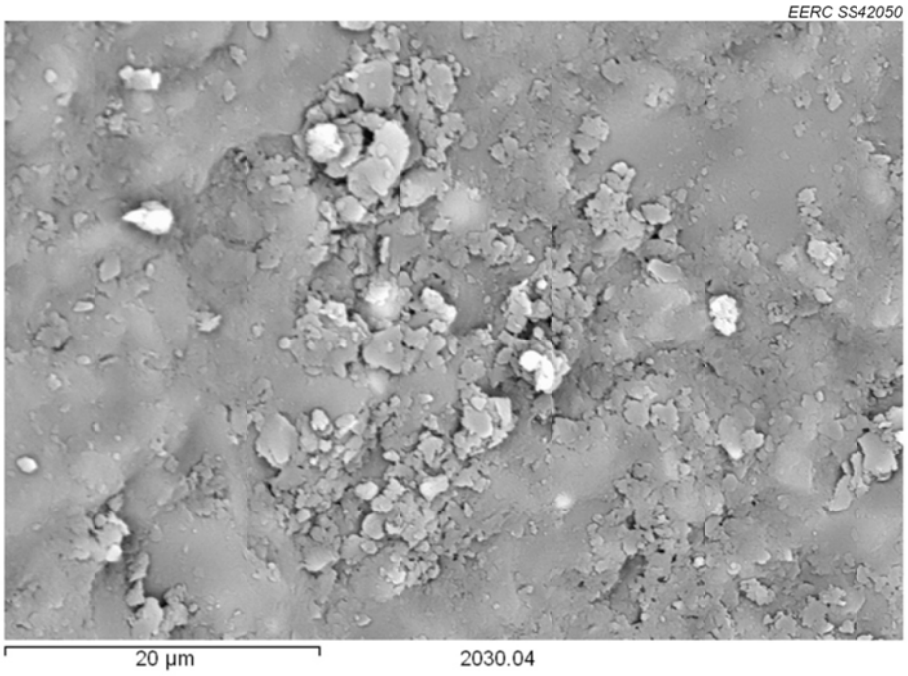

Figure C-5. SEM photomicrograph of TH-1, fractured, 5000× magnification, showing primarily illite clay.

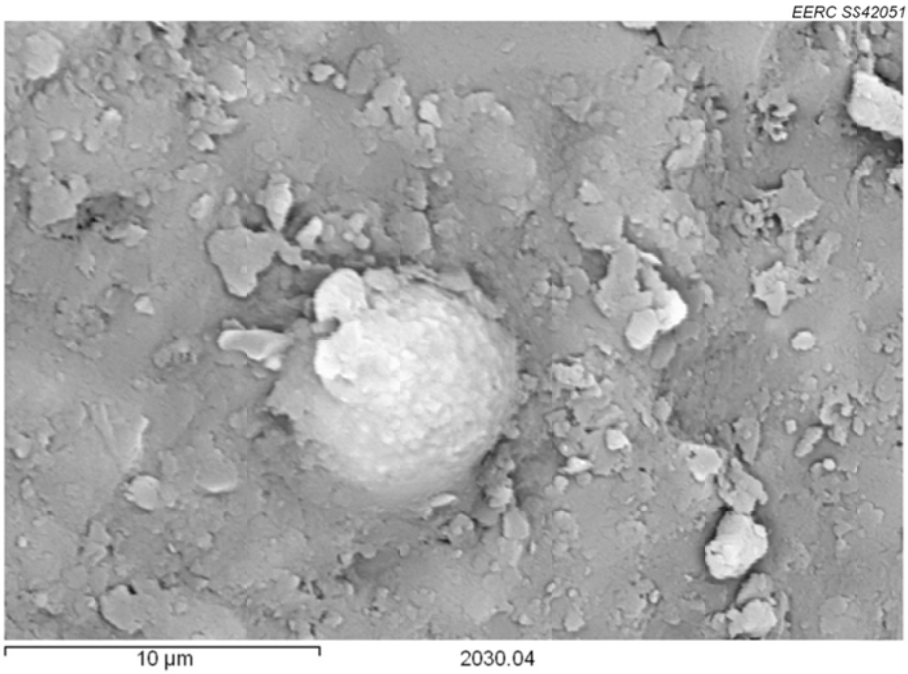

Figure C-6. SEM photomicrograph of TH-1, fractured, 5000× magnification, showing radial pyrite growth in clay.

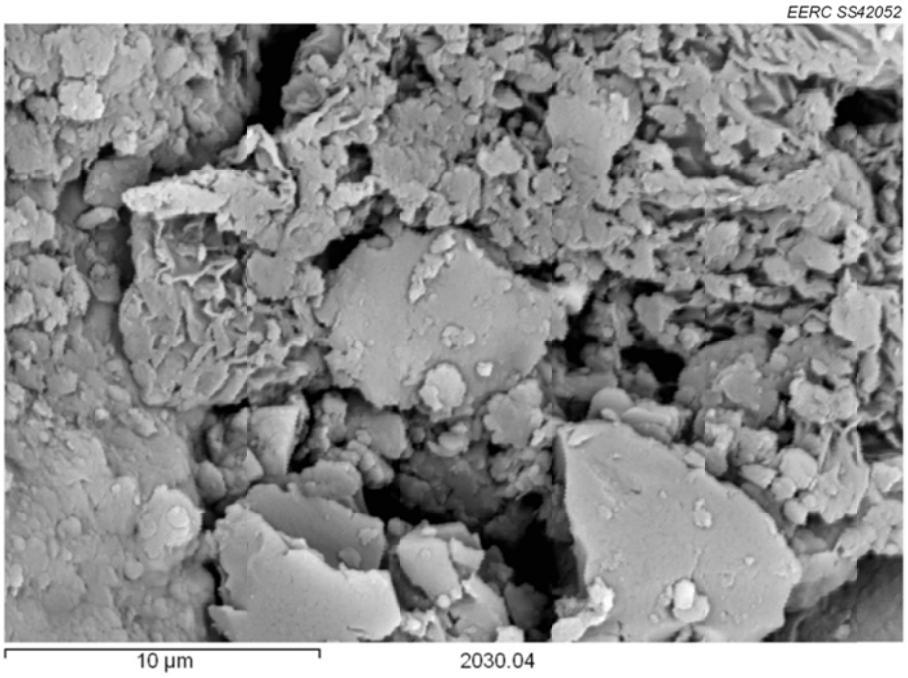

Figure C-7. SEM photomicrograph of TH-1, fractured, 5000× magnification, showing structure of clay matrix.

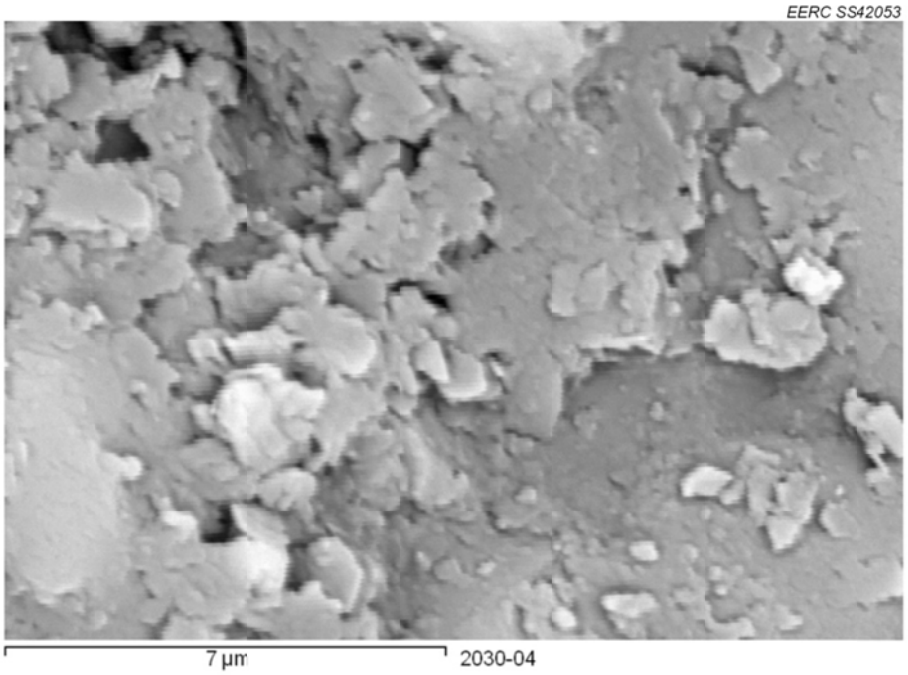

Figure C-8. SEM photomicrograph of TH-1, fractured, 10,000× magnification, showing structure of clay matrix.

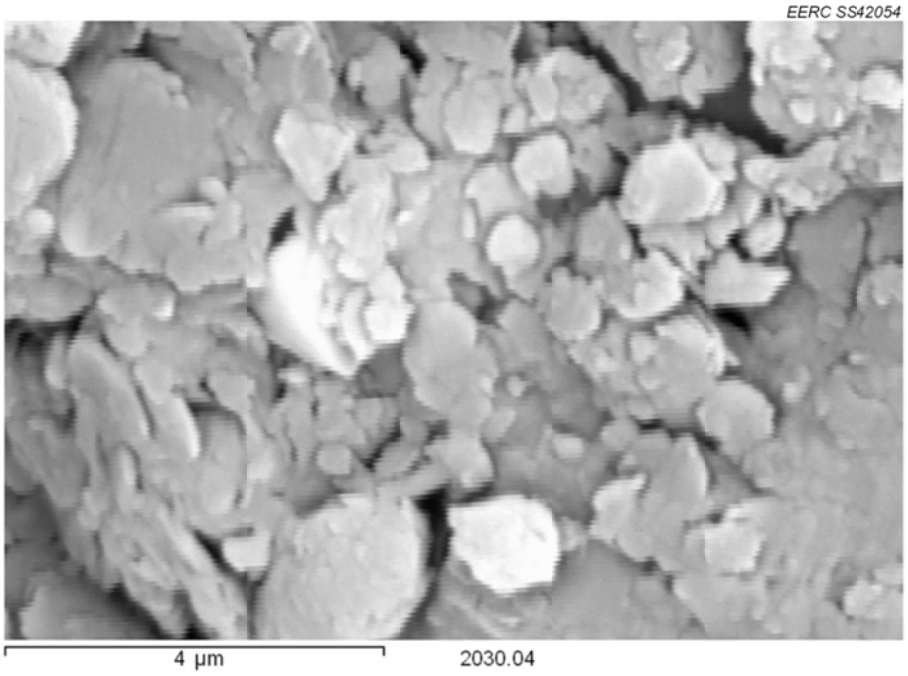

Figure C-9. SEM photomicrograph of TH-1, fractured, 15,000× magnification, showing structure of clay matrix.

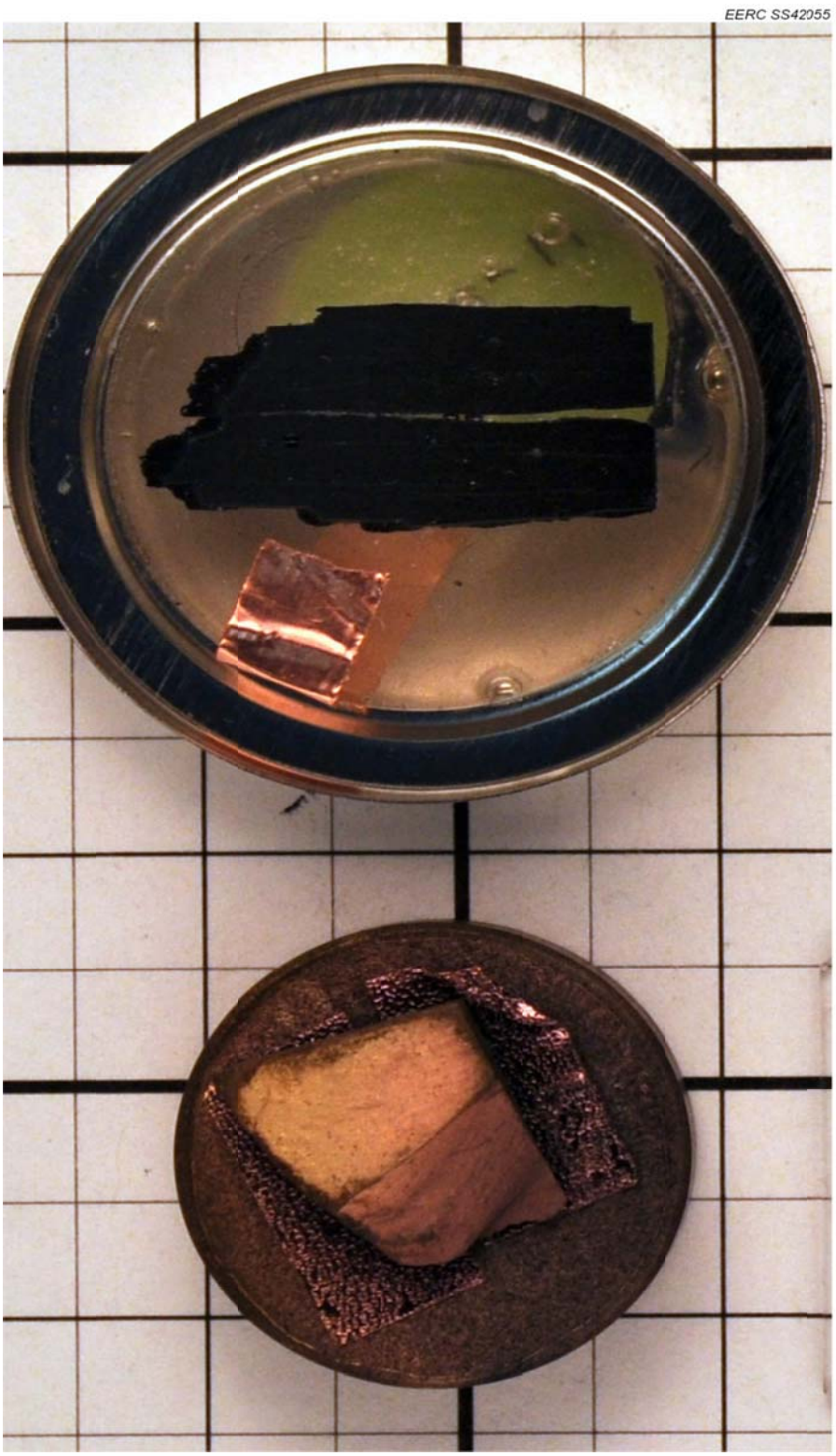

Figure C-10. Photograph of the T-1 specimens after experiment, the polished SEM sample (above) was used for SEM–EDS and QEMSEM measurements, while the fractured, gold-dusted SEM sample (below) was used for imagery.

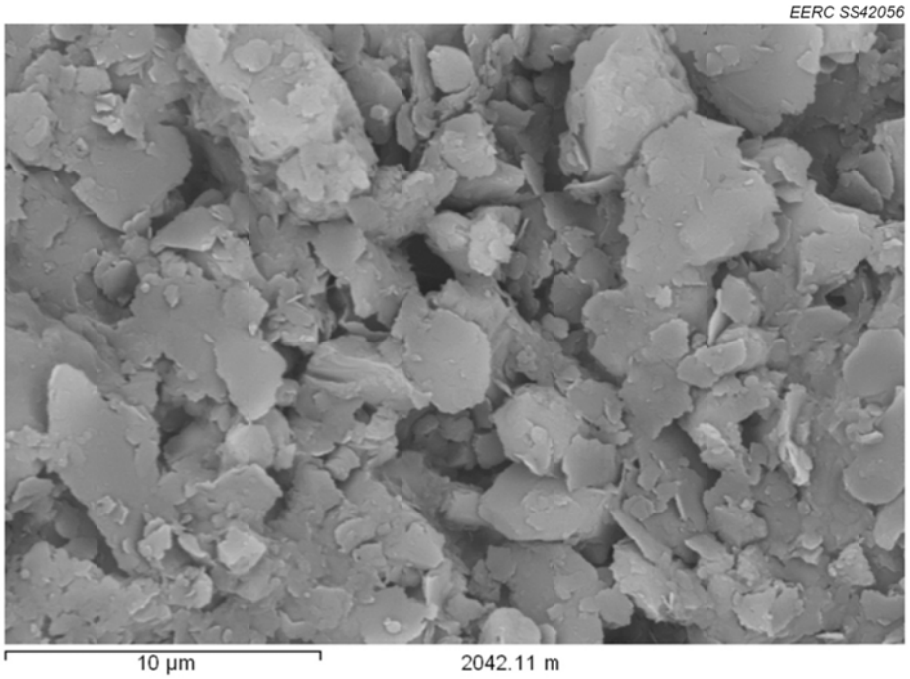

Figure C-11. SEM photomicrograph of T-1, fractured, 5000× magnification, showing structure of clays.

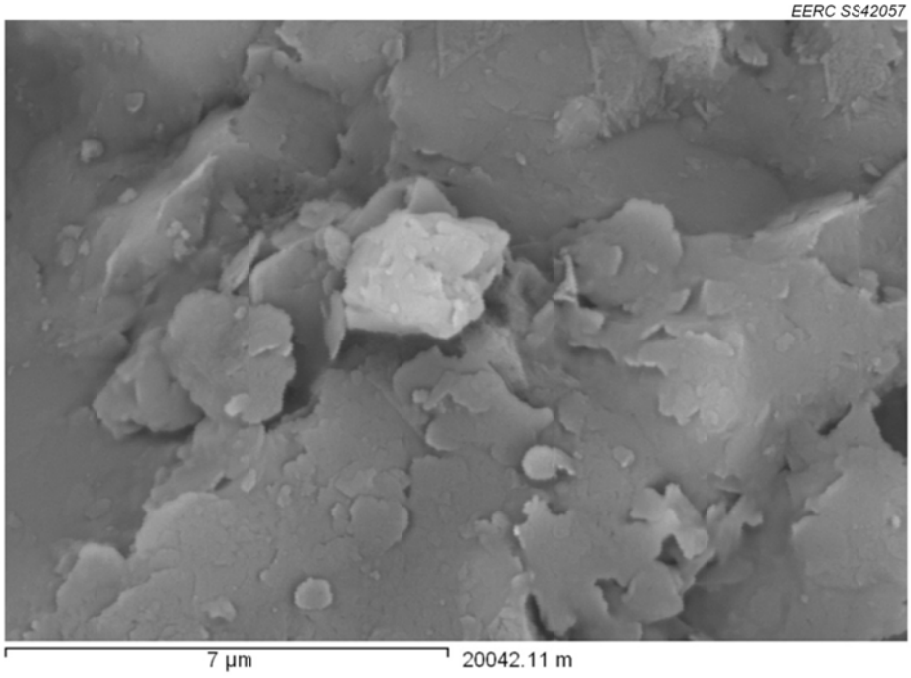

Figure C-12. SEM photomicrograph of T-1, fractured, 10,000× magnification, showing structure of clays.

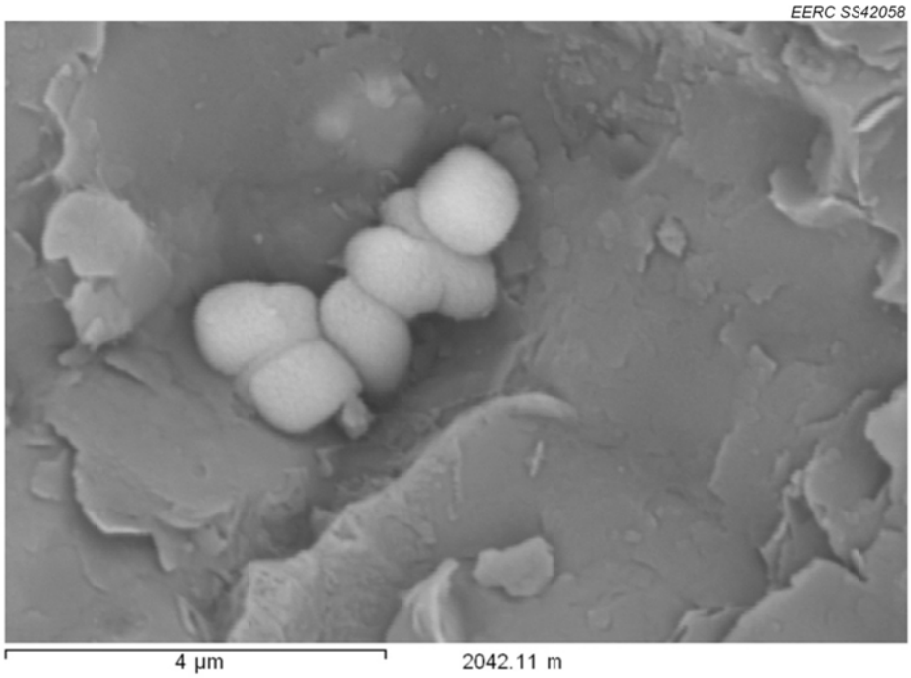

Figure C-13. SEM photomicrograph of T-1, fractured, 15,000× magnification, showing radial pyrite in illite.

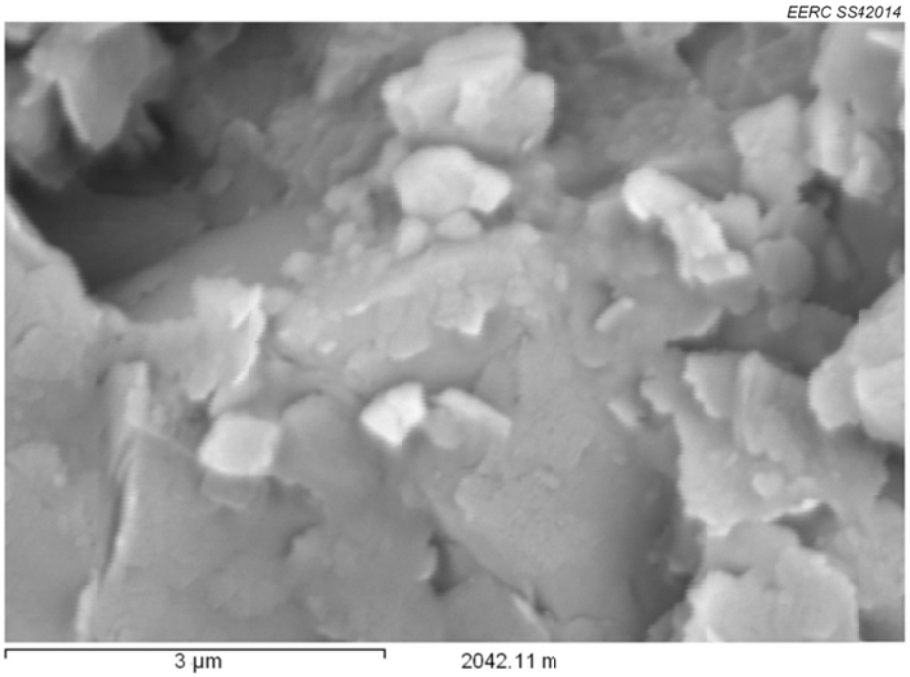

Figure C-14. SEM photomicrograph, of T-1, fractured, 20,000× magnification, showing clay structure.

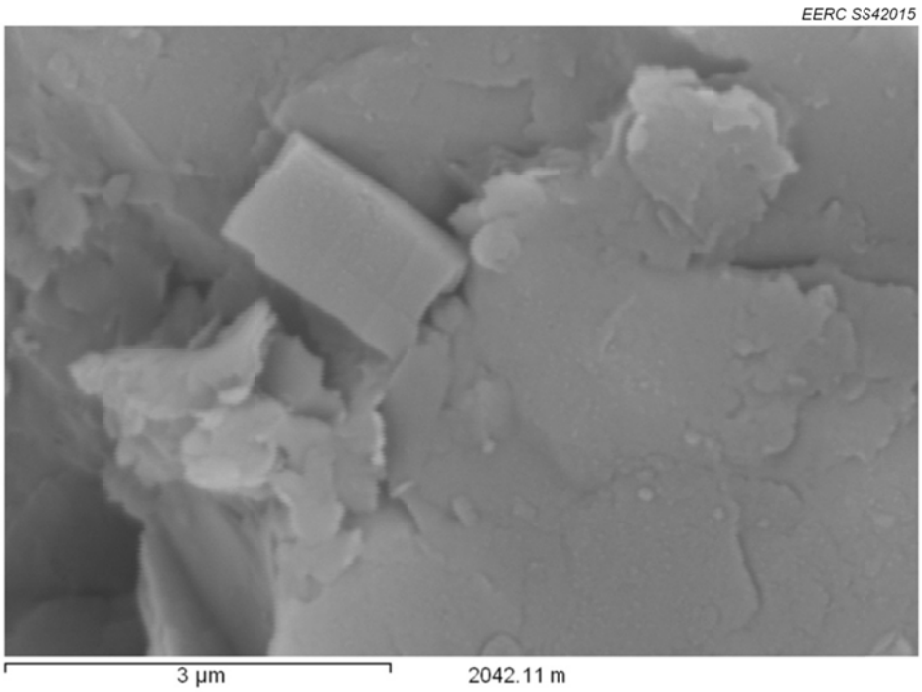

Figure C-15. SEM photomicrograph of T-1, fractured, 20,000× magnification, showing euhedral dolomite in illite.

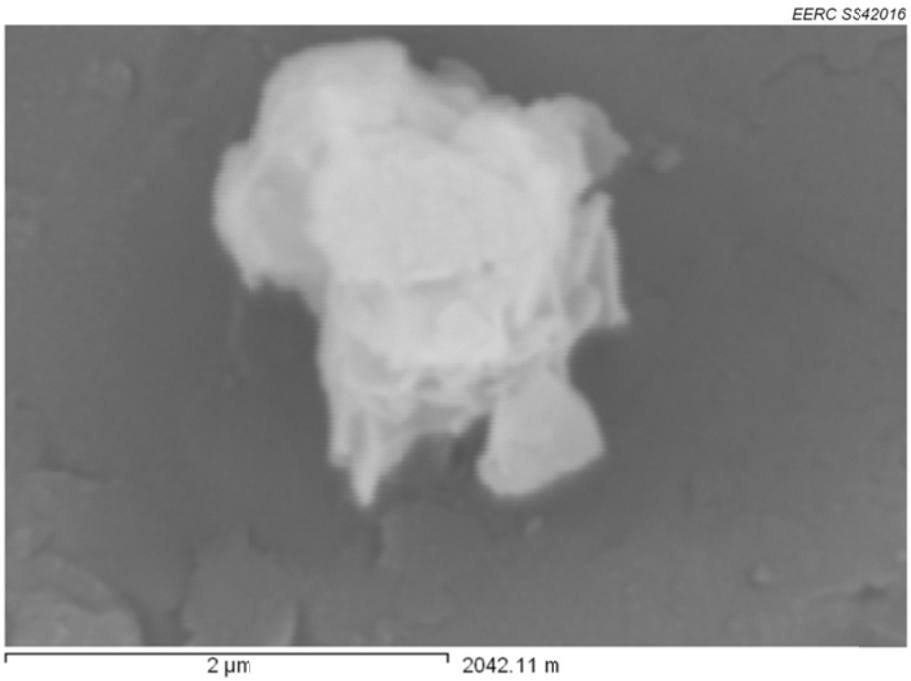

Figure C-16. SEM photomicrograph of T-1, fractured, 35,000× magnification, showing barite in pyrite.

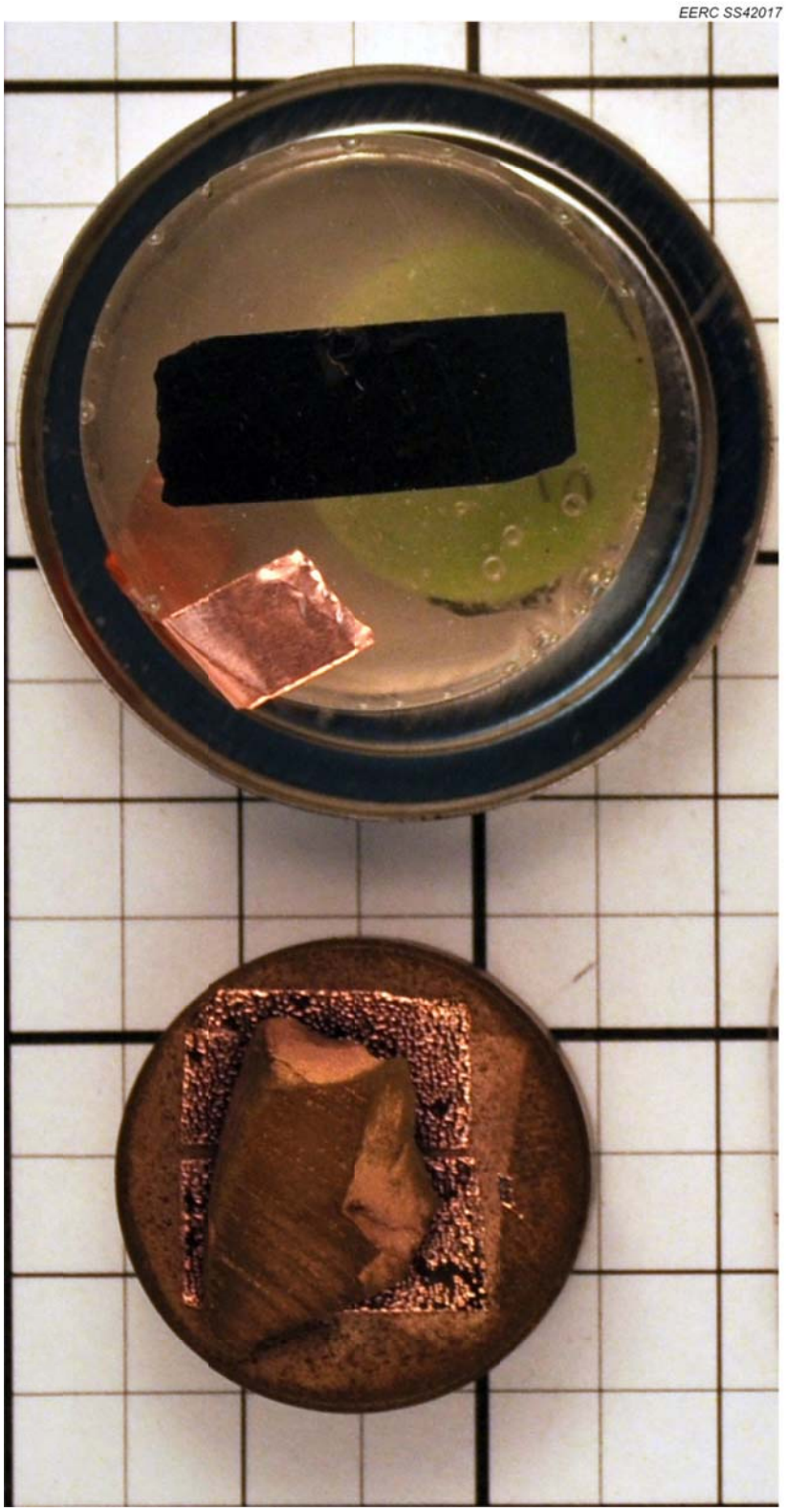

Figure C-17. Photograph of the T-3 specimens after experiment. The polished SEM sample (above) was used for SEM–EDS and QEMSEM measurements and the fractured, gold-dusted SEM sample (below) was used for imagery.

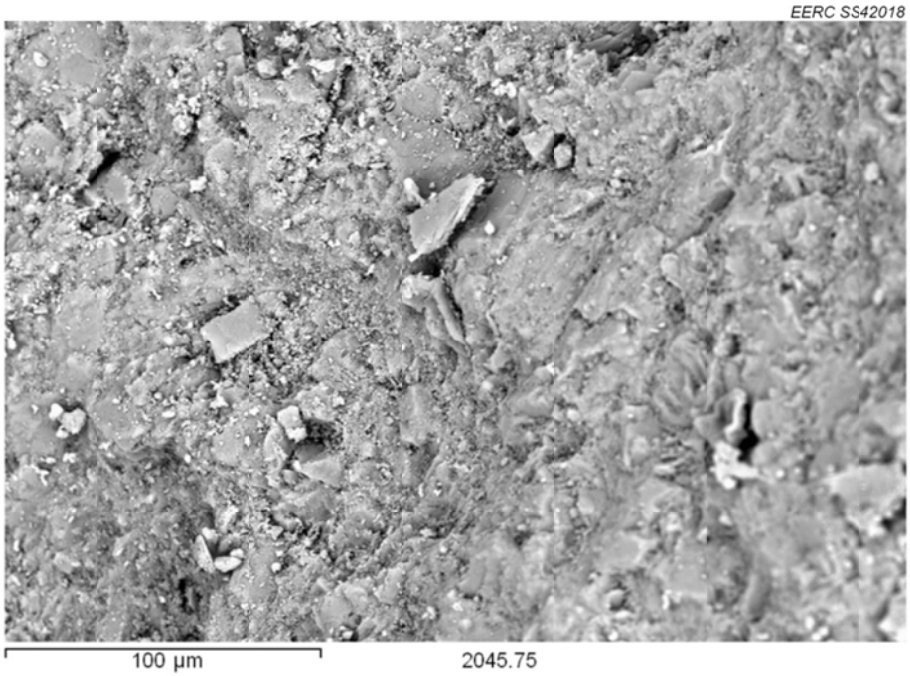

Figure C-18. SEM photomicrograph of T-3, fractured, 500× magnification, showing dolomite and clay structure.

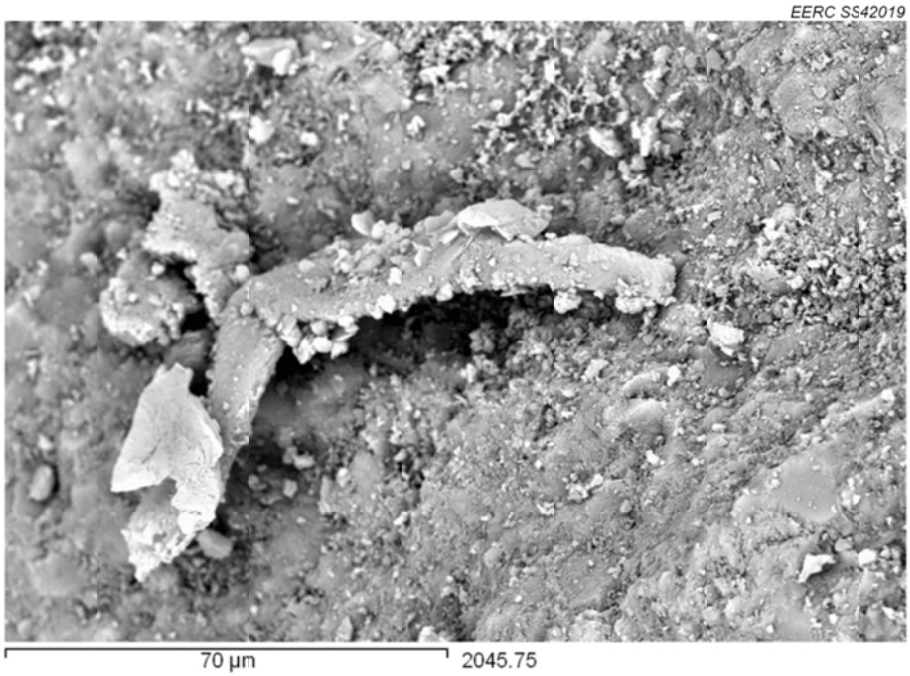

Figure C-19. SEM photomicrograph of T-3, fractured, 1000× magnification, showing intricate structures in the dolomite–clay matrix.

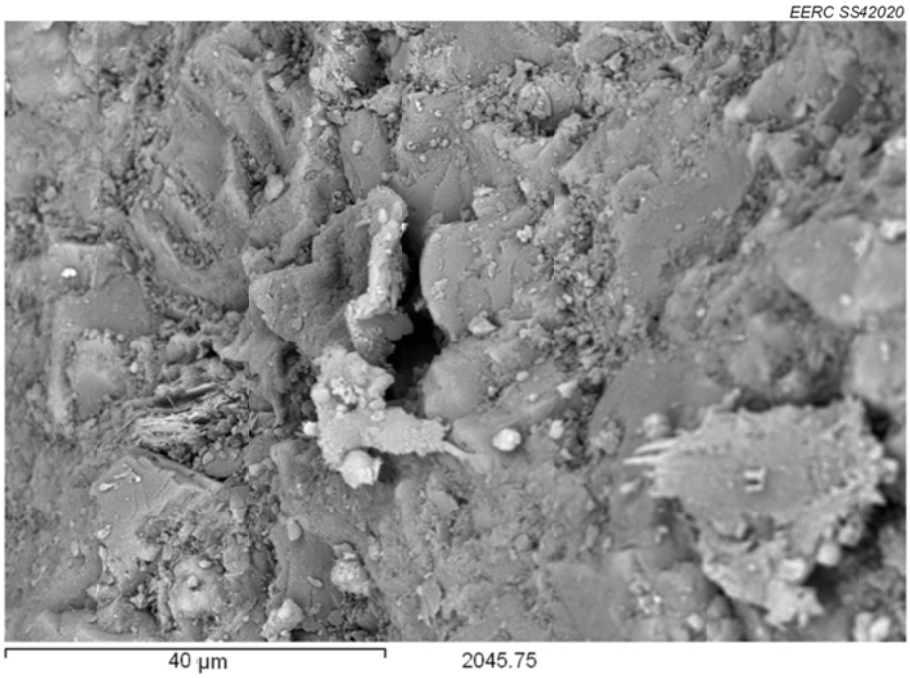

Figure C-20. SEM photomicrograph of T-3, fractured, 1500× magnification, showing mixed dolomite and clay matrix.

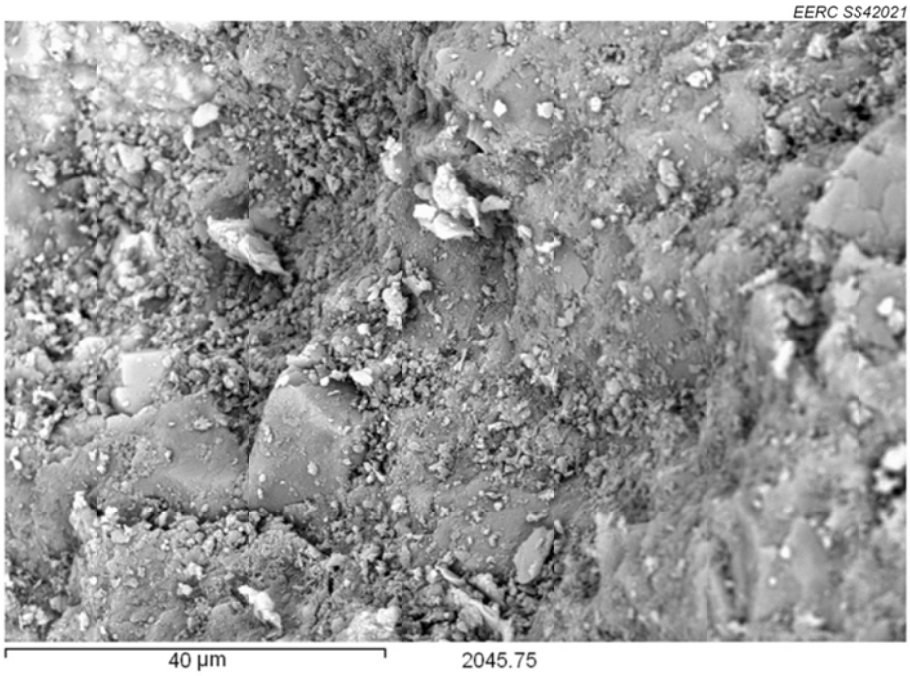

Figure C-21. SEM photomicrograph of T-3, fractured, 1500× magnification, showing dolomite and pyrite in illite clay.

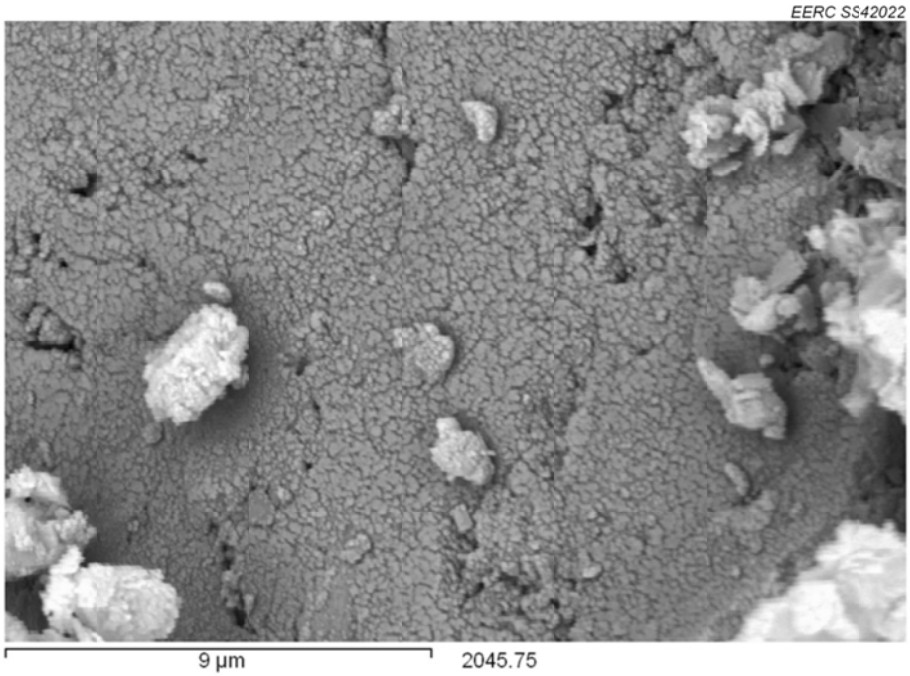

Figure C-22. SEM photomicrograph of T-3, fractured, 1500× magnification, showing pyrite on dolomite.

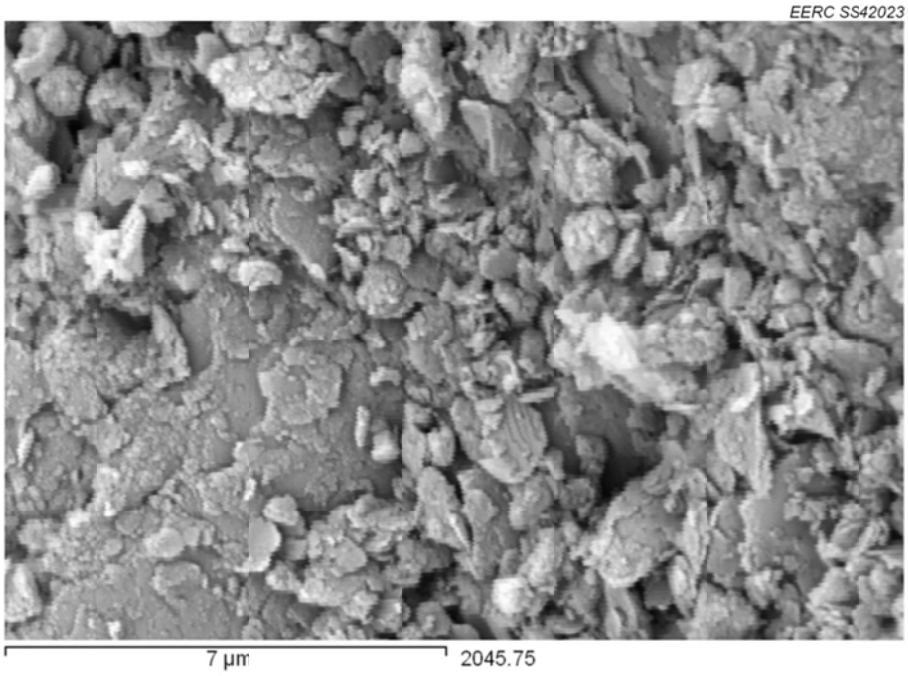

Figure C-23. SEM photomicrograph of T-3, fractured, 10,000× magnification, showing clay and dolomite structures.

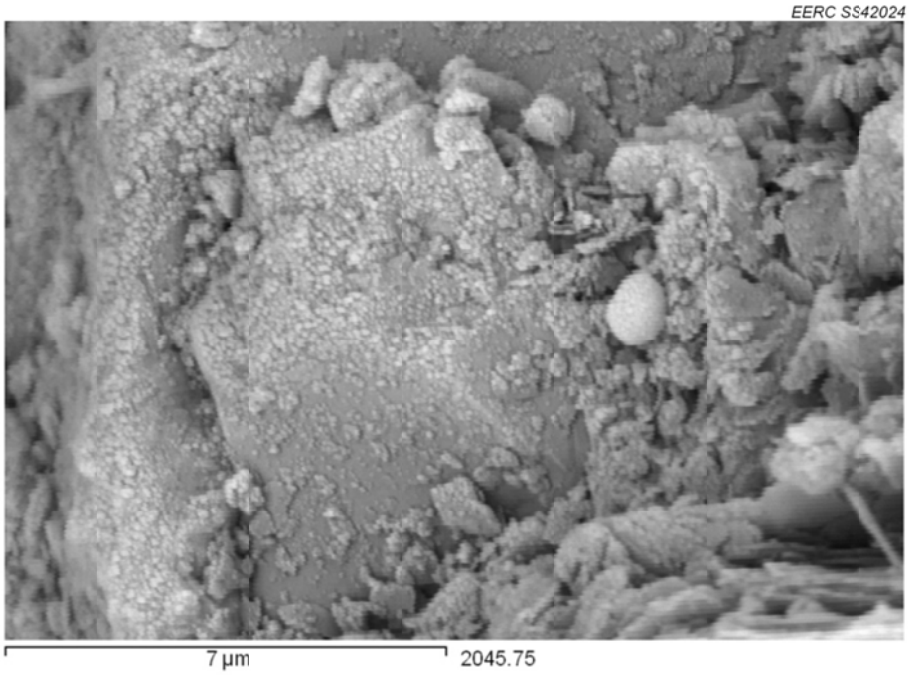

Figure C-24. SEM photomicrograph of T-3, fractured, 10,000× magnification, showing ultrafine pyrite on dolomite.

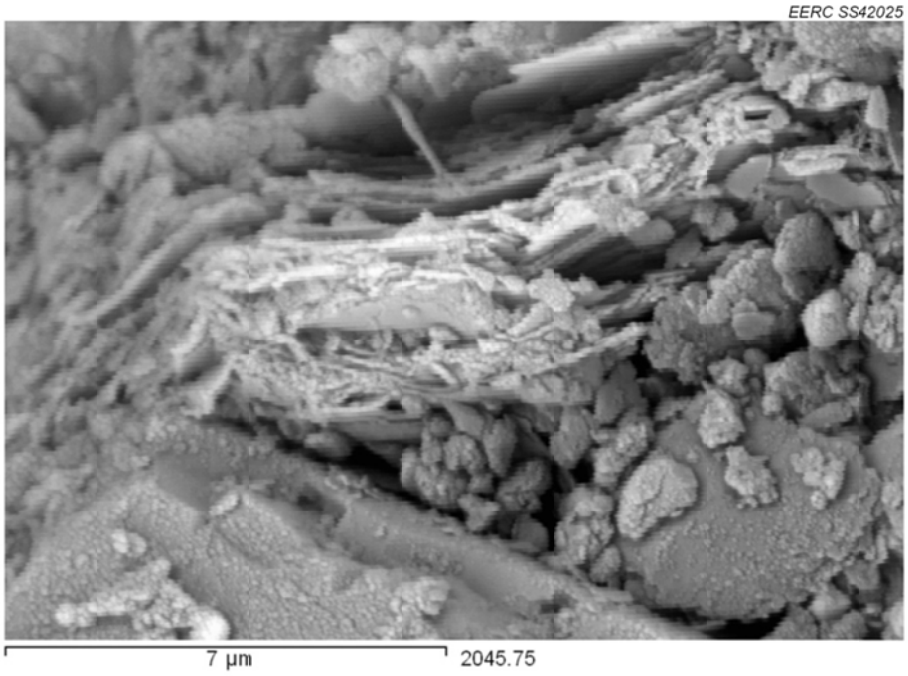

Figure C-25. SEM photomicrograph of T-3, fractured, 10,000× magnification, showing barite around pyrite and ultrafine pyrite on dolomite.

APPENDIX D

SEM–EDS DATA

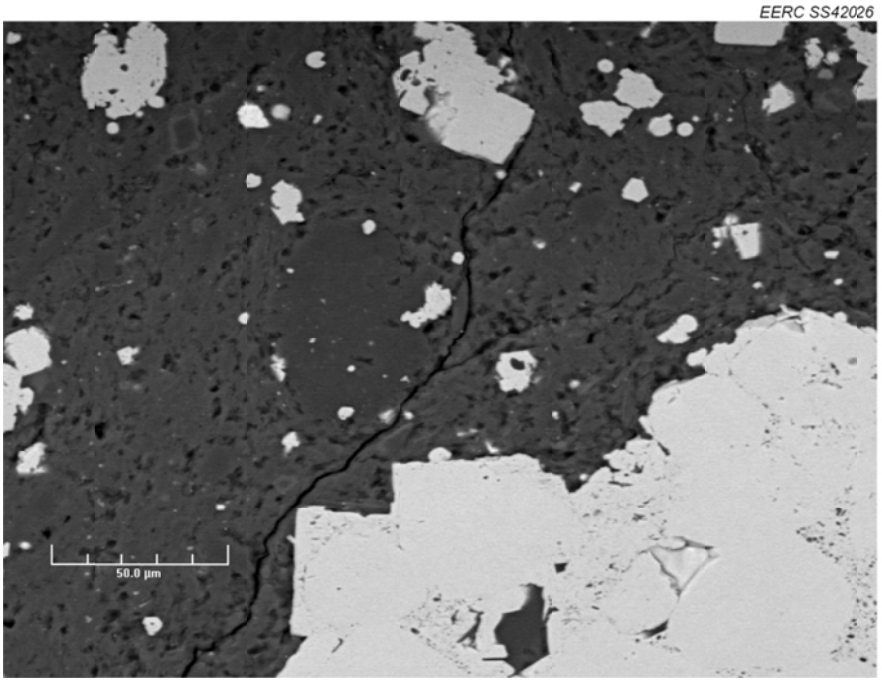

Figure D-1. Field for EDS testing on Sample TH-1 at 500× magnification. Yellow crosshairs indicate the tag number and location.

Table D-1. Results of SEM–EDS Measurements for Points Present in Figure D-1, wt%

Tag	Na	Mg	Al	Si	P	S	Cl	K	Ca	Ti	Fe	Ba	Mineralogy
1	0.00	0.00	1.24	93.07	0.33	1.67	0.00	2.74	0.00	0.01	0.93	0.00	**Clay**
2	0.00	0.00	0.39	95.44	0.00	0.89	0.00	2.66	0.00	0.00	0.62	0.00	**Quartz**
3	0.00	0.00	7.34	84.49	0.00	0.00	0.00	6.95	0.00	0.31	0.91	0.00	**Clay**
4	0.00	29.31	0.78	3.67	0.25	0.13	0.06	0.39	60.09	0.00	5.31	0.00	**Dolomite**
5	0.00	0.56	15.26	70.22	0.00	0.21	0.00	10.81	0.01	1.10	1.83	0.00	**Clay**
6	0.00	0.00	1.94	93.98	0.00	0.00	0.00	3.49	0.00	0.17	0.42	0.00	**Clay**
7	0.00	0.79	16.37	70.11	0.00	0.00	0.00	11.20	0.01	0.37	1.16	0.00	**Clay**
8	0.00	0.84	17.24	66.44	0.00	0.27	0.00	12.81	0.00	0.10	2.30	0.00	**Clay**
9	0.00	0.00	0.00	0.05	0.33	55.57	0.35	0.00	0.04	1.57	42.10	0.00	**Pyrite**
10	0.00	0.00	2.190	2.12	0.11	53.19	0.14	0.25	0.00	1.48	40.53	0.00	**Pyrite**

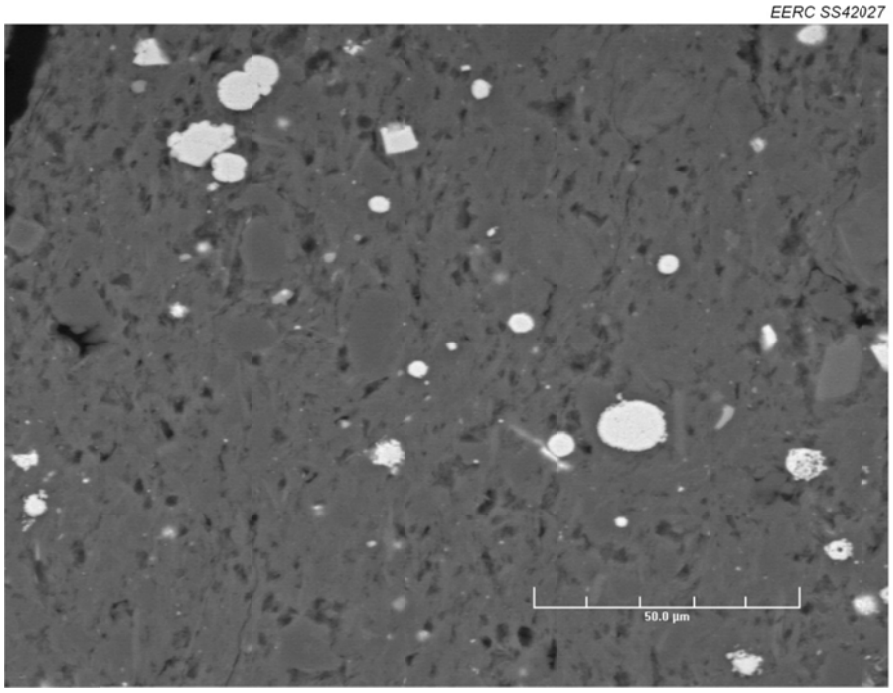

Figure D-2. Field for EDS testing on Sample TH-1 at 750× magnification. Yellow crosshairs indicate the tag number and location.

Table D-2. Results of SEM–EDS Measurements for Points Present in Figure D-2, wt%

Tag	Na	Mg	Al	Si	P	S	Cl	K	Ca	Ti	Fe	Ba	Mineralogy
1	0.00	12.59	7.63	28.23	0.00	0.02	0.00	5.27	33.09	0.23	12.93	0.00	**Dolomite**
2	0.00	0.00	3.74	88.94	0.00	1.18	0.00	4.80	0.00	0.02	1.32	0.00	**Clay**
3	0.00	0.00	4.27	89.67	0.00	0.00	0.00	5.33	0.00	0.06	0.67	0.00	**Clay**
4	0.00	0.00	2.35	92.88	0.00	0.00	0.00	4.06	0.00	0.09	0.61	0.00	**Clay**
5	0.00	0.00	4.16	89.86	0.00	0.00	0.00	5.11	0.00	0.08	0.69	0.09	**Clay**
6	0.00	1.34	22.26	55.58	0.00	0.00	0.00	16.63	0.06	1.01	2.96	0.16	**Clay**
7	0.00	1.57	21.35	50.44	0.00	0.00	0.00	17.48	0.14	0.06	7.82	1.14	**Clay**
8	0.00	0.40	9.63	79.23	0.00	0.00	0.00	9.62	0.00	0.00	1.11	0.00	**Clay**
9	0.00	0.75	15.68	69.92	0.00	0.00	0.00	11.31	0.09	0.37	1.48	0.39	**Clay**
10	0.00	0.35	11.71	76.40	0.00	0.00	0.00	9.64	0.07	0.38	1.18	0.28	**Clay**

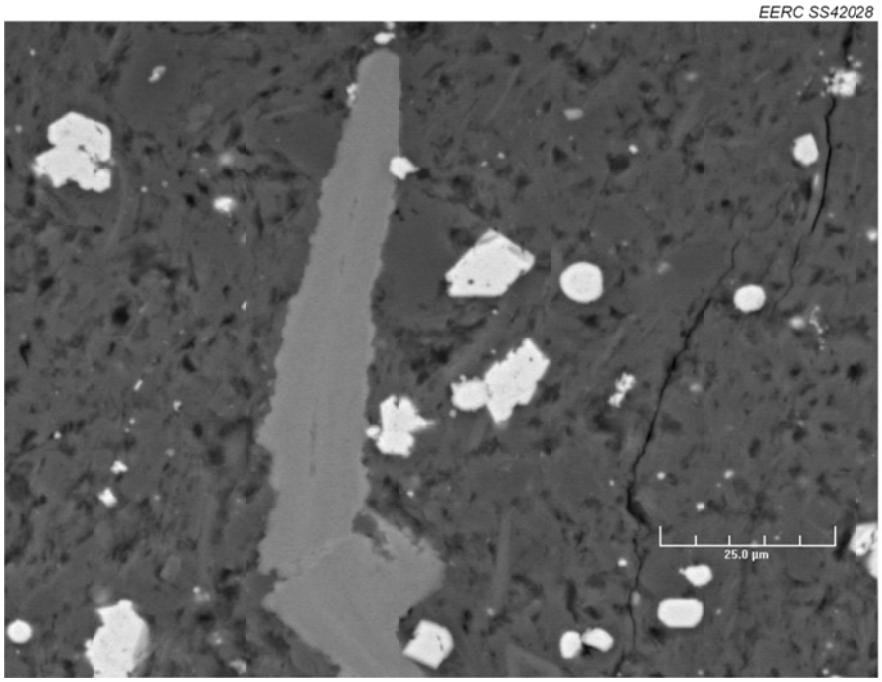

Figure D-3. Field for EDS testing on Sample TH-1 at 1000× magnification. Yellow crosshairs indicate the tag number and location.

Table D-3. Results of SEM–EDS Measurements for Points Present in Figure D-3, wt%

Tag	Na	Mg	Al	Si	P	S	Cl	K	Ca	Ti	Fe	Ba	Mineralogy
1	0.00	0.00	2.99	92.77	0.00	0.00	0.00	3.96	0.00	0.00	0.27	0.00	**Clay**
2	0.00	0.00	1.03	95.11	0.00	0.00	0.00	2.79	0.74	0.00	0.32	0.00	**Quartz**
3	0.00	0.00	0.05	96.95	0.00	0.25	0.00	2.29	0.00	0.00	0.45	0.00	**Quartz**
4	0.00	0.41	13.18	73.80	0.00	0.00	0.00	10.64	0.00	0.71	1.26	0.00	**Clay**
5	0.00	0.84	19.85	55.91	0.58	2.11	0.00	12.62	2.69	1.61	3.79	0.00	**Clay**
6	0.00	0.74	15.83	70.26	0.00	0.08	0.00	11.47	0.00	0.19	1.33	0.10	**Clay**
7	0.00	0.00	0.00	0.51	32.96	0.00	0.00	0.08	66.25	0.00	0.20	0.00	**Apatite**
8	0.00	0.00	0.04	0.51	33.27	0.00	0.00	0.06	65.85	0.00	0.28	0.00	**Apatite**
9	0.00	0.00	0.74	1.62	0.16	54.55	0.04	0.22	0.00	1.34	41.33	0.00	**Pyrite**
10	0.00	0.00	0.05	0.60	0.15	55.53	0.17	0.01	0.00	1.46	42.02	0.00	**Pyrite**

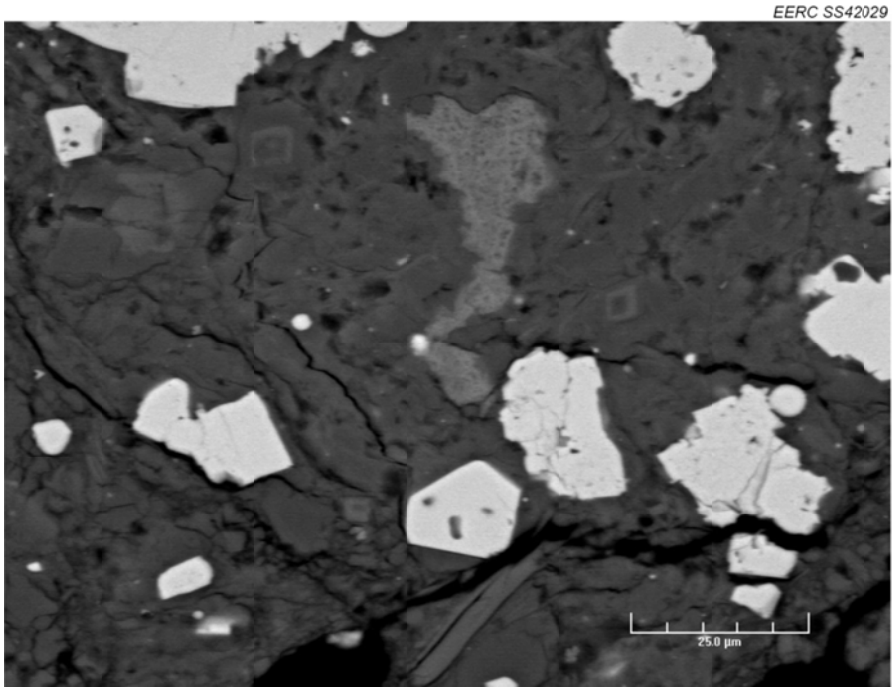

Figure D-4. Field for EDS testing on Sample TH-1 at 1000× magnification. Yellow crosshairs indicate the tag number and location.

Table D-4. Results of SEM–EDS Measurements for Points Present in Figure D-4, wt%

Tag	Na	Mg	Al	Si	P	S	Cl	K	Ca	Ti	Fe	Ba	Mineralogy
1	0.00	30.90	0.55	2.02	0.35	0.51	0.00	0.11	64.61	0.00	0.94	0.00	**Dolomite**
2	0.00	18.14	1.86	5.53	0.25	0.09	0.00	0.95	51.00	0.00	22.19	0.00	**Dolomite**
3	0.00	23.72	0.54	4.00	0.42	0.18	0.07	0.31	59.60	0.45	10.70	0.00	**Dolomite**
4	0.00	25.89	1.44	4.91	0.21	0.01	0.00	0.71	55.01	0.00	11.80	0.00	**Dolomite**
5	0.00	0.00	0.00	0.42	32.71	0.68	0.00	0.00	66.07	0.00	0.13	0.00	**Apatite**
6	0.00	0.00	0.60	3.34	32.10	0.62	0.00	0.36	62.78	0.00	0.19	0.00	**Apatite**
7	0.06	0.73	25.39	50.34	0.00	0.00	0.00	16.93	0.17	0.79	4.76	0.82	**Clay**
8	0.00	0.48	14.56	71.84	0.00	0.00	0.00	11.15	0.00	0.54	1.43	0.00	**Clay**
9	0.00	0.00	0.05	0.04	0.18	55.54	0.15	0.00	0.00	1.42	42.62	0.00	**Pyrite**
10	0.00	0.00	0.16	0.58	0.15	55.37	0.05	0.00	0.00	1.36	42.33	0.00	**Pyrite**

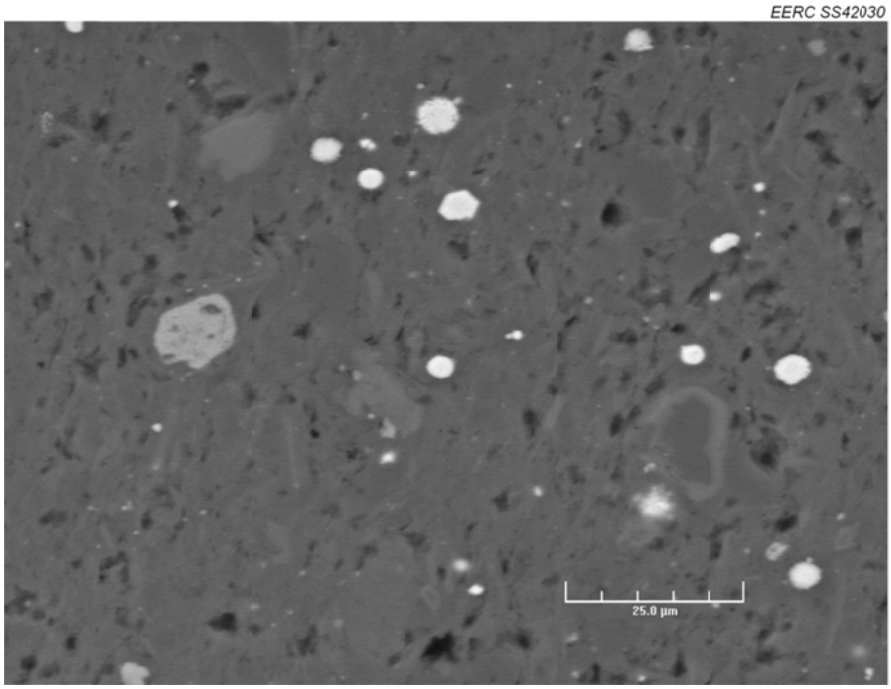

Figure D-5. Field for EDS testing on Sample TH-1 at 1000× magnification. Yellow crosshairs indicate the tag number and location.

Table D-5. Results of SEM–EDS Measurements for Points Present in Figure D-5, wt%

Tag	Na	Mg	Al	Si	P	S	Cl	K	Ca	Ti	Fe	Ba	Mineralogy
1	0.00	12.90	0.31	1.31	0.29	0.07	0.00	0.09	53.60	0.00	31.44	0.00	**Dolomite**
2	0.00	15.28	2.93	12.81	0.43	0.19	0.00	1.88	45.60	0.00	20.89	0.00	**Ankerite**
3	0.00	1.25	22.94	57.21	0.00	0.00	0.00	15.74	0.13	0.36	2.34	0.03	**Clay**
4	0.02	32.86	0.00	0.44	0.50	0.01	0.00	0.00	65.30	0.00	0.87	0.00	**Dolomite**
5	0.00	18.49	1.38	4.55	0.27	0.36	0.00	0.39	50.41	0.00	24.15	0.00	**Ankerite**
6	0.00	0.00	1.33	94.90	0.00	0.00	0.00	3.44	0.00	0.00	0.34	0.00	**Clay**
7*	0.00	0.00	32.53	17.24	33.10	0.29	0.00	3.96	2.45	0.00	0.04	10.39	**Clay**
8	0.00	0.00	1.84	93.86	0.44	0.00	0.00	3.54	0.00	0.00	0.33	0.00	**Clay**
9	0.00	3.89	4.83	60.91	0.00	0.00	0.00	3.18	21.93	0.00	5.27	0.00	**Clay**
10	0.00	0.61	16.99	67.97	0.00	0.00	0.00	12.35	0.00	0.72	1.36	0.00	**Clay**

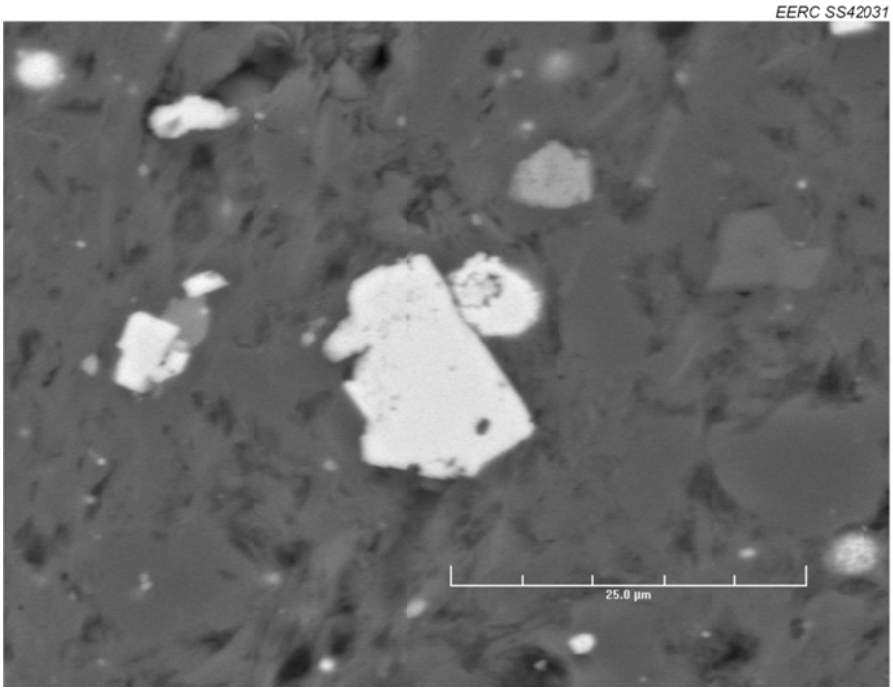

Figure D-6. Field for EDS testing on Sample TH-1 at 2000× magnification. Yellow crosshairs indicate the tag number and location.

Table D-6. Results of SEM–EDS Measurements for Points Present in Figure D-6, wt%

Tag	Na	Mg	Al	Si	P	S	Cl	K	Ca	Ti	Fe	Ba	Mineralogy
1	0.00	0.00	5.36	14.21	21.25	10.98	0.00	2.70	37.87	0.00	7.63	0.00	**Multiple**
2	0.00	0.00	4.51	8.73	0.00	0.46	0.00	1.59	0.01	84.05	0.64	0.00	**High-Ti**
3	0.00	17.76	1.67	6.34	0.08	0.00	0.00	0.68	49.37	0.00	24.10	0.00	**Dolomite**
4	0.00	0.00	2.92	92.11	0.00	0.15	0.00	4.14	0.00	0.00	0.67	0.00	**Clay**
5	0.00	0.07	5.27	86.08	0.00	1.56	0.00	5.74	0.00	0.04	1.25	0.00	**Clay**
6	0.00	0.00	1.44	94.93	0.00	0.00	0.00	3.15	0.00	0.00	0.46	0.02	**Clay**
7	0.00	0.00	0.40	96.40	0.00	0.05	0.15	2.66	0.00	0.00	0.34	0.00	**Quartz**
8	0.00	0.00	0.94	1.72	0.24	54.07	0.24	0.25	0.33	1.34	40.85	0.00	**Pyrite**
9	0.00	0.00	0.00	0.00	0.26	55.47	0.14	0.00	0.11	1.54	42.47	0.00	**Pyrite**
10	0.00	0.00	3.87	91.51	0.00	0.00	0.00	4.30	0.00	0.00	0.32	0.00	**Clay**

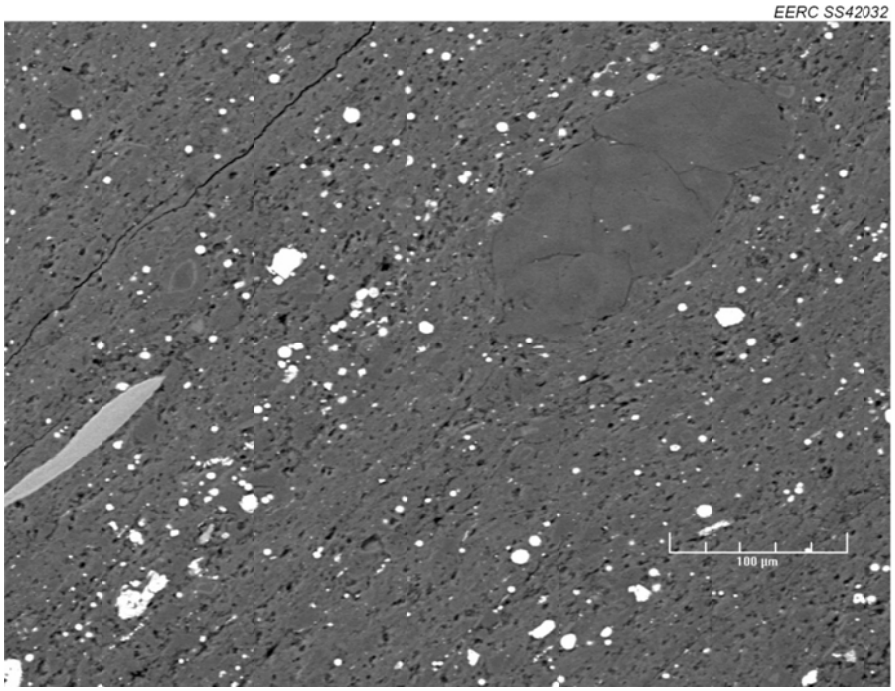

Figure D-7. Field for EDS testing on Sample T-1 at 250× magnification. Yellow crosshairs indicate the tag number and location.

Table D-7. Results of SEM–EDS Measurements for Points Present in Figure D-7, wt%

Tag	Na	Mg	Al	Si	P	S	Cl	K	Ca	Ti	Fe	Ba	Zn	Mineralogy
1	0.00	29.79	0.38	1.12	0.55	0.00	0.00	0.14	67.56	0.00	0.25	0.00	0.20	**Dolomite**
2	0.00	30.29	0.00	0.07	0.70	0.09	0.00	0.00	68.85	0.00	0.00	0.00	0.00	**Dolomite**
3	0.21	31.47	0.03	0.31	0.52	0.05	0.00	0.00	67.41	0.00	0.00	0.00	0.00	**Dolomite**
4	0.00	24.07	0.00	1.09	0.43	0.01	0.15	0.04	64.97	0.00	9.24	0.00	0.00	**Dolomite**
5	0.00	0.00	4.80	88.57	0.00	0.00	0.00	5.73	0.00	0.19	0.57	0.00	0.13	**Clay**
6	0.00	0.00	5.26	11.29	28.19	0.00	0.00	3.07	51.95	0.00	0.24	0.00	0.00	**Clay**
7	0.12	0.00	0.14	1.19	32.00	0.00	0.01	0.20	66.33	0.00	0.00	0.00	0.00	**Apatite**
8	0.00	0.00	3.65	90.60	0.00	0.00	0.00	5.06	0.00	0.13	0.56	0.00	0.00	**Clay**
9	0.00	0.00	0.12	3.35	0.22	51.36	0.22	0.07	0.20	1.05	41.44	0.00	1.98	**Pyrite**
10	0.00	0.00	0.00	0.93	0.24	52.68	0.19	0.00	0.11	1.45	41.93	0.00	2.48	**Pyrite**

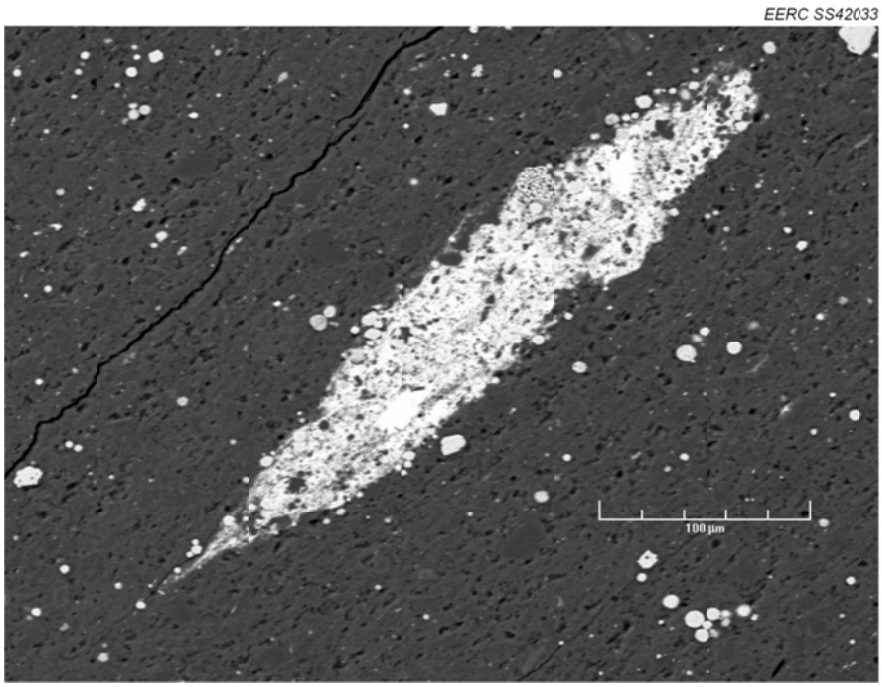

Figure D-8. Field for EDS testing on Sample T-1 at 300× magnification. Yellow crosshairs indicate the tag number and location.

Table D-8. Results of SEM–EDS Measurements for Points Present in Figure D-8, wt%

Tag	Na	Mg	Al	Si	P	S	Cl	K	Ca	Ti	Fe	Ba	Zn	Mineralogy
1	10.01	0.00	5.65	17.38	0.00	25.38	0.09	2.36	0.04	0.11	0.69	0.00	38.28	**Sphalerite**
2	12.40	0.03	1.47	2.99	0.09	31.35	0.00	1.12	0.00	0.15	0.64	0.00	49.75	**Sphalerite**
3	0.00	0.12	1.83	8.51	0.12	44.82	0.46	0.74	0.18	0.69	40.29	0.00	2.25	**Pyrite**
4	15.20	0.00	0.00	0.01	0.11	31.28	0.00	0.66	0.00	0.20	0.44	0.00	52.10	**Sphalerite**
5	14.21	0.00	0.52	0.89	0.00	31.08	0.00	0.82	0.00	0.26	0.52	0.00	51.70	**Sphalerite**
6	0.00	0.00	0.22	96.80	0.00	0.00	0.00	2.68	0.00	0.00	0.15	0.00	0.15	**Quartz**
7	0.00	0.00	0.12	96.37	0.00	0.00	0.00	2.65	0.00	0.00	0.34	0.00	0.51	**Quartz**
8	0.00	0.00	0.22	96.38	0.00	0.13	0.00	2.81	0.00	0.00	0.16	0.17	0.13	**Quartz**
9	0.00	0.09	7.61	81.93	0.08	0.00	0.00	8.85	0.00	0.44	0.88	0.00	0.11	**Clay**
10	0.00	1.13	16.50	67.29	0.00	0.46	0.00	12.61	0.00	0.43	1.56	0.00	0.04	**Clay**

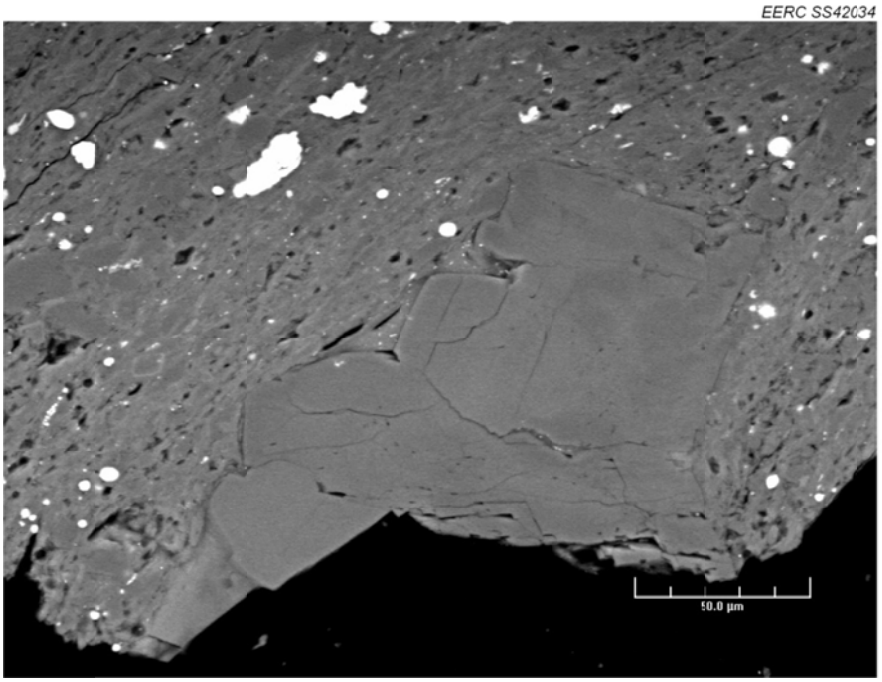

Figure D-9. Field for EDS testing on Sample T-1 at 500× magnification. Yellow crosshairs indicate the tag number and location.

Table D-9. Results of SEM–EDS Measurements for Points Present in Figure D-9, wt%

Tag	Na	Mg	Al	Si	P	S	Cl	K	Ca	Ti	Fe	Ba	Mineralogy
1	0.00	29.53	0.33	1.11	0.58	0.00	0.00	0.00	68.45	0.00	0.00	0.00	**Dolomite**
2	0.00	27.78	0.13	0.22	0.59	0.22	0.00	0.00	71.02	0.00	0.04	0.00	**Dolomite**
3	0.00	30.04	0.00	0.07	0.83	0.07	0.00	0.00	68.90	0.00	0.09	0.00	**Dolomite**
4	0.00	0.08	3.71	89.69	0.02	0.00	0.00	4.90	0.00	0.87	0.73	0.00	**Clay**
5	0.00	26.10	1.06	14.47	0.11	0.00	0.00	0.87	57.10	0.00	0.29	0.00	**Dolomite**
6	0.36	0.83	21.19	60.17	0.00	0.50	0.00	14.23	0.28	0.60	1.84	0.00	**Clay**
7	0.00	1.29	19.72	60.96	0.00	0.00	0.00	14.63	1.17	0.40	1.52	0.30	**Clay**
8	0.00	1.11	19.70	61.24	0.00	0.10	0.00	15.14	0.10	0.65	1.95	0.00	**Clay**
9	0.00	0.01	1.03	1.60	0.17	52.55	0.15	0.38	0.07	1.22	42.82	0.00	**Pyrite**
10	0.00	0.00	0.10	1.12	0.17	54.18	0.08	0.00	0.00	1.19	43.15	0.00	**Pyrite**

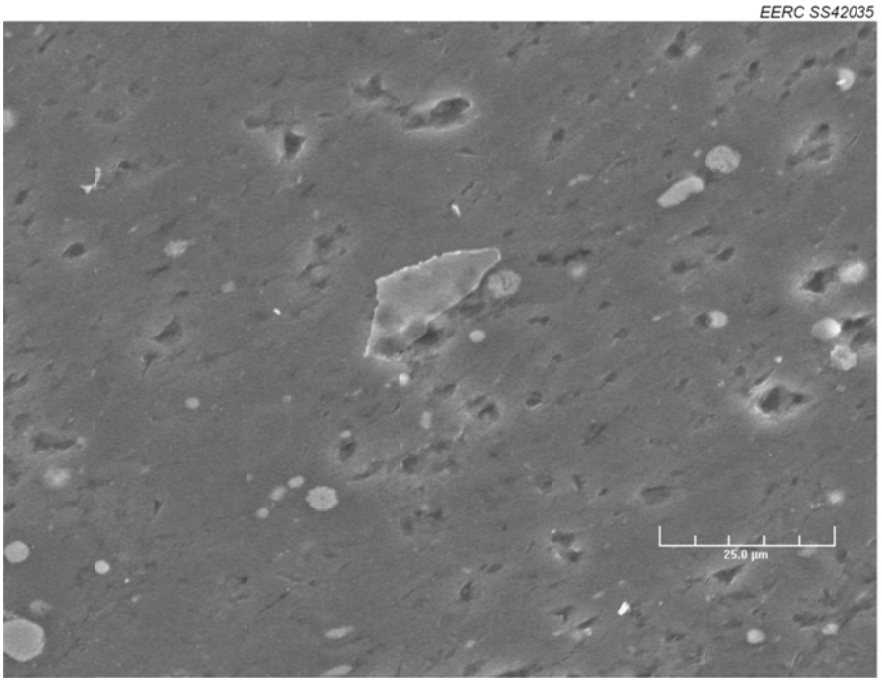

Figure D-10. Field for EDS testing on Sample T-1 at 1000× magnification. Yellow crosshairs indicate the tag number and location.

Table D-10. Results of SEM–EDS Measurements for Points Present in Figure D-10, wt%

Tag	Na	Mg	Al	Si	P	S	Cl	K	Ca	Ti	Fe	Ba	Mineralogy
1	0.00	0.25	8.56	83.61	0.00	0.00	0.00	7.00	0.00	0.00	0.58	0.00	**Clay**
2	0.00	0.23	8.48	81.97	0.00	0.00	0.00	8.29	0.00	0.04	1.00	0.00	**Clay**
3	0.00	0.46	14.94	70.59	0.00	0.00	0.00	12.65	0.00	0.27	1.08	0.00	**Clay**
4	0.00	0.00	2.66	9.92	0.00	47.64	0.00	1.32	0.00	0.08	38.37	0.00	**Pyrite**
5	0.00	0.00	1.56	8.95	0.00	49.76	0.00	0.72	0.00	0.00	39.01	0.00	**Pyrite**
6	0.00	0.00	1.64	6.70	0.00	50.75	0.00	0.56	0.00	0.00	40.35	0.00	**Pyrite**
7	0.00	0.26	13.36	73.86	0.00	0.00	0.00	11.00	0.00	0.00	1.52	0.00	**Clay**
8	0.00	0.29	15.79	71.34	0.00	0.00	0.00	11.22	0.11	0.00	1.26	0.00	**Clay**

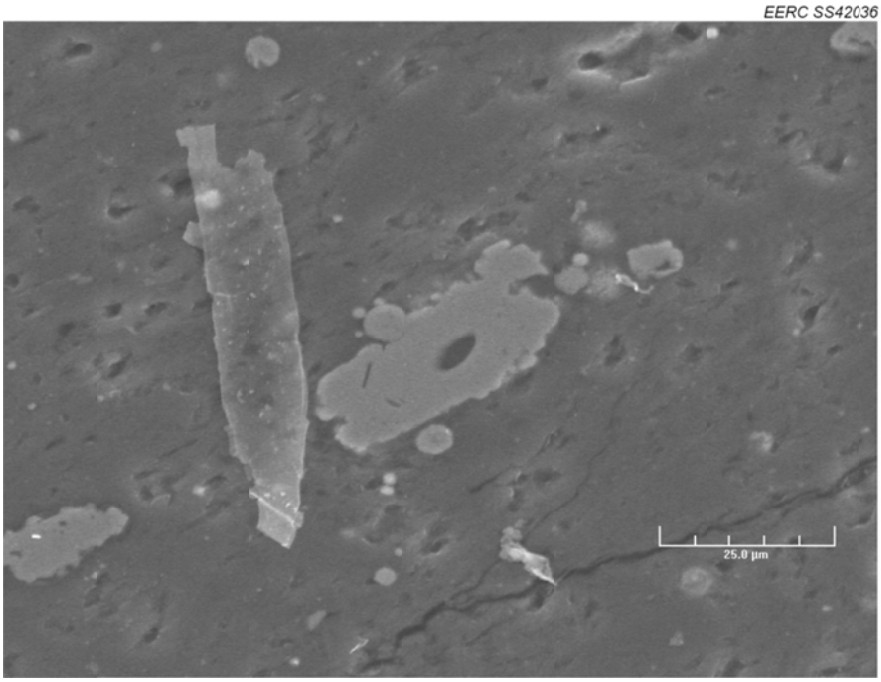

Figure D-11. Field for EDS testing on Sample T-1 at 1000× magnification. Yellow crosshairs indicate the tag number and location.

Table D-11. Results of SEM–EDS Measurements for Points Present in Figure D-11, wt%

Tag	Na	Mg	Al	Si	P	S	Cl	K	Ca	Ti	Fe	Ba	Mineralogy
1	0.00	0.47	14.80	68.06	0.00	0.90	0.01	11.93	2.14	0.00	1.69	0.00	**Clay**
2	0.00	0.00	17.22	67.57	0.00	0.15	0.00	13.46	0.00	0.39	1.20	0.00	**Clay**
3	0.00	0.00	0.40	1.93	0.00	53.98	0.00	0.38	0.06	0.00	43.24	0.00	**Pyrite**
4	0.00	0.00	2.65	10.04	0.00	49.81	0.00	0.94	0.19	0.00	36.36	0.00	**Pyrite**
5	0.00	0.00	0.00	2.28	0.00	52.76	0.00	0.19	0.03	0.31	44.42	0.00	**Pyrite**
6	0.00	0.00	0.23	14.00	0.00	47.69	0.00	0.20	0.00	0.00	37.88	0.00	**Pyrite**
7	0.00	0.00	0.13	99.79	0.00	0.00	0.00	0.08	0.00	0.00	0.00	0.00	**Quartz**
8	0.00	0.71	20.36	60.11	0.00	1.38	0.00	14.27	0.15	0.00	3.04	0.00	**Clay**

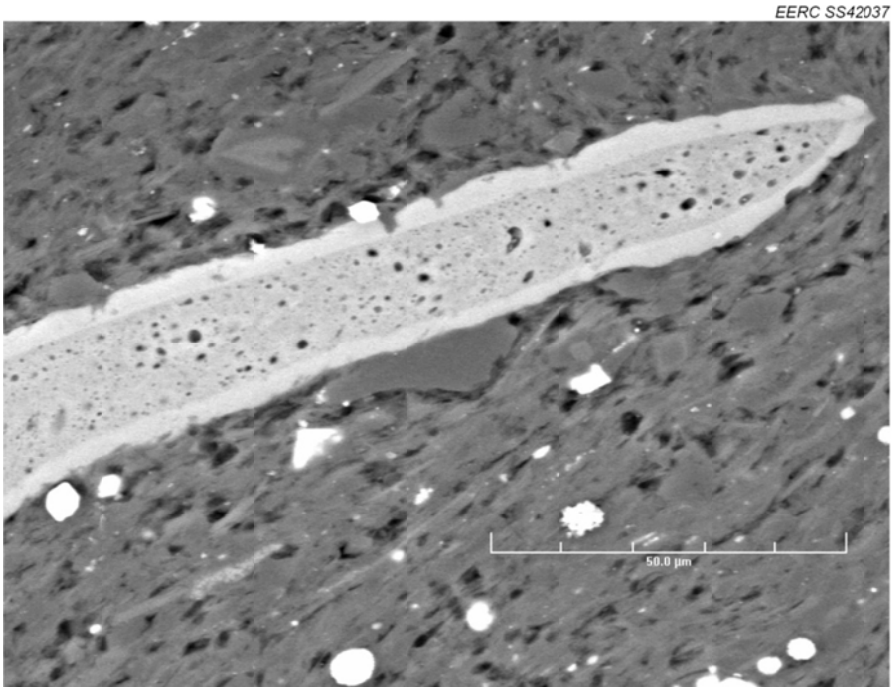

Figure D-12. Field for EDS testing on Sample T-1 at 1000× magnification. Yellow crosshairs indicate the tag number and location.

Table D-12. Results of SEM–EDS Measurements for Points Present in Figure D-12, wt%

Tag	Na	Mg	Al	Si	P	S	Cl	K	Ca	Ti	Fe	Ba	Mineralogy
1	0.00	18.69	0.74	2.74	0.20	0.08	0.00	0.39	58.14	0.00	19.02	0.00	**Ankerite**
2	0.00	0.58	10.15	76.85	0.00	0.50	0.00	9.74	0.88	0.09	1.20	0.00	**Clay**
3	0.00	0.04	5.12	86.45	0.24	0.00	0.00	6.29	1.06	0.00	0.59	0.20	**Clay**
4	0.00	0.00	0.10	0.92	32.81	0.00	0.00	0.12	66.01	0.00	0.03	0.00	**Apatite**
5	0.00	0.00	0.18	1.19	32.04	0.00	0.00	0.14	66.45	0.00	0.00	0.00	**Apatite**
6	0.09	0.00	0.05	0.52	32.61	0.00	0.00	0.12	66.54	0.00	0.07	0.00	**Apatite**
7	0.00	0.00	0.00	0.44	32.80	0.00	0.10	0.06	66.60	0.00	0.00	0.00	**Apatite**
8	0.00	0.00	0.63	95.95	0.39	0.00	0.00	2.70	0.21	0.00	0.11	0.00	**Quartz**
9	0.00	0.00	4.52	88.54	0.00	0.00	0.00	5.39	0.00	0.81	0.74	0.00	**Clay**
10	0.00	0.00	4.71	88.32	0.00	0.00	0.00	5.99	0.00	0.33	0.65	0.00	**Clay**

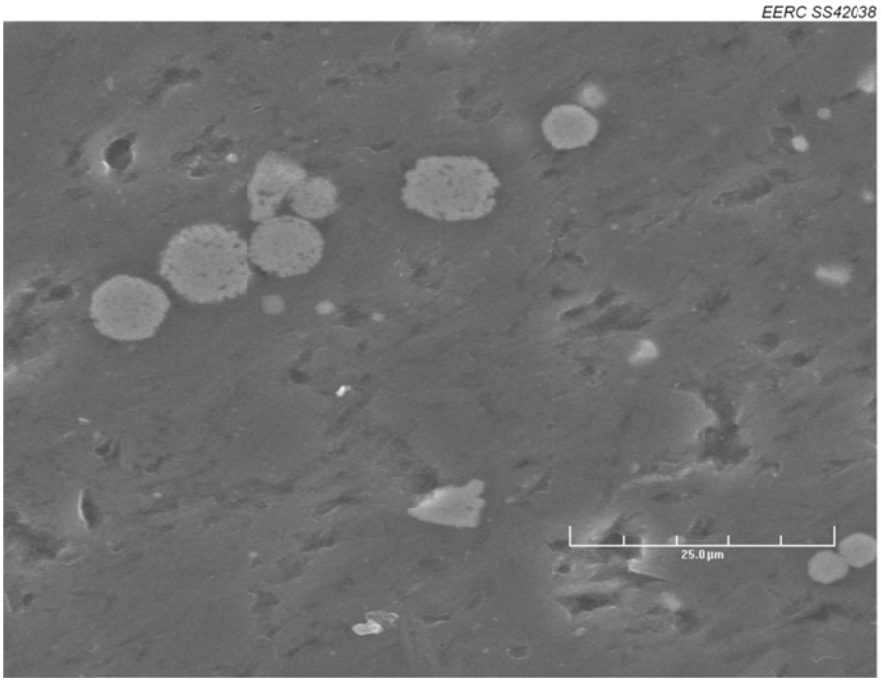

Figure D-13. Field for EDS testing on Sample T-1 at 1500× magnification. Yellow crosshairs indicate the tag number and location.

Table D-13. Results of SEM–EDS Measurements for Points Present in Figure D-13, wt%

Tag	Na	Mg	Al	Si	P	S	Cl	K	Ca	Ti	Fe	Ba	Mineralogy
1	0.00	0.00	0.19	0.56	0.00	54.92	0.00	0.27	0.06	0.00	44.00	0.00	**Pyrite**
2	0.00	0.08	0.16	0.70	0.15	54.70	0.00	0.00	0.00	0.08	44.14	0.00	**Pyrite**
3	0.00	0.00	0.05	0.48	0.00	54.99	0.00	0.32	0.05	0.00	43.46	0.65	**Pyrite**
4	0.00	0.00	0.73	1.97	0.12	53.65	0.00	0.34	0.00	0.40	42.79	0.00	**Pyrite**
5	0.00	0.31	17.06	66.83	0.00	0.00	0.00	13.15	0.33	0.07	2.25	0.00	**Clay**
6	0.05	0.26	3.09	7.10	0.00	49.43	0.03	0.60	0.00	0.00	39.45	0.00	**Pyrite**
7	0.00	0.00	3.98	8.97	0.00	47.86	0.00	1.50	0.00	0.23	37.46	0.00	**Pyrite**
8	0.00	0.39	21.61	59.22	0.00	0.00	0.00	17.17	0.00	0.00	1.61	0.00	**Clay**
9	0.00	0.75	18.14	63.11	0.00	0.00	0.00	15.69	0.22	0.17	1.92	0.00	**Clay**
10	0.00	0.94	17.47	65.51	0.00	0.00	0.00	13.39	0.29	0.84	1.56	0.00	**Clay**

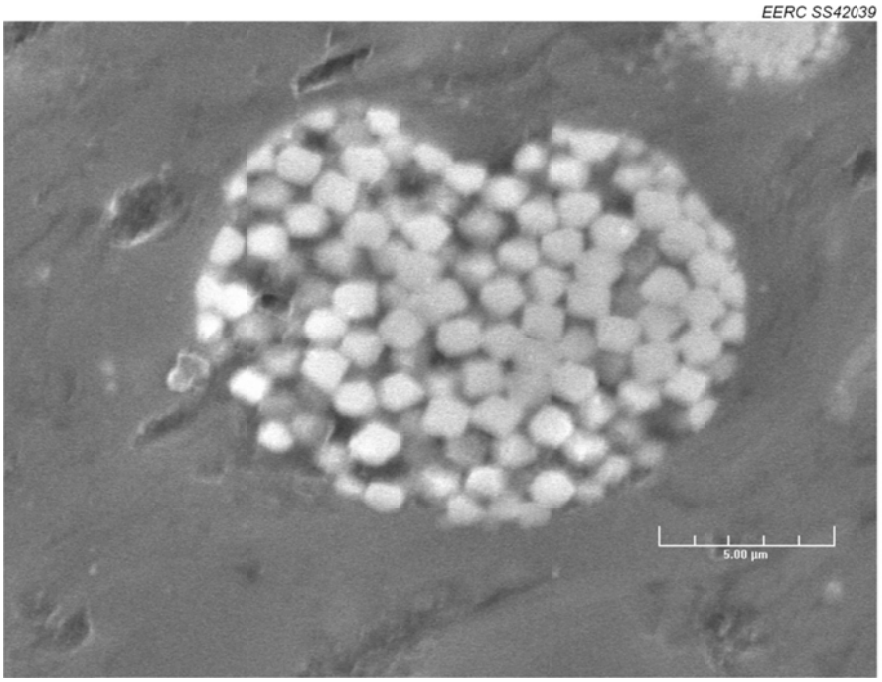

Figure D-14. Field for EDS testing on Sample T-1 at 5000× magnification. Yellow crosshairs indicate the tag number and location.

Table D-14. Results of SEM–EDS Measurements for Points Present in Figure D-14, wt%

Tag	Na	Mg	Al	Si	P	S	Cl	K	Ca	Ti	Fe	Ba	Mineralogy
1	0.00	0.30	15.08	67.07	0.00	2.43	0.00	12.22	0.02	0.91	1.96	0.00	**Clay**
2	0.00	0.00	0.99	3.76	0.00	53.34	0.00	0.47	0.00	0.21	41.24	0.00	**Pyrite**
3	0.00	0.00	0.18	0.30	0.00	56.00	0.00	0.03	0.00	0.07	43.42	0.00	**Pyrite**
4	0.00	0.00	0.00	0.00	0.00	55.54	0.00	0.14	0.00	0.18	44.07	0.07	**Pyrite**
5	0.00	0.00	2.25	5.84	0.00	52.41	0.00	1.14	0.09	0.00	38.28	0.00	**Pyrite**
6	0.00	0.63	16.90	66.77	0.00	0.23	0.00	13.84	0.00	0.49	1.14	0.00	**Clay**

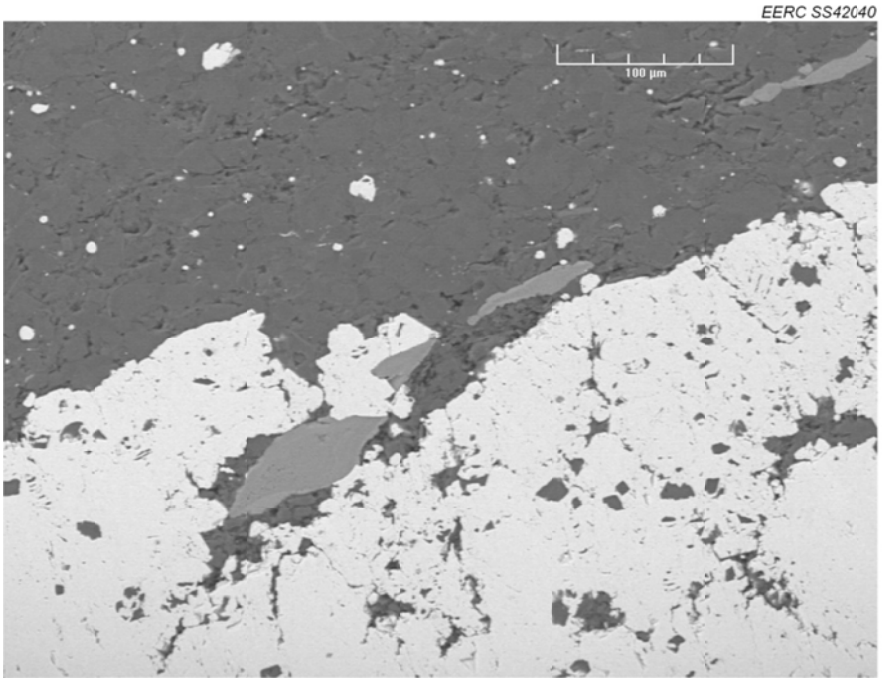

Figure D-15. Field for EDS testing on Sample T-3 at 250× magnification. Yellow crosshairs indicate the tag number and location.

Table D-15. Results of SEM–EDS Measurements for Points Present in Figure D-15, wt%

Tag	Na	Mg	Al	Si	P	S	Cl	K	Ca	Ti	Fe	Ba	Mineralogy
1	0.07	0.00	0.00	0.58	32.02	0.00	0.00	0.02	67.21	0.00	0.11	0.00	**Apatite**
2	0.00	0.00	0.02	0.51	32.41	0.02	0.00	0.00	66.96	0.00	0.07	0.00	**Apatite**
3	0.12	0.02	0.00	0.44	31.68	0.00	0.28	0.18	67.28	0.00	0.00	0.00	**Apatite**
4	0.00	14.63	10.56	20.59	0.00	0.00	0.00	3.38	48.85	0.05	1.94	0.00	**Dolomite**
5	0.00	25.25	0.00	0.88	0.56	0.31	0.00	0.00	72.58	0.00	0.42	0.00	**Dolomite**
6	0.00	24.30	0.14	0.43	0.47	0.06	0.20	0.05	73.37	0.00	0.98	0.00	**Dolomite**
7	0.00	26.46	0.36	0.86	0.50	0.20	0.00	0.19	70.74	0.00	0.70	0.00	**Dolomite**
8	0.00	12.96	0.00	0.45	0.07	30.42	0.00	0.00	30.83	0.00	25.28	0.00	**Pyrite**
9	0.00	23.98	2.14	6.60	0.17	0.73	0.00	2.01	61.34	0.25	2.79	0.00	**Dolomite**
10	0.00	0.00	0.01	0.00	0.10	53.73	0.20	0.00	0.00	1.49	44.48	0.00	**Pyrite**

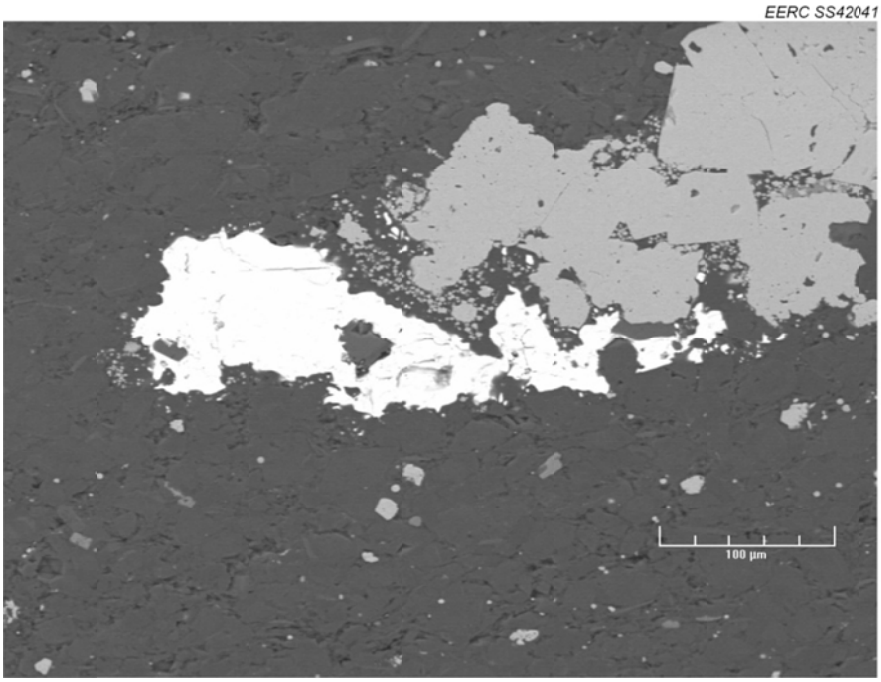

Figure D-16. Field for EDS testing on Sample T-3 at 250× magnification. Yellow crosshairs indicate the tag number and location.

Table D-16. Results of SEM–EDS Measurements for Points Present in Figure D-16, wt%

Tag	Na	Mg	Al	Si	P	S	Cl	K	Ca	Ti	Fe	Ba	Mineralogy
1	0.10	0.00	0.00	0.42	0.02	19.05	0.00	0.00	0.00	9.88	0.00	70.52	**Barite**
2	0.07	0.00	0.00	0.66	0.01	19.48	0.00	0.00	0.00	9.33	0.00	70.45	**Barite**
3	0.00	0.00	0.00	0.03	0.34	53.64	0.24	0.00	0.29	1.38	44.08	0.00	**Pyrite**
4	0.00	0.00	0.00	0.04	0.32	54.00	0.20	0.00	0.06	1.58	43.80	0.00	**Pyrite**
5	0.00	0.03	1.63	4.37	0.14	49.65	0.11	0.44	0.42	1.02	42.20	0.00	**Pyrite**
6	0.00	2.04	1.04	13.78	0.03	0.21	0.00	0.38	2.46	80.01	0.04	0.00	**High-Ti**
7	0.00	0.00	0.00	0.37	0.26	53.79	0.20	0.00	0.44	1.49	43.46	0.00	**Pyrite**
8	0.00	26.24	0.68	2.28	0.42	0.00	0.00	0.29	69.93	0.00	0.17	0.00	**Dolomite**
9	0.00	25.32	1.42	3.14	0.31	0.17	0.35	0.52	68.26	0.00	0.51	0.00	**Dolomite**
10	0.00	26.79	0.04	0.55	0.39	0.30	0.09	0.07	71.46	0.00	0.32	0.00	**Dolomite**

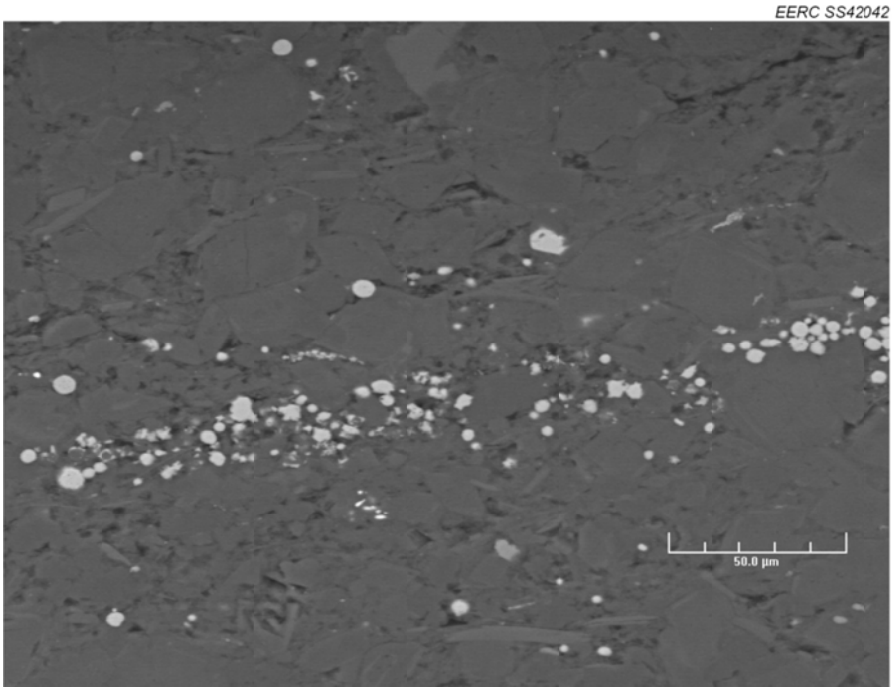

Figure D-17. Field for EDS testing on Sample T-3 at 500× magnification. Yellow crosshairs indicate the tag number and location.

Table D-17. Results of SEM–EDS Measurements for Points Present in Figure D-17, wt%

Tag	Na	Mg	Al	Si	P	S	Cl	K	Ca	Ti	Fe	Ba	Mineralogy
1	0.00	0.30	0.30	0.91	0.64	0.13	0.00	0.08	97.66	0.00	0.00	0.00	**Calcite**
2	0.00	1.44	22.55	50.30	0.00	0.00	0.00	19.11	0.90	0.58	4.68	0.45	**Clay**
3	0.01	26.17	0.23	1.15	0.53	0.35	0.00	0.00	70.64	0.00	0.91	0.00	**Dolomite**
4	0.00	25.72	0.07	0.54	0.53	0.47	0.00	0.02	72.58	0.00	0.06	0.00	**Dolomite**
5	0.00	0.00	0.00	0.08	0.11	54.06	0.04	0.00	0.29	1.51	43.91	0.00	**Pyrite**
6	0.00	24.34	0.07	8.97	0.22	0.23	0.00	0.08	65.29	0.00	0.81	0.00	**Dolomite**
7	0.00	0.00	0.00	1.36	0.38	53.54	0.33	0.01	0.20	1.43	42.75	0.00	**Pyrite**
8	0.00	0.00	0.10	1.88	0.24	53.72	0.12	0.00	0.34	1.38	42.21	0.00	**Pyrite**
9	0.00	1.56	18.50	62.95	0.00	1.39	0.00	13.12	0.63	0.34	1.51	0.00	**Clay**
10	0.00	1.18	24.60	46.85	0.00	0.00	0.00	19.25	0.69	1.43	6.01	0.00	**Clay**
11	0.00	0.00	0.94	1.57	0.13	0.08	0.04	0.20	0.59	96.05	0.39	0.00	**High-Ti**
12	0.00	26.66	0.22	0.45	0.59	0.12	0.00	0.00	71.58	0.00	0.37	0.00	**Dolomite**

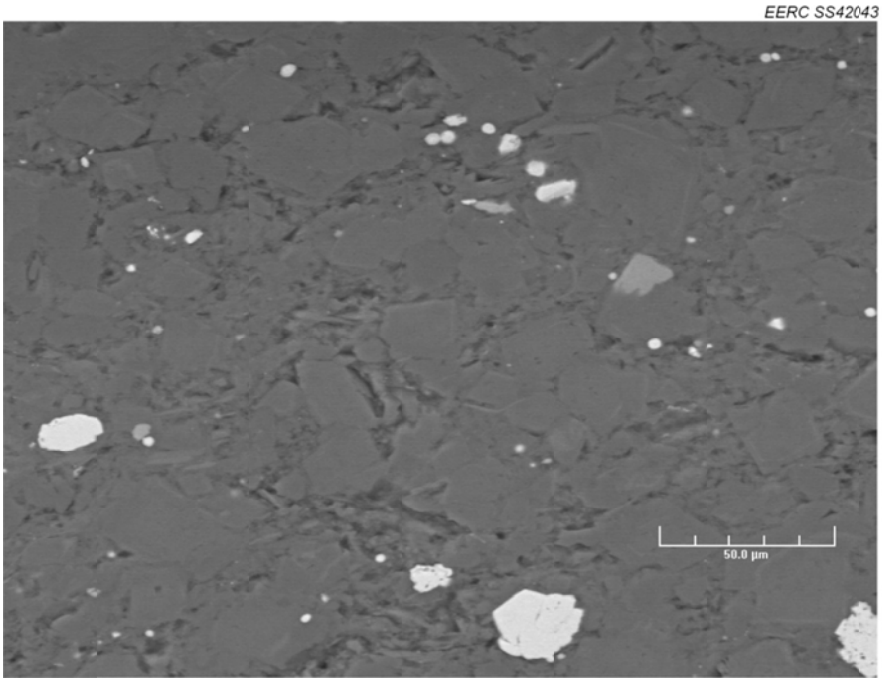

Figure D-18. Field for EDS testing on Sample T-3 at 500× magnification. Yellow crosshairs indicate the tag number and location.

Table D-18. Results of SEM–EDS Measurements for Points Present in Figure D-18, wt%

Tag	Na	Mg	Al	Si	P	S	Cl	K	Ca	Ti	Fe	Ba	Mineralogy
1	0.00	25.71	1.09	3.06	0.15	0.00	0.00	0.66	65.92	0.00	3.40	0.00	**Dolomite**
2	0.00	27.63	0.54	3.34	0.29	0.04	0.29	0.23	67.36	0.00	0.29	0.00	**Dolomite**
3	0.00	26.66	0.03	0.77	0.49	0.13	0.00	0.04	71.79	0.00	0.08	0.00	**Dolomite**
4	0.00	28.22	0.44	1.40	0.39	0.18	0.00	0.33	68.78	0.00	0.27	0.00	**Dolomite**
5	0.00	1.52	6.15	78.75	0.00	1.61	0.00	5.00	6.26	0.00	0.71	0.00	**Clay**
6	0.00	1.11	15.09	65.59	0.00	3.66	0.00	12.12	0.43	0.46	1.53	0.00	**Clay**
7	0.29	0.13	24.18	54.07	0.00	0.00	0.00	16.69	0.31	0.36	3.55	0.40	**Clay**
8	0.00	1.18	18.12	60.40	0.00	0.67	0.00	15.89	1.24	0.38	1.75	0.37	**Clay**
9	0.16	0.17	0.20	0.77	32.23	0.00	0.00	0.23	66.24	0.00	0.00	0.00	**Apatite**
10	0.00	4.34	0.54	1.37	0.08	1.69	0.00	0.12	16.18	74.50	1.19	0.00	**High-Ti**

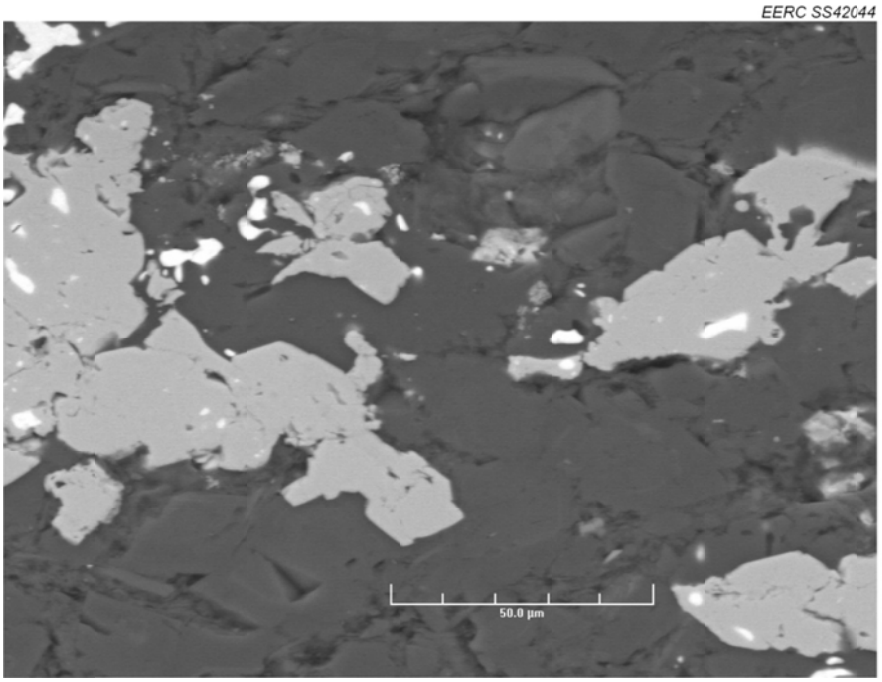

Figure D-19. Field for EDS testing on Sample T-3 at 750× magnification. Yellow crosshairs indicate the tag number and location.

Table D-19. Results of SEM–EDS Measurements for Points Present in Figure D-19, wt%

Tag	Na	Mg	Al	Si	P	S	Cl	K	Ca	Ti	Fe	Ba	Mineralogy
1	0.00	25.08	0.32	1.65	0.29	0.41	0.00	0.14	70.47	0.00	1.65	0.00	**Dolomite**
2	0.00	27.27	0.00	0.58	0.50	0.12	0.00	0.00	70.43	0.00	1.09	0.00	**Dolomite**
3	0.00	30.16	0.13	0.29	0.41	0.15	0.00	0.00	67.63	0.00	1.22	0.00	**Dolomite**
4	0.00	0.00	0.00	0.30	0.24	54.14	0.10	0.00	0.05	1.48	43.69	0.00	**Pyrite**
5	0.00	0.00	0.00	8.89	0.05	16.91	0.00	0.00	0.03	9.17	1.11	63.85	**Barite**
6	0.00	0.00	0.00	0.03	0.33	53.97	0.22	0.00	0.08	1.55	43.80	0.00	**Barite**
7	0.01	0.00	0.00	0.04	0.10	30.05	0.00	0.00	0.00	6.89	14.83	48.08	**Barite**
8	0.00	0.00	0.00	0.59	0.00	28.67	0.00	0.00	0.00	7.46	12.22	51.06	**Barite**
9	0.00	25.68	0.87	3.01	0.68	0.31	0.09	0.42	67.94	0.00	1.00	0.00	**Dolomite**
10	0.00	27.13	0.21	0.62	0.48	0.12	0.00	0.00	69.61	0.00	1.83	0.00	**Dolomite**

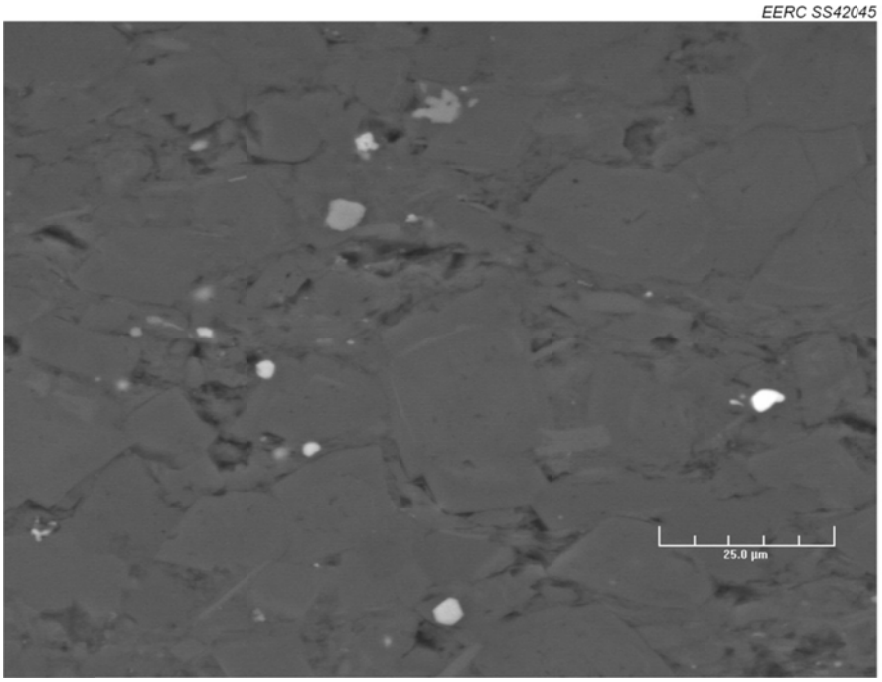

Figure D-20. Field for EDS testing on Sample T-3 at 1000× magnification. Yellow crosshairs indicate the tag number and location.

Table D-20. Results of SEM–EDS Measurements for Points Present in Figure D-20, wt%

Tag	Na	Mg	Al	Si	P	S	Cl	K	Ca	Ti	Fe	Ba	Mineralogy
1	0.00	30.25	0.81	1.86	0.35	0.25	0.10	0.17	65.88	0.00	0.35	0.00	**Dolomite**
2	0.00	25.42	0.82	3.35	0.30	0.06	0.00	0.39	69.23	0.00	0.43	0.00	**Dolomite**
3	0.00	26.96	0.15	0.85	0.46	0.07	0.00	0.05	70.87	0.00	0.53	0.06	**Dolomite**
4	0.00	26.97	0.00	2.34	0.23	0.09	0.00	0.00	70.17	0.00	0.19	0.00	**Dolomite**
5	0.00	1.05	2.74	6.08	0.00	0.02	0.00	1.30	2.48	85.95	0.39	0.00	**High-Ti**
6	0.00	0.41	1.42	4.19	0.10	0.53	0.02	0.47	1.64	89.79	1.42	0.00	**High-Ti**
7	0.00	1.29	22.58	52.68	0.00	0.00	0.00	18.39	0.30	0.81	3.94	0.00	**Clay**
8	0.00	1.56	0.18	0.69	0.21	49.46	0.09	0.01	7.41	0.64	39.73	0.00	**Pyrite**
9	0.00	0.00	0.81	15.18	0.00	17.08	0.00	0.16	0.38	8.33	0.00	58.06	**Barite**
10	0.00	23.02	0.47	1.00	0.47	0.40	0.47	0.21	73.13	0.00	0.83	0.00	**Dolomite**

APPENDIX B

FORT NELSON CCS PROJECT RESERVOIR QUALITY ASSESSMENT AND ACID GAS INJECTION STUDY LABORATORY EVALUATION